NATIONAL ADVISORY COMMITTEE FOR AERONAUTICS

TECHNICAL NOTE 2045

APPROXIMATE TURBULENT BOUNDARY-LAYER DEVELOPMENT IN PLANE COMPRESSIBLE FLOW ALONG THERMALLY INSULATED SURFACES WITH APPLICATION TO SUPERSONIC-TUNNEL CONTOUR CORRECTION

By Maurice Tucker

Lewis Flight Propulsion Laboratory
Cleveland, Ohio

Washington
March 1950

NATIONAL ADVISORY COMMITTEE FOR AERONAUTICS

TECHNICAL NOTE 2045

APPROXIMATE TURBULENT BOUNDARY-LAYER DEVELOPMENT IN PLANE COMPRESSIBLE FLOW ALONG THERMALLY INSULATED SURFACES WITH APPLICATION TO SUPERSONIC-TUNNEL CONTOUR CORRECTION

By Maurice Tucker

SUMMARY

Numerical solutions of the differential equation obtained from the momentum theorem for the development of a turbulent boundary layer along a thermally insulated surface in two-dimensional and in radial shock-free flow are presented in tabular form for a range of Mach numbers from 0.100 to 10. The solution can be used in a stepwise procedure with any given distribution of favorable pressure gradients and for zero pressure gradients. Solutions are also given for use with moderate adverse pressure gradients. The mean velocity in the boundary layer is approximated by a power-law profile. In view of the stepwise integration methods to be used, the exponent designating the profile shape can be varied along the surface between the integral fraction limits 1/5 and 1/11 through interpolation. Agreement obtained between theoretical and experimental boundary-layer development in a supersonic nozzle at a nominal Mach number of 2 indicates the general validity of the approximations used in the analysis - in particular, the method of extrapolating low-speed skin-friction relations to high Mach number flows. The extrapolation method used assumes that the skin-friction coefficients depend primarily on Reynolds number, provided that the density and the kinematic viscosity are evaluated at surface conditions.

The tabulated results are directly applicable to the correction of supersonic-tunnel contours for the effects of boundary-layer growth. In connection with this problem, an idealized analysis of the Mach wave boundary-layer interaction is presented, which leads to a method of contour correction that differs in principle from the conventional method based on use of displacement thickness. A brief discussion of the two methods is given.

INTRODUCTION

Computation of turbulent-boundary-layer development is required in numerous flow problems. Inasmuch as the fundamental processes governing turbulent boundary-layer flow are not yet completely understood, it becomes necessary to resort to semiempirical methods. The Kármán momentum equation in reference 1 provides such a method for obtaining the approximate growth of a compressible turbulent boundary layer in shock-free flow under the action of pressure gradient, provided that the streamwise variation of the local skin-friction coefficient and of the boundary-layer velocity profile are known. A summary of recent contributions to the computation of compressible boundary-layer flows is presented in reference 2. Tetervin makes use of the Kármán momentum equation to indicate the integrations needed for obtaining the turbulent boundary-layer quantities in compressible flow.

The method used at the NACA Lewis laboratory for this report differs from that of reference 2 primarily in the manner whereby the local skin-friction coefficients for compressible flow are extrapolated from low-speed values. In the absence of sufficiently decisive experimental data, the present computations have been extended to include the extrapolation method of reference 2. The stepwise integration method included herein makes it possible to present integrated results for two-dimensional and for radial turbulent boundary-layer flows along thermally insulated surfaces with stream Mach numbers from 0.100 to 10 in a form that is applicable to a variety of cases.

As one application of the tabulated results, the correction of supersonic-tunnel contours for effects of boundary-layer growth is discussed. The conventional method of contour correction is based on continuity of mass flow, which leads to selection of displacement thickness as the correction criterion. In this report the problem is also treated from the concept of Mach wave interaction with the boundary layer, giving rise to a contour correction that differs from the conventional correction.

BOUNDARY-LAYER DEVELOPMENT

Physical Assumptions

Application of the Kármán momentum equation to turbulent flow requires a knowledge of the local skin-friction coefficient and the boundary-layer velocity profile. Falkner (reference 3) has reviewed

the low-speed data available on turbulent flow over flat plates (zero pressure gradient) and concludes that local skin-friction coefficients can be obtained with fair accuracy from an empirical formula which, in the notation of reference 3, is

$$c_f \equiv \frac{f}{\frac{1}{2}\rho v^2} = 0.0262 \left(\frac{\nu}{vl}\right)^{1/7} \tag{1}$$

where

c_f local skin-friction coefficient

f local skin-friction stress

ρ fluid density

v tangential velocity at outer edge of boundary layer

ν kinematic viscosity

l distance to given point from leading edge of plate

Reference 3, being concerned only with low-speed flow, does not further specify the density and the kinematic viscosity. In reference 2, equation (1) is applied for compressible flow in a modified form which, in the present notation (appendix A), is equivalent to

$$\frac{\tau}{\rho_1 u_1^2} = 0.0131 \left(\frac{\nu_1}{u_1 x}\right)^{1/7} \equiv \frac{0.0131}{R_s^{1/7}} \tag{1a}$$

where

τ local skin-friction stress

ρ_1 density at outer edge of boundary layer

u_1 velocity at outer edge of boundary layer

ν_1 kinematic viscosity at outer edge of boundary layer

x distance from start of boundary-layer development

R_s stream Reynolds number

The friction relation of equation (1a) is in accordance with established procedure for subsonic flow.

This analysis considers another assumption; namely, that the local skin-friction coefficient for turbulent flow under pressure gradient is dependent only on Reynolds number, provided that the density and the kinematic viscosity are evaluated for the temperature and the pressure prevailing at the bounding surface or wall. Equation (1) is then modified as

$$\frac{\tau}{\rho_w u_1^2} = 0.0131 \left(\frac{\nu_w}{u_1 x}\right)^{1/7} \equiv \frac{0.0131}{R_w^{1/7}} \tag{1b}$$

where the subscript w designates surface or wall values. This formulation was suggested by the observation that the laminar-flow flat-plate drag coefficients calculated by von Kármán and Tsien in reference 4 become practically independent of Mach number if the density and the kinematic viscosity are evaluated at wall conditions instead of stream conditions. Evidence to support the assumption implied by equation (1b) is given in reference 5, which presents the results of heat-transfer investigations of turbulent air flow at high subsonic speeds in an electrically heated tube. In reference 5, better correlation of turbulent friction coefficient and Reynolds number was obtained by use of ρ_w and ν_w than by use of "bulk values." The analysis that follows utilizes both equations (1a) and (1b). (It has come to the attention of the author that von Kármán in reference 6 proposed an assumption similar to that implied in equation (1b)).

Some assumption must also be made regarding the mean velocity profile in a compressible turbulent boundary layer. Figure 1 presents a comparison of the power-law profile given by

$$\frac{u}{u_1} = \left(\frac{y}{\delta}\right)^{1/N} \equiv z^{1/N} \tag{2}$$

where

u boundary-layer velocity at distance y from surface

y normal distance from plate surface

δ nominal boundary-layer thickness

N velocity-profile parameter

with an experimental profile obtained from measurements taken slightly upstream of the test section in a supersonic tunnel with a design Mach number of 2.08. The power-law profile appears to offer a satisfactory approximation to the profiles obtained in compressible flow under favorable (negative) pressure gradients and is used in the analysis for both favorable and adverse (positive) pressure gradients.

Dependable relations for the variation of the velocity-profile parameter N of equation (2) with Reynolds number, pressure gradient, and Mach number are not yet known for compressible turbulent flows. An approximate guide for the selection of N insofar as Reynolds number effect is concerned may be obtained as follows: Dryden (reference 7) rearranges Kármán's logarithmic velocity-profile relation to obtain

$$e^{\left(\frac{u}{u_1} - 1\right)} = z^{\frac{1}{k}\sqrt{c_f}} = \left(\frac{u}{u_1}\right)^{\frac{N\sqrt{c_f}}{k}}$$

which, with the use of equation (1a) or (1b), results in

$$N = \frac{k}{\sqrt{0.0131}} (R_{s,w})^{1/14} \left(\frac{\frac{u}{u_1} - 1}{\log_e \frac{u}{u_1}}\right) \tag{3}$$

The subscript s,w indicates that the quantity in question may be based on stream or wall values. The value of N obtained from equation (3) will obviously depend upon the value selected for u/u_1. Experimental investigations would be required to determine whether the effect of pressure gradient and of Mach number could be approximately accounted for by proper selection of the ratio u/u_1. In the absence of such data arbitrary selection of the velocity ratio at the outer portion of the boundary layer, that is, $u/u_1 = 1$, gives

$$N = 8.7\ k(R_{s,w})^{1/14} \tag{4a}$$

Figure 8 of reference 8 indicates that the constant k should be given the value 0.3; thus,

$$N = 2.6 \left(R_{s,w}\right)^{1/14} \tag{4b}$$

A plot of equation (4b) is given in figure 2. The qualitative nature of this relation should be noted.

The foregoing assumptions as to skin friction and velocity profile are primarily based on results obtained for the case of zero pressure gradient. Figure 4 of reference 9 indicates that use of a flat-plate skin-friction relation may provide a satisfactory approximation for favorable pressure gradients and even for very moderate adverse pressure gradients. Unpublished data for low speed turbulent flow show no significant changes in velocity profile for pressure gradients varying from favorable to moderately adverse. The lack of sufficient data precludes consideration of the possible effect of Mach number on the turbulent boundary-layer velocity profile.

The customary assumption of zero static-pressure gradient normal to the wall is made for the boundary-layer region, inasmuch as curvature effects are neglected in the analysis. The wall or bounding surfaces are considered to be thermally insulated and the effective Prandtl number is taken as unity. The stream stagnation temperature and the surface or wall temperature are thus equal. The energy equation $c_p t + \frac{u^2}{2} = \text{constant}$ is then applicable to the boundary-layer flow. The ratio of specific heats γ is taken as 1.40, independent of temperature.

Treatment of Boundary-Layer Equation

In the present notation, the Kármán momentum equation of reference 1 for two-dimensional compressible flow

$$\tau = \frac{d}{dx}\left(\rho_1 u_1^2 \theta\right) + \rho_1 u_1 \delta^* \frac{du_1}{dx}$$

can be written as

$$\frac{d\theta}{dx} + \left[\frac{(2-M_1^2) + \frac{\delta^*}{\theta}\frac{dM_1}{dx}}{M_1(1+m^2)}\right]\theta = \frac{\rho_w}{\rho_1}\frac{\tau}{\rho_w u_1^2} \tag{5}$$

where

θ boundary-layer momentum thickness

x distance along surface from effective start of boundary-layer development

M_1 Mach number at outer edge of boundary layer

δ^* boundary-layer displacement thickness

$$m^2 \equiv \frac{\gamma-1}{2} M_1^2 = \frac{M_1^2}{5}$$

With the use of the substitutions $f \equiv \theta/\delta$, $g \equiv \delta^*/\delta$, and $H \equiv g/f$, equation (5) takes the form

$$\frac{d\delta}{dx} + \left[\frac{1}{f}\frac{df}{dx} + \frac{(2-M_1^2) + H\frac{dM_1}{dx}}{M_1(1+m^2)}\right]\delta = \frac{\rho_w}{\rho_1}\frac{\tau}{f\rho_w u_1^2} \tag{6}$$

The development that follows will be concerned with obtaining a solution of equation (6) in a form convenient for stepwise integration. It will be found convenient to retain Mach number M_1 and velocity-profile parameter N as the working parameters in the solution of equation (6) or related equations. The boundary-layer ratios f and g must therefore be obtained in terms of these parameters. From the assumptions of constant static pressure through the boundary layer and applicability of the energy equation and through use of the perfect gas law, the density ratio may be obtained as

$$\frac{\rho}{\rho_1} = \frac{1}{m^2\left[\frac{1+m^2}{m^2} - \left(\frac{u}{u_1}\right)^2\right]} \tag{7}$$

From the defining equations for δ^* and θ given in the list of symbols (appendix A), the ratios f and g can be obtained as

$$g = 1 - \int_0^1 \frac{\rho u}{\rho_1 u_1}\, dz$$

$$f = 1-g - \int_0^1 \frac{\rho u^2}{\rho_1 u_1^2}\, dz$$

and, through use of equations (2) and (7), can be put in the form

$$f = \frac{N}{1+m^2} \int_0^1 \frac{(s^N - s^{N+1})\, ds}{1 - \frac{m^2 s^2}{1+m^2}} \tag{8}$$

$$g = 1 - \frac{N}{1+m^2} \int_0^1 \frac{s^N\, ds}{1 - \frac{m^2 s^2}{1+m^2}} \tag{9}$$

where s is a variable of integration ($s \equiv z^{1/N}$). Although equations (8) and (9) can be integrated in closed form, evaluation by numerical methods (Simpson's one-third rule) using punch-card equipment was much faster for comparable accuracy. Values of the momentum thickness ratios f and of the displacement thickness ratios g for Mach numbers from 0.100 to 10 and for velocity-profile parameters $N = 5$, 7, 9, and 11 are listed in tables I and II, respectively. Corresponding values of the parameter $H \equiv \frac{\delta^*}{\theta}$ are listed in table III.

By means of equations (7), (8), (9), and (1a) or (1b), equation (6) may be written as

$$\frac{d\delta}{dx} + \varphi \frac{dM_1}{dx}\, \delta = \frac{K\Psi_{s,w}}{x^{1/7}} \tag{10}$$

where

$$\varphi \equiv \frac{g+f(2-7m^2) + \frac{2m^2N}{(1+m^2)^2}\int_0^1 \frac{s^2(s^N-s^{N+1})\,ds}{\left(1-\frac{m^2s^2}{1+m^2}\right)^2}}{\sqrt{5}\,fm(1+m^2)} \tag{11}$$

$$K \equiv 0.0131\left(\frac{\mu_0}{\rho_0 a_0}\right)^{1/7}$$

$$\Psi_s \equiv \frac{(1+m^2)^{2/7}}{fM_1^{1/7}} \quad \text{with equation (1a)}$$

$$\Psi_w \equiv \frac{1}{(1+m^2)^{3/7}\,fM_1^{1/7}} \quad \text{with equation (1b)}$$

and the zero subscript denotes stagnation values. In evaluation of df/dx from equation (8), the differentiation has been conducted with respect to the Mach number parameter only. The qualitative nature of the relation given by equation (4b) does not appear to warrant differentiation with respect to the parameter N. For most of the range of interest the important variable is M rather than N. In deriving equation (10) for the skin-friction relation given by equation (1a), the assumption has been made that $\mu_1 = \mu_0\left(\frac{t_1}{T_0}\right)$.

For the case of zero pressure gradient $\left(\frac{dM_1}{dx} = 0\right)$, equation (10) simplifies to

$$\frac{d\delta}{dx} = \frac{K\Psi_{s,w}}{x^{1/7}} \tag{12}$$

For constant velocity-profile parameter N and thus constant f and noting that $f\delta = \theta$, the solution of equation (12) may be put in the form:

$$\theta_b = \frac{7K}{6}\left[\frac{(1+m^2)^2}{M_1}\right]^{1/7}\left(x_b^{6/7}-x_a^{6/7}\right) + \theta_a \quad \text{(using stream values)} \quad (13a)$$

or

$$\theta_b = \frac{7K}{6}\left[\frac{1}{M_1(1+m^2)^3}\right]^{1/7}\left(x_b^{6/7}-x_a^{6/7}\right) + \theta_a \quad \text{(using wall values)} \quad (13b)$$

where x_a and x_b designate the start and the end, respectively, of the integration interval. The velocity-profile parameter is obtained from equation (4b) or by use of figure 2 and the ratios θ/δ and δ^*/δ from the value of N and tables I and II. The parameter N is taken as constant for the integration interval and is based on the average Reynolds number prevailing for the interval. For the case where an initial boundary layer exists at the start of the constant Mach number run, the effective value of x_a at the start is obtained by computing the distance required for development of the initial momentum thickness θ_a. The distance x_b is also measured from the apparent origin.

For the case of pressure gradient, equation (10) has the general solution

$$\delta = e^{-\int \varphi \frac{dM_1}{dx}\,dx}\left(K\int \frac{\Psi_{s,w}}{x^{1/7}}\, e^{\int \varphi \frac{dM_1}{dx}\,dx}\,\frac{dx}{dM_1}\,dM_1 + B\right) \quad (14)$$

where B is a constant of integration. Certain simplifications of the numerical work required for evaluation of equation (14) can be obtained if the stream Mach number variation under consideration is approximated, as shown in figure 3, so that dx/dM_1 and, in effect, $x^{1/7}$ are constant for a given surface interval. With M_a and M_b denoting the stream Mach numbers at the start and the end, respectively, of an interval and with the parameter N constant for the interval, equation (14) is approximated by

$$\delta_{M_b} = e^{-\int_{M_a}^{M_b} \varphi \, dM_1} \left(\frac{K \frac{dx}{dM_1}}{\bar{x}^{1/7}} \int_{M_a}^{M_b} \psi_{s,w} e^{\int_{M_a}^{M_1} \varphi \, dM_1} dM_1 + \delta_{M_a} \right)$$

or, in a form more convenient for the necessary numerical integrations,

$$\delta_{M_b} = e^{-\int_{1}^{M_b} \varphi \, dM_1} \frac{K \frac{dx}{dM}}{\bar{x}^{1/7}} \left(\int_{1}^{M_b} \psi_{s,w} e^{\int_{1}^{M_1} \varphi \, dM_1} dM_1 - \int_{1}^{M_a} \psi_{s,w} e^{\int_{1}^{M_1} \varphi \, dM_1} dM_1 \right) +$$

$$\delta_{M_a} e^{\int_{1}^{M_a} \varphi \, dM_1} e^{-\int_{1}^{M_b} \varphi \, dM} \qquad (15)$$

where $\bar{x}$ denotes the mean distance of the interval designated by M_a and M_b from the effective starting point of boundary-layer development. This starting point is obtained by use of equation (13). The assumption is made that δ_{M_a} or θ_{M_a} develops under action of a zero pressure gradient at the Mach number M_a. This assumption is consistent with the use of a flat-plate skin-friction relation for the case of pressure gradient. The action of pressure gradient is thus taken into account only in calculation of the boundary-layer quantities through equation (15). With subsonic flow, the Mach number for the lower limit of integration is chosen as 0.100.

The various quantities (designated $\underline{A}$ to $\underline{F}$) needed to obtain the variation of the boundary-layer thickness δ in two-dimensional flow using equation (15) have been obtained by means of punch-card equipment. These quantities are listed in tables IV to IX for $N = 5$, 7, 9, and 11 and for Mach numbers from 0.100 to 10. The following variations of equation (15) will be found convenient for computation of two-dimensional flows:

For favorable pressure gradients (dM_1/dx positive),

$$\delta_{M_b} = \underline{E}_{M_b} \frac{K \frac{dx}{dM_1}}{\overline{x}^{1/7}} \left[\left(\underline{A} \text{ or } \underline{B} \right)_{M_b} - \left(\underline{A} \text{ or } \underline{B} \right)_{M_a} \right] + \delta_{M_a} \underline{F}_{M_a} \underline{E}_{M_b} \qquad (15a)$$

where

$$\underline{A} \equiv \int_1^M \Psi_w \, e^{\int_1^{M_1} \varphi \, dM_1} \, dM_1 \qquad \text{(from table IV)}$$

$$\underline{B} \equiv \int_1^M \Psi_s \, e^{\int_1^{M_1} \varphi \, dM_1} \, dM_1 \qquad \text{(from table V)}$$

$$\underline{E} \equiv e^{-\int_1^M \varphi \, dM_1} \qquad \text{(from table VIII)}$$

$$F \equiv e^{\int_1^M \varphi \, dM_1} \qquad \text{(from table IX)}$$

For adverse pressure gradients (dM_1/dx negative),

$$\delta_{M_b} = \underline{F}_{M_b} \frac{K \frac{dx}{dM_1}}{\overline{x}^{1/7}} \left[\left(\underline{C} \text{ or } \underline{D} \right)_{M_b} - \left(\underline{C} \text{ or } \underline{D} \right)_{M_a} \right] + \delta_{M_a} \underline{E}_{M_a} \underline{F}_{M_b} \tag{15b}$$

where

$$\underline{C} \equiv \int_1^M \Psi_w \, e^{-\int_1^{M_1} \varphi \, dM_1} \, dM_1 \quad \text{(from table VI)}$$

$$\underline{D} \equiv \int_1^M \Psi_s \, e^{-\int_1^{M_1} \varphi \, dM_1} \, dM_1 \quad \text{(from table VII)}$$

For diverging radial boundary-layer flows, the momentum equation (equation (16), reference 10) can be written in the present notation as

$$\frac{d\theta}{dr} + \left[\frac{(2-M_1^2) + \frac{\delta^*}{\theta}}{M_1(1+m^2)} \frac{dM_1}{dr} + \frac{1}{r} \right] \theta = \frac{\rho_w}{\rho_1} \frac{\tau}{\rho_w u_1^2} \tag{16}$$

where r designates the distance from the apparent origin of the radial flow to the point in question. With the substitutions used in obtaining equation (10), equation (16) becomes

$$\frac{d\delta}{dr} + \left(\varphi \frac{dM_1}{dr} + \frac{1}{r} \right) \delta = \frac{K \Psi_{s,w}}{x^{1/7}} \tag{17a}$$

where x designates the effective distance from the start of the boundary-layer development in radial flow. As indicated in reference 10, the following variation of equation (17a) is convenient for converging radial flow:

$$\frac{d\delta}{dr_1} + \left(\varphi \frac{dM_1}{dr_1} + \frac{1}{r_1 - r_0}\right)\delta = \frac{K\Psi_{s,w}}{x^{1/7}} \tag{17b}$$

where

r_1 distance from start of integration interval to point in question

r_0 distance from start of integration interval to apparent sink in converging radial flow

With the approximations used for equation (13), the respective solutions of equations (17a) and (17b) are

$$\delta_{M_b} = e^{-\int_1^{M_b} \varphi \, dM_1} \frac{K \frac{dr}{dM_1} \frac{1}{r}}{r_b \bar{x}^{1/7}} \left(\int_1^{M_b} \Psi_{s,w} e^{\int_1^{M_1} \varphi \, dM_1} dM_1 - \int_1^{M_a} \Psi_{s,w} e^{\int_1^{M_1} \varphi \, dM_1} dM_1 \right) +$$

$$\delta_{M_a} \frac{r_a}{r_b} e^{\int_1^{M_a} \varphi \, dM_1} e^{-\int_1^{M_b} \varphi \, dM_1} \tag{18a}$$

and

$$\delta_{M_b} = e^{-\int_1^{M_b} \varphi \, dM_1} \left[\frac{K \frac{dr_1}{dM_1}(r_1 - r_0)}{(r_b - r_0)\bar{x}^{1/7}} \right] \left(\int_1^{M_b} \Psi_{s,w} e^{\int_1^{M_1} \varphi \, dM_1} dM_1 - \int_1^{M_a} \Psi_{s,w} e^{\int_1^{M_1} \varphi \, dM_1} dM_1 \right) +$$

$$\delta_{M_a} \frac{(r_a - r_0)}{(r_b - r_0)} e^{\int_1^{M_a} \varphi \, dM_1} e^{-\int_1^{M_b} \varphi \, dM_1} \tag{18b}$$

where

r mean distance of interval designated by M_a and M_b from apparent source in diverging radial flow

$(\overline{r_1-r_0})$ mean distance of interval designated by M_a and M_b to apparent sink in converging radial flow

Here also the assumption is made that θ_{M_a} develops under the action of a zero pressure gradient at M_a. With subsonic flow, the Mach number for the lower limit of integration is chosen as 0.100.

The following variations of equations (18a) and (18b) are convenient for computation of radial flows:

Subsonic flow under adverse pressure gradient (dM_1/dr negative):

$$\delta_{M_b} = \underline{F}_{M_b} \left\{ \frac{K \frac{dr}{dM_1} \frac{\bar{r}}{r_b}}{\bar{x}^{1/7}} \left[(\underline{C} \text{ or } \underline{D})_{M_b} - (\underline{C} \text{ or } \underline{D})_{M_a} \right] + \delta_{M_a} \frac{r_a}{r_b} \underline{E}_{M_a} \right\} \tag{19a}$$

Subsonic flow under favorable pressure gradient (dM_1/dr positive):

$$\delta_{M_b} = \underline{E}_{M_b} \left\{ \frac{K \frac{dr_1}{dM_1} (\overline{r_1-r_0})}{(r_b-r_0)\ \bar{x}^{1/7}} \left[(\underline{A} \text{ or } \underline{B})_{M_b} - (\underline{A} \text{ or } \underline{B})_{M_a} \right] + \delta_{M_a} \frac{(r_a-r_0)}{(r_b-r_0)} \underline{F}_{M_a} \right\} \tag{19b}$$

Supersonic flow under adverse pressure gradient (dM_1/dr_1 negative):

$$\delta_{M_b} = \underline{F}_{M_b} \left\{ \frac{K \frac{dr_1}{dM_1} (\overline{r_1-r_0})}{(r_b-r_0)\ \bar{x}^{1/7}} \left[(\underline{C} \text{ or } \underline{D})_{M_b} - (\underline{C} \text{ or } \underline{D})_{M_a} \right] + \delta_{M_a} \frac{(r_a-r_0)}{(r_b-r_0)} \underline{E}_{M_a} \right\} \tag{19c}$$

Supersonic flow under favorable pressure gradient (dM_1/dr positive):

$$\delta_{M_b} = \underline{E}_{M_b}\left\{\frac{K\,\frac{dr}{dM_1}\,\frac{\bar{r}}{\bar{x}^{1/7}}}{r_b}\left[(\underline{A}\text{ or }\underline{B})_{M_b} - (\underline{A}\text{ or }\underline{B})_{M_a}\right] + \delta_{M_a}\frac{r_a}{r_b}\underline{F}_{M_a}\right\} \qquad (19d)$$

Divergent or convergent flow fields may be regarded as radial flows for which the position of the apparent source or sink is variable. For the boundary-layer calculations, this continuous variation may be approximated as a stepwise variation such as shown in figure 4. The distances r, r_1, and r_0 are determined from the geometry of the flow field under consideration, as indicated in figure 4.

The approximate development of a turbulent boundary layer can be obtained from the preceding analysis. For two-dimensional flow, equations (15a) and (15b) are used for favorable and adverse pressure gradients, respectively, to obtain the variation of the boundary-layer thickness δ along the surface under consideration. Equations (19a) to (19d) are used to obtain corresponding results for radial flow. The various quantities needed to evaluate these equations are listed in tables IV to IX. Equation (13) is applicable to the case of zero pressure gradient. With the variation of the boundary-layer thickness δ along the surface thus known, the local values of momentum thickness θ and of displacement thickness δ^* are calculated from the ratios f and g of tables I and II, respectively, because the Mach number is known and appropriate values of the parameter N can be obtained from equation (4b). Linear interpolation for M and N is within the accuracy of the various approximations. The constant K may be written

$$K = 0.0218\left(\frac{\mu_0\sqrt{T_0}}{p_0}\right)^{1/7} \qquad (20)$$

provided that the coefficient of viscosity, temperature, and pressure are assigned the following units, respectively: slugs per foot-second, $^{\circ}R$, and pounds per square foot. All distances must then be expressed in feet and the boundary-layer quantities obtained will be given in feet.

APPLICATION TO SUPERSONIC-TUNNEL CONTOUR CORRECTION

Analytical and graphical procedures (references 11 and 12) based on the method of characteristics are available for the design of two-dimensional supersonic nozzles with potential flow. The effect of the wall boundary layers on the performance of such nozzles must be considered, however, if shock-free flow at the desired Mach number is to be obtained. The assumption is customarily made that effects of boundary-layer growth on the flow can be accounted for by a correction of the potential-flow nozzle contours. The preceding analysis is directly applicable to the contour-correction problem.

Displacement-Thickness Contour Correction

The displacement thickness δ^* is generally considered as the proper criterion for correction of supersonic-tunnel contours in that the continuity of mass-flow requirement is thereby satisfied. This basis for selection of δ^* will be reviewed. Contours of the potential-flow nozzle and of the corrected nozzle are designated by AA' and BB', respectively, in figure 5. The contour correction at any nozzle station is represented by the quantity e. The boundary layer is contained between contours BB' and CC'. The line DC' represents a potential-flow streamline that is tangent to the boundary layer at C'. The mass flow in a two-dimensional boundary layer is obtained from the defining equation for δ^* as

$$\int_0^{\delta} \rho u \, dy = \rho_1 u_1 (\delta - \delta^*) \tag{21}$$

From the continuity equation and equation (21),

$$(\rho_1 u_1)_t \, (DC + \delta_t - \delta_t^*) = (\rho_1 u_1)_e \, (\delta_e - \delta_e^*)$$

where subscripts t and e designate the throat and nozzle-exit stations, respectively. The quantity $\frac{(\rho_1 u_1)_t}{(\rho_1 u_1)_e} \equiv A$ represents the the one-dimensional area ratio corresponding to the Mach number of the potential flow at O'C'; thus,

$$DC + \delta_t = \frac{1}{A}(\delta_e - \delta_e^*) + \delta_t^* \tag{22}$$

With the area ratio also given by $A = \frac{Y_e - \delta_e}{Y_t - (DC + \delta_t)}$, the quantity A, through use of equation (22), may be written

$$A = \frac{Y_e - \delta_e^*}{Y_t - \delta_t^*} \tag{23}$$

If the exit Mach numbers of the initial potential-flow contour nozzle and of the flow bounded by streamlines DC' and OO' are to be equal,

$$A = \frac{Y_e - e_e}{Y_t - e_t}$$

Thus,

$$\frac{Y_e - e_e}{Y_t - e_t} = \frac{Y_e - \delta_e^*}{Y_t - \delta_t^*} \tag{24}$$

Equation (24) is obviously satisfied by the requirement that $e_e = \delta_e^*$ and that $e_t = \delta_t^*$. With the additional assumption that $e = \delta^*$ throughout the nozzle, consistent with the neglect of curvature effects, the displacement-thickness contour-correction method then consists of "opening" each wall of the potential-flow nozzle by the displacement thickness δ^* applicable to each station.

Puckett suggests in reference 13 that an approximation to the contour-correction method just described may be obtained by adding the displacement-thickness cross-sectional area at the nozzle exit to the potential-flow nozzle-exit area and then designing the nozzle contour by the method of characteristics for the higher Mach number thus obtained. Reference 13 also contains a method for estimating the thickness of a turbulent boundary layer at the outlet of a supersonic nozzle. This method is briefly discussed in appendix B.

Reflection-Thickness Contour Correction

The contour-correction methods just described take into account the change in mass flow due to frictional retardation and thereby

satisfy one of the requirements for a contour correction - that flow should be obtained at the desired Mach number. It is not obvious that these methods will satisfy the second requirement; namely, that the flow in the test section should be free of expansion waves and shock waves.

Consideration of the basic process of supersonic-nozzle design, that is, cancellation of the Mach waves set up through expansive turning of the walls in the forepart of the nozzle by compressive turning of the walls in the straightening portion of the nozzle, indicates that a method of contour correction should logically be based on interaction of the Mach waves and the boundary layer. Certain simplifying assumptions are required to make the Mach wave boundary-layer interaction amenable to analysis. Suppose that the interaction is idealized by assuming that the curvature of a Mach wave penetrating the boundary layer is entirely due to the extension of the wave into a region of variable Mach number and that the Mach wave reflection from the sonic line is a solid-boundary reflection, the sonic line remaining undeformed. This assumption of a solid boundary reflection is compatible with the results obtained by Tsien and Finston in reference 14. The turbulent state of the boundary-layer flow enters the analysis only to the extent that the mean velocity profiles assumed determine the Mach wave curvature and the thickness of the subsonic portion of the boundary layer. Changes in local Mach number resulting from the wave penetration and dissipation effects are considered negligible. The interaction under these assumptions is schematically represented in figure 6 and results in the Mach wave being apparently reflected from point B. Point A is the reflection point for potential flow. The Mach wave boundary-layer interaction is further considered in appendix C. In this treatment the boundary layer is regarded as a discontinuous rotational flow field. The results of this analysis indicate a general agreement with the preceding simplified picture.

The reflection thickness ratio λ/δ is given by

$$\frac{\lambda}{\delta} = 1 - \frac{x_B}{\delta\sqrt{M_1^2-1}} \tag{25}$$

where x_B, λ are the coordinates of the reflection point B of figure 6. The differential equation for the deflection path of the incident wave from which x_B is obtained is

$$\frac{dz}{dx} = -\frac{1}{\delta\sqrt{M^2-1}} \tag{26}$$

For a given velocity-profile parameter N, the quantity $z \equiv y/\delta$ is readily obtainable in terms of the applicable boundary-layer Mach number from the assumption that the energy equation

$c_p t + \frac{u^2}{2} = \text{constant}$ holds for the boundary layer. Formal integration of equation (26) and substitution into equation (25) give the following expression for the reflection-thickness ratio:

$$\frac{\lambda}{\delta} = 1 - N\left(\frac{5+M_1^2}{5M_1^2}\right)^{N/2}\left(\frac{1}{M_1^2-1}\right)^{1/2}\int_1^{M_1}\frac{M^{N-1}(M^2-1)^{1/2}\,dM}{\left(1+\frac{M^2}{5}\right)^{\frac{N+2}{2}}} \qquad (27)$$

Equation (27) has been numerically integrated for values of velocity-profile parameter N of 5, 7, 9, and 11. The reflection-thickness ratio λ/δ for Mach numbers from 1 to 10 are listed in table X. The contour correction using λ/δ is applied in the same manner as the displacement-thickness method and consists in opening each wall of the potential-flow nozzle by the value of λ applicable to each station.

DISCUSSION

Boundary-Layer Development

A discussion of the effect on the boundary-layer development of the various parameters entering into the analysis may prove helpful in the applications thereof. Inasmuch as K is the only quantity that depends on the pressure and the temperature, equation (20) indicates that the development is not critically dependent on these parameters. The manner in which such chosen quantities as the velocity profile and skin-friction relations affect the development is not immediately apparent and may be best indicated by numerical computation.

Calculations of the boundary-layer development in two typical supersonic nozzles (one at a Mach number of 2.08, the other at a Mach number of 7.00) were made using equation (15a) with wall density and kinematic viscosity. The results are summarized in table XI and indicate that the momentum thickness θ is not appreciably affected by comparatively large changes in the profile parameter N. The parameter N enters into equation (5), which

provides the basis for the analysis, only through the ratio $H \equiv \delta^*/\theta$. As shown in table III, the ratio H is relatively insensitive to changes in N so that a small effect of N on θ might be expected. The variation of δ^* listed in table XI with changes in N is a consequence of the insensitivity of H to this parameter.

In view of the preceding discussion, it appears that for a given pressure distribution the proper selection of a skin-friction relation is the decisive factor in the determination of the boundary-layer quantities δ, δ^*, and θ. The effect of the skin-friction relations of equations (1a) and (1b) on the boundary-layer development is shown in figure 7 for the curved wall or contour plate of a Mach number 2.08 supersonic tunnel with a contour plate width of 3.84 inches and test-section dimensions of 3.84 by 10 inches. The boundary-layer momentum thickness θ at the throat was chosen to correspond with the experimental data, which are plotted in figure 7 for comparison. For these calculations, the flow along the contour plate was assumed to be two dimensional and equations (15a) and (13) were used for the nozzle and the test section, respectively. Use of the skin-friction relation of equation (1a), which is based upon stream values of density and kinematic viscosity, leads to excessively high values for the important boundary-layer quantities δ^* and θ; whereas use of equation (1b), which is based on wall values of density and kinematic viscosity, offers a relatively good check with experiment. The experimental boundary-layer development along the center line of the flat side plate is compared in figure 8 with the calculated development using the skin-friction relation of equation (1b), which involves wall density and kinematic viscosity. The side-plate nozzle flow was approximated as a stepwise distribution of radial divergent flows and equations (19d) and (13) were used for the nozzle and the test section, respectively. An absolute stagnation temperature of 590° R and absolute stagnation pressures of 37 and 29 inches of mercury were used in the contour-plate and side-plate calculations, respectively, consistent with the experimental values.

It should be noted that the presence of some secondary flows in the nozzle section was indicated by pressure distributions observed along the contour plate transverse to the stream direction and that the test-section flow is traversed by shock waves that originate at the start of the test section, that is, at the 38.3-inch station. The shock waves from each contour plate meet along the side-plate center line at about the 46-inch station. The secondary flows in the nozzle section are probably caused by the proximity of the side plates. The shock waves would have the effect of increasing the momentum and displacement thicknesses (fig. 30, reference 15) and of setting up additional secondary flows. The lack of data

makes it difficult to estimate the effect of the secondary flows on the boundary-layer development. It appears reasonable to suppose that if the potential-flow conditions postulated are obtained the accuracy of the calculated development would come between the limits indicated by figures 7 and 8.

CONTOUR-CORRECTION METHODS

The variation of the reflection-thickness ratio λ/δ with stream Mach number for the velocity profile $\frac{u}{u_1} = \left(\frac{y}{\delta}\right)^{1/7}$ is shown in figure 9. Use of the assumption that the sonic line remains undeformed by impingement of the Mach wave accounts for the relatively sharp increase in the value of λ/δ as the stream Mach number approaches unity. This assumption is probably invalid at the low supersonic stream Mach numbers where the boundary layer consists for the most part of subsonic flow. The variation of displacement-thickness ratio δ^*/δ with stream Mach number for the same velocity profile is also plotted in figure 9 for comparison.

Use of δ^* as the correction criterion satisfies, within the accuracy of the present boundary-layer analysis, the requirement that the flow be obtained at the desired Mach number. Inasmuch as a proper criterion for contour correction must in addition satisfy the requirement that the flow be free of expansion waves and shock waves, the comparison shown in figure 9 might have been expected to show an approximate equivalence of δ^*/δ and λ/δ for at least the higher Mach numbers. In the absence of a rigorous calculation for λ/δ and δ^*/δ, the choice of contour-correction method would appear to remain an open question.

CONCLUDING REMARKS

With the tabulations presented herein, the approximate development of a turbulent boundary layer in plane shock-free flow along a thermally insulated surface under arbitrary pressure gradient variation may be obtained through routine arithmetic computation. The agreement between the results of such computations and the experimental data obtained in a supersonic tunnel at a nominal Mach number of 2 suggests that Falkner's empirical skin-friction relation for low speeds may be applicable to high Mach number flows under favorable and zero pressure gradients and possibly even very moderate adverse gradients provided the extrapolation method of the

present analysis is used; that is, provided that the local skin-friction coefficients depend primarily on Reynolds number when density and kinematic viscosity are evaluated at surface or wall conditions. It does not appear likely that the assumptions employed in the analysis will remain valid at the very high Mach numbers. The tabulations were extended to a Mach number of 10 primarily as a means of obtaining at least a first approximation to the boundary-layer development. Further experimental checks - particularly at Mach numbers considerably greater than 2 - are desirable.

The boundary-layer analysis presented is directly applicable to the problem of supersonic-tunnel contour correction and permits use of a correction method based upon the continuity of mass flow requirement (displacement-thickness method) or on the requirement that the test-section flow be free of expansion waves and shock waves (reflection-thickness method). Although it is impossible to decide, a priori, which method is most appropriate in principle, it appears advisable at present to use the displacement-thickness method in view of the drastic simplifying assumptions required for the reflection-thickness method.

Lewis Flight Propulsion Laboratory,
National Advisory Committee for Aeronautics,
Cleveland, Ohio, July 14, 1949.

APPENDIX A

SYMBOLS

The following symbols are used in this report:

A nozzle-area ratio

a_0 speed of sound based on stagnation temperature

c_f local skin-friction coefficient, $\frac{\tau}{\rho_1 u_1^2}$

e_e nozzle contour correction at nozzle exit

e_t nozzle contour correction at throat

f ratio of momentum thickness to boundary-layer thickness, θ/δ

g ratio of displacement thickness to boundary-layer thickness, δ^*/δ

H boundary-layer-shape parameter, $\frac{\delta^*}{\theta} = \frac{g}{f}$

j effective thickness of stream tube (used in appendix C)

K constant based on stagnation conditions, $0.0131\left(\frac{\mu_0}{\rho_0 a_0}\right)^{1/7}$ (See also equation (20).)

k "universal" constant used in Kármán logarithmic velocity-profile relation (references 6 and 7)

M Mach number in boundary layer

M_1 Mach number at outer edge of boundary layer

m^2 Mach number parameter, $m^2 \equiv \frac{\gamma-1}{2} M_1^2 = \frac{M_1^2}{5}$

N velocity-profile parameter, $\frac{u}{u_1} = z^{1/N}$

P_0 tunnel-inlet stagnation pressure

R_s stream Reynolds number, $\frac{\rho_1 u_1 x}{\mu_1}$

R_w wall Reynolds number, $\frac{\rho_w u_1 x}{\mu_w} = \frac{\rho_w u_1 x}{\mu_0}$

r radial distance of line of constant Mach number from apparent source in diverging radial flow

r_0 radial distance from start of integration to apparent sink in converging radial flow

r_1 radial distance of line of constant Mach number from start of integration to point in question for converging radial flow

s variable of integration

T_0 absolute stagnation temperature

t absolute static temperature in boundary layer

t_1 absolute static temperature at outer edge of boundary layer

u velocity in boundary layer

u_1 velocity at outer edge of boundary layer

x distance along surface measured from effective start of boundary-layer development

$\bar{x}$ mean distance of surface interval from effective start of boundary-layer development

x_B coordinate (abscissa) of effective wave reflection point measured in streamwise direction from penetration point of incident wave

y normal distance from surface

$2Y_e$ nozzle-exit ordinate

$2Y_t$ nozzle-throat ordinate

z normal distance parameter, y/δ

γ ratio of specific heats, 1.40

δ nominal boundary-layer thickness, distance from surface to point in boundary layer where velocity is approximately equal to stream velocity

δ^* boundary-layer displacement thickness, $\frac{1}{\rho_1 u_1}\int_0^\delta (\rho_1 u_1 - \rho u)dy$

θ boundary-layer momentum thickness, $\frac{1}{\rho_1 u_1^2}\int_0^\delta \rho u(u_1 - u)dy$

λ coordinate (ordinate) of effective wave reflection point measured from bounding surface

μ_w coefficient of viscosity based on wall temperature

μ_0 coefficient of viscosity based on stagnation temperature

μ_1 coefficient of viscosity based on stream static temperature

ν_w wall kinematic viscosity, μ_w/ρ_w

ν_1 stream kinematic viscosity at outer edge of boundary layer, μ_1/ρ_1

ρ density in boundary layer

ρ_w density at wall or bounding surface

ρ_0 stagnation density

ρ_1 density at outer edge of boundary layer

τ local skin-friction stress

φ coefficient defined by equation (11)

Ψ_s friction parameter, $\dfrac{(1+m^2)^{2/7}}{fM_1^{1/7}}$

Ψ_w friction parameter, $\dfrac{1}{(1+m^2)^{3/7} fM_1^{1/7}}$

APPENDIX B

APPROXIMATE DETERMINATION OF BOUNDARY-LAYER DEVELOPMENT

In many instances a comparatively rapid method of estimating the boundary-layer quantities at the exit of a supersonic nozzle is of value during the initial design stage. The method devised by Puckett in reference 13 is especially adapted for such a purpose. In applying the momentum equation to obtain δ at the nozzle exit, Puckett assumes that the boundary-layer velocity profile is linear and that the variation of stream Mach number along the nozzle contour is also linear. The local skin-friction coefficient is taken as constant, being evaluated for stream conditions at the nozzle exit and the boundary-layer thickness at the nozzle throat is neglected. The integration interval extends from the nozzle throat to the nozzle exit. In order to obtain δ^* from δ, the ratio δ^*/δ evaluated for the profile $\frac{u}{u_1} = \left(\frac{y}{\delta}\right)^{1/7}$ is apparently used. This procedure results in a serious underestimation of the boundary-layer quantities when applied to the experimental data of this report; whereas consistent use of the linear boundary-layer velocity profile, that is, in obtaining δ^*/δ and in solving for δ, yields much better agreement.

The basic procedure of reference 13 may be followed using the tabulations of this report by reducing the number of integration intervals. The use of a single integration interval for the nozzle with the assumption of a linear variation of Mach number along the nozzle contour will generally lead to an underestimation of the boundary-layer values. A minimum of two integration intervals is suggested for the nozzle section. The Mach number variation along the contour might be approximated by the following elliptic distribution in the event that the exact distribution is unavailable:

$$M_{l_i}^2 = M_e^2 \left[1 - \left(\frac{l_i}{l} - 1\right)^2 \left(1 - \frac{1}{M_e^2}\right)\right] \qquad \text{(B1)}$$

where

M_{l_i} stream Mach number at distance l_i

x_1 distance from nozzle throat

l length of nozzle section

M_e test-section Mach number

The use of a single integration interval with a linear contour distribution of Mach number is probably adequate for the portion of the tunnel upstream of the throat. The velocity-profile parameters to use are obtained from equation (4b).

APPENDIX C

CHARACTERISTICS ANALYSIS OF MACH WAVE BOUNDARY-LAYER INTERACTION

The Mach wave boundary-layer interaction may also be analyzed through use of the method of characteristics. The boundary-layer region is regarded as a discontinuous medium composed of parallel stream tubes with the flow in each tube irrotational. The static pressure in the boundary layer upstream of the initial incident wave is assumed constant for all stream tubes.

For ease in computation, the effective thickness of each stream tube constituting the supersonic portion of the boundary layer is so chosen that the product j of the actual thickness and of the local value of $\sqrt{\bar{M}^2-1}$ is constant for all stream tubes, $\bar{M}$ designating the Mach number representative of the stream tube under consideration. Such spacing insures wave intersections at desired intervals, as schematically shown in figure 10.

I. Irving Pinkel of the Lewis laboratory has shown that the following relations apply if no discontinuity in pressure is to exist across the plane separating two stream tubes downstream of a wave interaction, such as DG, EH, and so forth, of figure 10:

$$\left.\begin{aligned} \Delta\alpha_t &= \frac{\Delta\alpha_i}{w} \\ \Delta\alpha_r &= \Delta\alpha_i \left(1 - \frac{1}{w}\right) \end{aligned}\right\} \qquad (C1)$$

where

$\Delta\alpha_i$ flow deviation produced by characteristic incident on plane of separation

$\Delta\alpha_t$ flow deviation produced by characteristic transmitted through plane of separation

$\Delta\alpha_r$ flow deviation produced by characteristic reflected from plane of separation

$w \equiv \frac{1}{2}\left(\frac{b_2}{b_1} + 1\right)$ if, for example, the characteristic AB is incident at B (fig. 10)

$\equiv \frac{1}{2}\left(\frac{b_1}{b_2} + 1\right)$ if, for example, the characteristic CE is incident at E (fig. 10)

$b \equiv \frac{\rho u^2}{\sqrt{\bar{M}^2-1}}$, pressure index

With a selected velocity profile and an assumed strength (flow deviation) of the Mach wave impinging on the boundary layer, equations (C1) can be used to determine the two sets of characteristics throughout the simulated boundary layer. The Mach number representative of each stream tube is assumed to be unchanged by the interactions. In the numerical example considered, the stream Mach number was taken as 2.44 and the profile $u/u_1 = z^{1/5}$ was chosen. Under these conditions the subsonic portion of the boundary layer represents 5.2 percent of the total thickness δ. The quantity $z\sqrt{M^2-1}$ from $M = 1$ to $M = 2.44$ was divided into 25 equal intervals and average values of the pressure index b corresponding to each interval were determined. Application of equations (C1), which are based upon linearized theory, becomes questionable when the Mach number $\bar{M}$ of the stream tube approaches the sonic value so that the index b approaches infinity. For the present case, the value of the index b was arbitrarily taken as 100 times the value obtained for the next adjacent stream tube. The strengths of the characteristics entering the potential flow from the boundary-layer region as determined from the analysis are listed in table XII for an incident compression Mach wave of unit strength. Compression and expansion waves are denoted by positive and negative signs, respectively. The location number represents the distance of the secondary waves from the primary incident wave measured in intervals of the quantity $2j\sqrt{M_1^2-1}$. The strengths of the secondary waves are inappreciable relative to the primary incident wave strength except for the wave at location number 24. The interaction represented by the data in table XII is in general agreement with the interaction shown in figure 6 in that the wave at location 24 has about the same strength and sign as the original incident wave. It is of interest to note the attenuation of wave

strength downstream of location 24. On the basis of some preliminary computations, it would appear that no physical significance can be attached to the oscillatory nature of these secondary waves, inasmuch as the use of 24 intervals rather than 25 gave rise to secondary compression waves having approximately the same strength as would be obtained by grouping the wave strengths of table XII as follows: 25 and 26, 27 and 28, 29 and 30, and so forth.

REFERENCES

1. Goldstein, Sidney: Modern Developments in Fluid Dynamics. Vol. I. Clarendon Press (Oxford), 1938, pp. 131-134.

2. Tetervin, Neal: Approximate Formulas for the Computation of Turbulent Boundary-Layer Momentum Thicknesses in Compressible Flows. NACA ACR L6A22, 1946.

3. Falkner, V. M.: A New Law for Calculating Drag. Aircraft Eng., vol. XV, no. 169, March 1943, pp. 65-69.

4. von Kármán, Th., and Tsien, H. S.: Boundary Layer in Compressible Fluids. Jour. Aero. Sci., vol. 5, no. 6, April 1938, pp. 227-232.

5. Lowdermilk, Warren H., and Grele, Milton D.: Heat Transfer from High-Temperature Surfaces to Fluids. II - Correlation of Heat-Transfer and Friction Data for Air Flowing in Inconel Tube with Rounded Entrance. NACA RM E8L03, 1949.

6. de Kármán, Th.: The Problem of Resistance in Compressible Fluids. Quinto Convegno "Volta", Reale Accademia d'Italia (Roma), Sett. 30-Ott. 6, 1935, pp. 3-57.

7. Dryden, Hugh L.: Air Flow in the Boundary Layer near a Plate. NACA Rep. 562, 1936.

8. Gurjienko, G.: Universal Logarithmic Law of Velocity Distribution as Applied to the Investigation of Boundary Layer and Drag of Streamline Bodies at Large Reynolds Numbers. NACA TM 842, 1937.

9. Garner, H. C.: The Development of Turbulent Boundary Layers. R. & M. No. 2133, British A.R.C., June 1944.

10. Tetervin, Neal: Boundary-Layer Momentum Equations for Three-Dimensional Flow. NACA TN 1479, 1947.

11. Pinkel, I. Irving: Equations for the Design of Two-Dimensional Supersonic Nozzles. NACA Rep. 907, 1948.

12. Puckett, A. E.: Supersonic Nozzle Design. Jour. Appl. Mech., vol. 13, no. 4, Dec. 1946, pp. A265-A270.

13. Puckett, Allen E.: Final Report on the Model Supersonic Wind Tunnel Project. OSRD No. 3569, Armor and Ordnance Rep. No. A-269, NDRC, April 30, 1944.

14. Tsien, H. S., and Finston, M.: Interaction between Parallel Streams of Subsonic and Supersonic Velocities. Jour. Aero. Sci., vol. 16, no. 9, Sept. 1949, pp. 515-528.

15. Ackeret, J., Feldmann, F., and Rott, N.: Investigations of Compression Shocks and Boundary Layers in Gases Moving at High Speed. NACA TM 1113, 1947.

TABLE I - VARIATION OF MOMENTUM-THICKNESS RATIO f WITH MACH NUMBER M AND VELOCITY-PROFILE PARAMETER N

$$\left[f = \frac{\theta}{\delta}\right]$$

(a) Subsonic flow

Mach number M	Velocity-profile parameter, N			
	5	7	9	11
0.100	0.11894	0.09715	0.08176	0.07460
.200	.11865	.09695	.08162	.07448
.300	.11816	.09662	.08138	.07427
.400	.11748	.09616	.08105	.07398
.500	.11663	.09557	.08063	.07361
.600	.11560	.09487	.08012	.07317
.700	.11442	.09406	.07953	.07266
.800	.11309	.09315	.07887	.07208
.900	.11162	.09214	.07813	.07144
1.000	.11004	.09104	.07735	.07074

TABLE I - VARIATION OF MOMENTUM-THICKNESS RATIO f WITH MACH NUMBER M AND VELOCITY-PROFILE PARAMETER N - Continued

$$\left[f = \frac{\theta}{\delta}\right]$$

(b) Supersonic flow

Mach number	Velocity-profile parameter, N				Mach number	Velocity-profile parameter, N			
M	5	7	9	11	M	5	7	9	11
1.00	0.11004	0.09104	0.07733	0.06711	3.40	0.06441	0.05708	0.05107	0.04617
1.04	.10938	.09058	.07699	.06685	3.44	.06377	.05657	.05066	.04582
1.08	.10870	.09010	.07664	.06658	3.48	.06314	.05607	.05024	.04548
1.12	.10801	.08962	.07628	.06631	3.52	.06251	.05557	.04984	.04514
1.16	.10730	.08912	.07592	.06603	3.56	.06189	.05507	.04943	.04480
1.20	.10658	.08862	.07555	.06574	3.60	.06128	.05458	.04903	.04447
1.24	.10585	.08810	.07516	.06545	3.64	.06067	.05410	.04863	.04413
1.28	.10511	.08758	.07478	.06515	3.68	.06007	.05361	.04823	.04380
1.32	.10435	.08704	.07438	.06485	3.72	.05948	.05314	.04784	.04347
1.36	.10359	.08650	.07398	.06454	3.76	.05889	.05266	.04745	.04314
1.40	.10281	.08595	.07357	.06422	3.80	.05832	.05219	.04706	.04282
1.44	.10203	.08540	.07315	.06390	3.84	.05774	.05173	.04668	.04250
1.48	.10124	.08483	.07273	.06357	3.88	.05718	.05127	.04630	.04217
1.52	.10045	.08427	.07231	.06324	3.92	.05662	.05082	.04592	.04186
1.56	.09965	.08369	.07188	.06291	3.96	.05606	.05037	.04555	.04154
1.60	.09884	.08311	.07144	.06257	4.00	.05551	.04992	.04518	.04123
1.64	.09803	.08253	.07100	.06223	4.04	.05497	.04948	.04481	.04092
1.68	.09721	.08194	.07056	.06188	4.08	.05444	.04904	.04445	.04061
1.72	.09640	.08135	.07011	.06153	4.12	.05391	.04861	.04409	.04030
1.76	.09557	.08075	.06966	.06118	4.16	.05339	.04818	.04373	.04000
1.80	.09475	.08016	.06921	.06083	4.20	.05287	.04775	.04337	.03969
1.84	.09393	.07956	.06875	.06047	4.24	.05236	.04733	.04302	.03939
1.88	.09310	.07895	.06830	.06011	4.28	.05186	.04692	.04267	.03910
1.92	.09228	.07835	.06784	.05974	4.32	.05136	.04651	.04233	.03880
1.96	.09145	.07774	.06737	.05938	4.36	.05087	.04610	.04198	.03851
2.00	.09063	.07714	.06691	.05901	4.40	.05038	.04570	.04164	.03822
2.04	.08980	.07653	.06644	.05864	4.44	.04990	.04530	.04131	.03793
2.08	.08898	.07592	.06598	.05827	4.48	.04942	.04490	.04098	.03765
2.12	.08816	.07532	.06551	.05790	4.52	.04895	.04451	.04065	.03736
2.16	.08734	.07471	.06504	.05753	4.56	.04849	.04412	.04032	.03708
2.20	.08653	.07410	.06457	.05716	4.60	.04803	.04374	.03999	.03680
2.24	.08572	.07350	.06410	.05678	4.64	.04758	.04336	.03967	.03653
2.28	.08491	.07289	.06364	.05641	4.68	.04713	.04299	.03936	.03626
2.32	.08410	.07229	.06317	.05603	4.72	.04669	.04262	.03904	.03598
2.36	.08330	.07168	.06270	.05566	4.76	.04625	.04225	.03873	.03571
2.40	.08250	.07108	.06223	.05528	4.80	.04582	.04189	.03842	.03545
2.44	.08171	.07049	.06176	.05491	4.84	.04539	.04153	.03811	.03518
2.48	.08092	.06989	.06130	.05453	4.88	.04497	.04117	.03781	.03492
2.52	.08014	.06930	.06083	.05416	4.92	.04455	.04082	.03751	.03466
2.56	.07936	.06870	.06037	.05378	4.96	.04414	.04047	.03721	.03440
2.60	.07859	.06812	.05990	.05341	5.00	.04373	.04013	.03692	.03415
2.64	.07782	.06753	.05944	.05304	5.04	.04333	.03979	.03663	.03389
2.68	.07706	.06695	.05898	.05266	5.08	.04293	.03945	.03634	.03364
2.72	.07630	.06637	.05852	.05229	5.12	.04254	.03912	.03605	.03339
2.76	.07555	.06579	.05807	.05192	5.16	.04215	.03879	.03577	.03315
2.80	.07480	.06522	.05761	.05155	5.20	.04177	.03846	.03549	.03290
2.84	.07407	.06465	.05716	.05118	5.24	.04139	.03814	.03521	.03266
2.88	.07333	.06408	.05671	.05081	5.28	.04102	.03782	.03493	.03242
2.92	.07261	.06352	.05626	.05044	5.32	.04065	.03751	.03466	.03218
2.96	.07189	.06296	.05581	.05008	5.36	.04028	.03719	.03439	.03194
3.00	.07117	.06240	.05537	.04972	5.40	.03992	.03688	.03412	.03171
3.04	.07047	.06185	.05493	.04935	5.44	.03956	.03658	.03386	.03148
3.08	.06977	.06131	.05449	.04899	5.48	.03921	.03628	.03359	.03125
3.12	.06907	.06076	.05405	.04863	5.52	.03886	.03598	.03334	.03102
3.16	.06839	.06022	.05362	.04828	5.56	.03852	.03568	.03308	.03079
3.20	.06771	.05969	.05318	.04792	5.60	.03818	.03539	.03282	.03057
3.24	.06703	.05916	.05276	.04757	5.64	.03784	.03510	.03257	.03035
3.28	.06637	.05863	.05233	.04721	5.68	.03751	.03481	.03232	.03013
3.32	.06571	.05811	.05191	.04686	5.72	.03718	.03453	.03207	.02991
3.36	.06505	.05759	.05149	.04651	5.76	.03686	.03425	.03183	.02970

TABLE I - VARIATION OF MOMENTUM-THICKNESS RATIO f WITH MACH NUMBER M AND VELOCITY-PROFILE PARAMETER N - Concluded

$\left[f = \frac{\theta}{\delta}\right]$

(b) Supersonic flow - Concluded

Mach number	Velocity-profile parameter, N				Mach number	Velocity-profile parameter, N			
M	5	7	9	11	M	5	7	9	11
5.80	0.03653	0.03397	0.03159	0.02948	8.20	0.02264	0.02164	0.02060	0.01961
5.84	.03622	.03369	.03135	.02927	8.24	.02248	.02149	.02046	.01948
5.88	.03590	.03342	.03111	.02906	8.28	.02232	.02134	.02033	.01936
5.92	.03559	.03315	.03087	.02885	8.32	.02216	.02120	.02019	.01924
5.96	.03529	.03289	.03064	.02865	8.36	.02200	.02105	.02006	.01912
6.00	.03499	.03262	.03041	.02844	8.40	.02184	.02091	.01993	.01900
6.04	.03469	.03236	.03016	.02824	8.44	.02168	.02077	.01980	.01888
6.08	.03439	.03210	.02995	.02804	8.48	.02153	.02063	.01967	.01876
6.12	.03410	.03185	.02973	.02784	8.52	.02138	.02049	.01954	.01865
6.16	.03381	.03160	.02951	.02764	8.56	.02123	.02035	.01942	.01853
6.20	.03352	.03135	.02929	.02745	8.60	.02108	.02021	.01929	.01841
6.24	.03324	.03110	.02907	.02725	8.64	.02093	.02008	.01917	.01830
6.28	.03296	.03086	.02885	.02706	8.68	.02078	.01994	.01905	.01819
6.32	.03269	.03061	.02864	.02687	8.72	.02064	.01981	.01892	.01808
6.36	.03241	.03037	.02843	.02668	8.76	.02050	.01968	.01880	.01796
6.40	.03214	.03014	.02822	.02649	8.80	.02035	.01955	.01868	.01785
6.44	.03188	.02990	.02801	.02631	8.84	.02021	.01942	.01857	.01774
6.48	.03161	.02967	.02781	.02613	8.88	.02007	.01929	.01845	.01764
6.52	.03135	.02944	.02760	.02594	8.92	.01994	.01916	.01833	.01753
6.56	.03110	.02921	.02740	.02576	8.96	.01980	.01904	.01822	.01742
6.60	.03084	.02899	.02720	.02559	9.00	.01966	.01891	.01810	.01732
6.64	.03059	.02877	.02700	.02541	9.04	.01953	.01879	.01799	.01721
6.68	.03034	.02855	.02681	.02523	9.08	.01940	.01867	.01788	.01711
6.72	.03009	.02833	.02661	.02506	9.12	.01927	.01855	.01776	.01701
6.76	.02985	.02811	.02642	.02489	9.16	.01914	.01843	.01765	.01690
6.80	.02961	.02790	.02623	.02472	9.20	.01901	.01831	.01754	.01680
6.84	.02937	.02769	.02604	.02455	9.24	.01888	.01819	.01744	.01670
6.88	.02914	.02748	.02586	.02438	9.28	.01875	.01807	.01733	.01660
6.92	.02890	.02727	.02567	.02421	9.32	.01863	.01796	.01722	.01650
6.96	.02867	.02707	.02549	.02405	9.36	.01850	.01784	.01711	.01641
7.00	.02844	.02686	.02531	.02389	9.40	.01838	.01773	.01701	.01631
7.04	.02822	.02666	.02513	.02372	9.44	.01826	.01762	.01691	.01621
7.08	.02800	.02646	.02495	.02356	9.48	.01814	.01750	.01680	.01612
7.12	.02778	.02627	.02478	.02341	9.52	.01802	.01739	.01670	.01602
7.16	.02756	.02607	.02460	.02325	9.56	.01790	.01728	.01660	.01593
7.20	.02734	.02588	.02443	.02309	9.60	.01778	.01717	.01650	.01583
7.24	.02713	.02569	.02426	.02294	9.64	.01767	.01707	.01640	.01574
7.28	.02692	.02550	.02409	.02278	9.68	.01755	.01696	.01630	.01565
7.32	.02671	.02531	.02392	.02263	9.72	.01744	.01685	.01620	.01556
7.36	.02650	.02513	.02375	.02248	9.76	.01733	.01675	.01610	.01547
7.40	.02630	.02495	.02359	.02233	9.80	.01721	.01665	.01601	.01538
7.44	.02610	.02476	.02343	.02218	9.84	.01710	.01654	.01591	.01529
7.48	.02590	.02458	.02326	.02204	9.88	.01699	.01644	.01582	.01520
7.52	.02570	.02441	.02310	.02189	9.92	.01689	.01634	.01572	.01511
7.56	.02550	.02423	.02294	.02175	9.96	.01678	.01624	.01563	.01503
7.60	.02531	.02406	.02279	.02161	10.00	.01667	.01614	.01554	.01494
7.64	.02512	.02388	.02263	.02146					
7.68	.02493	.02371	.02248	.02132					
7.72	.02474	.02354	.02232	.02119					
7.76	.02456	.02338	.02217	.02105					
7.80	.02437	.02321	.02202	.02091					
7.84	.02419	.02305	.02187	.02078					
7.88	.02401	.02288	.02173	.02064					
7.92	.02384	.02272	.02158	.02051					
7.96	.02366	.02256	.02144	.02038					
8.00	.02349	.02241	.02129	.02026					
8.04	.02331	.02225	.02115	.02013					
8.08	.02314	.02209	.02101	.01999					
8.12	.02297	.02194	.02087	.01986					
8.16	.02281	.02179	.02073	.01973					

TABLE II - VARIATION OF DISPLACEMENT-THICKNESS RATIO g WITH MACH NUMBER M AND VELOCITY-PROFILE PARAMETER N

$$\left[g = \frac{\delta^*}{\delta}\right]$$

(a) Subsonic flow

Mach number M	Velocity-profile parameter, N			
	5	7	9	11
0.100	0.16708	0.12533	0.10026	0.08353
.200	.16832	.126375	.10115	.08431
.300	.17038	.12811	.10264	.08561
.400	.17324	.13052	.10471	.08742
.500	.17687	.13359	.10735	.08973
.600	.18124	.13728	.11054	.09253
.700	.18631	.14159	.11426	.09579
.800	.19204	.14647	.11848	.09951
.900	.19838	.15189	.12319	.10366
1.000	.20529	.15783	.12836	.10822

NACA

TABLE II - VARIATION OF DISPLACEMENT-THICKNESS RATIO g WITH MACH NUMBER M AND VELOCITY-PROFILE PARAMETER N - Continued

$$\left[g = \frac{\delta^*}{\delta}\right]$$

(b) Supersonic flow

Mach number	Velocity-profile parameter, N				Mach number	Velocity-profile parameter, N			
M	5	7	9	11	M	5	7	9	11
1.00	0.20530	0.15782	0.12836	0.10822	3.40	0.43230	0.36603	0.31894	0.28336
1.04	.20821	.16033	.13054	.11016	3.44	.43595	.36958	.32234	.28660
1.08	.21120	.16291	.13280	.11215	3.48	.43958	.37312	.32573	.28982
1.12	.21426	.16556	.13512	.11421	3.52	.44319	.37664	.32911	.29305
1.16	.21740	.16828	.13750	.11632	3.56	.44677	.38015	.33248	.29626
1.20	.22061	.17106	.13994	.11849	3.60	.45033	.38364	.33583	.29947
1.24	.22389	.17391	.14244	.12072	3.64	.45387	.38711	.33918	.30267
1.28	.22722	.17681	.14500	.12299	3.68	.45738	.39056	.34251	.30586
1.32	.23062	.17978	.14761	.12532	3.72	.46088	.39400	.34583	.30904
1.36	.23408	.18280	.15028	.12770	3.76	.46434	.39742	.34914	.31221
1.40	.23759	.18587	.15299	.13013	3.80	.46779	.40082	.35243	.31538
1.44	.24115	.18900	.15576	.13261	3.84	.47121	.40421	.35571	.31853
1.48	.24475	.19217	.15857	.13513	3.88	.47460	.40757	.35898	.32168
1.52	.24841	.19539	.16143	.13769	3.92	.47797	.41092	.36223	.32481
1.56	.25210	.19866	.16434	.14030	3.96	.48132	.41425	.36547	.32794
1.60	.25584	.20196	.16728	.14294	4.00	.48464	.41756	.36870	.33105
1.64	.25961	.20531	.17027	.14563	4.04	.48794	.42085	.37191	.33415
1.68	.26341	.20869	.17329	.14835	4.08	.49121	.42412	.37510	.33725
1.72	.26725	.21211	.17635	.15111	4.12	.49446	.42737	.37828	.34033
1.76	.27112	.21557	.17944	.15391	4.16	.49769	.43060	.38145	.34339
1.80	.27501	.21905	.18257	.15674	4.20	.50089	.43381	.38460	.34645
1.84	.27892	.22256	.18573	.15960	4.24	.50407	.43701	.38773	.34950
1.88	.28286	.22610	.18892	.16249	4.28	.50722	.44018	.39085	.35253
1.92	.28682	.22967	.19213	.16541	4.32	.51035	.44334	.39395	.35555
1.96	.29079	.23325	.19537	.16836	4.36	.51345	.44647	.39704	.35855
2.00	.29478	.23686	.19864	.17133	4.40	.51654	.44958	.40011	.36155
2.04	.29878	.24049	.20193	.17433	4.44	.51959	.45268	.40317	.36453
2.08	.30280	.24414	.20524	.17735	4.48	.52263	.45575	.40620	.36750
2.12	.30682	.24780	.20858	.18040	4.52	.52564	.45881	.40923	.37046
2.16	.31085	.25148	.21193	.18346	4.56	.52862	.46184	.41223	.37339
2.20	.31489	.25517	.21530	.18655	4.60	.53158	.46486	.41522	.37632
2.24	.31893	.25886	.21868	.18965	4.64	.53452	.46786	.41819	.37923
2.28	.32297	.26259	.22208	.19278	4.68	.53744	.47083	.42115	.38214
2.32	.32701	.26631	.22549	.19592	4.72	.54033	.47379	.42409	.38502
2.36	.33105	.27004	.22892	.19907	4.76	.54320	.47672	.42701	.38790
2.40	.33509	.27378	.23236	.20224	4.80	.54604	.47964	.42992	.39075
2.44	.33913	.27752	.23580	.20542	4.84	.54887	.48253	.43281	.39360
2.48	.34316	.28126	.23926	.20861	4.88	.55167	.48541	.43568	.39643
2.52	.34718	.28501	.24272	.21182	4.92	.55444	.48827	.43854	.39925
2.56	.35120	.28875	.24619	.21503	4.96	.55720	.49110	.44138	.40205
2.60	.35521	.29250	.24966	.21825	5.00	.55993	.49392	.44420	.40484
2.64	.35921	.29624	.25314	.22149	5.04	.56264	.49672	.44701	.40761
2.68	.36320	.29999	.25662	.22472	5.08	.56533	.49950	.44979	.41037
2.72	.36718	.30373	.26011	.22797	5.12	.56800	.50226	.45257	.41312
2.76	.37114	.30746	.26359	.23122	5.16	.57064	.50500	.45532	.41585
2.80	.37509	.31119	.26708	.23448	5.20	.57327	.50772	.45806	.41856
2.84	.37903	.31492	.27056	.23773	5.24	.57586	.51042	.46078	.42126
2.88	.38296	.31863	.27405	.24100	5.28	.57844	.51310	.46349	.42395
2.92	.38686	.32234	.27753	.24426	5.32	.58100	.51577	.46618	.42662
2.96	.39075	.32605	.28101	.24753	5.36	.58354	.51841	.46885	.42928
3.00	.39463	.32974	.28449	.25079	5.40	.58606	.52104	.47150	.43193
3.04	.39848	.33342	.28797	.25406	5.44	.58855	.52364	.47414	.43455
3.08	.40232	.33709	.29143	.25733	5.48	.59103	.52623	.47676	.43717
3.12	.40614	.34076	.29490	.26059	5.52	.59349	.52880	.47937	.43977
3.16	.40994	.34441	.29836	.26385	5.56	.59592	.53135	.48196	.44235
3.20	.41372	.34804	.30181	.26711	5.60	.59834	.53388	.48453	.44493
3.24	.41747	.35167	.30525	.27037	5.64	.60073	.53640	.48709	.44748
3.28	.42121	.35528	.30869	.27363	5.68	.60310	.53890	.48963	.45002
3.32	.42493	.35888	.31211	.27688	5.72	.60546	.54137	.49215	.45255
3.36	.42863	.36246	.31553	.28012	5.76	.60779	.54383	.49466	.45506

TABLE II - VARIATION OF DISPLACEMENT-THICKNESS RATIO g WITH MACH NUMBER M AND VELOCITY-PROFILE PARAMETER N - Concluded

$$\left[g = \frac{\delta^*}{\delta}\right]$$

(b) Supersonic flow - Concluded

Mach number	Velocity-profile parameter, N				Mach number	Velocity-profile parameter, N			
M	5	7	9	11	M	5	7	9	11
5.80	0.61012	0.54628	0.49715	0.45756	8.20	0.71964	0.66442	0.62011	0.58297
5.84	.61241	.54870	.49963	.46005	8.24	.72106	.66598	.62177	.58469
5.88	.61469	.55111	.50209	.46252	8.28	.72246	.66754	.62342	.58640
5.92	.61695	.55350	.50453	.46497	8.32	.72387	.66908	.62506	.58810
5.96	.61919	.55587	.50696	.46741	8.36	.72525	.67061	.62669	.58979
6.00	.62142	.55823	.50937	.46984	8.40	.72663	.67213	.62830	.59146
6.04	.62362	.56056	.51177	.47225	8.44	.72800	.67364	.62991	.59313
6.08	.62580	.56288	.51415	.47465	8.48	.72934	.67514	.63151	.59479
6.12	.62798	.56519	.51651	.47704	8.52	.73070	.67663	.63309	.59644
6.16	.63012	.56748	.51886	.47941	8.56	.73204	.67811	.63466	.59807
6.20	.63226	.56975	.52120	.48176	8.60	.73337	.67957	.63623	.59970
6.24	.63437	.57200	.52352	.48411	8.64	.73468	.68103	.63778	.60132
6.28	.63647	.57424	.52582	.48643	8.68	.73598	.68248	.63932	.60292
6.32	.63856	.57646	.52811	.48875	8.72	.73729	.68391	.64086	.60452
8.36	.64062	.57866	.53038	.49105	8.76	.73857	.68534	.64238	.60611
6.40	.64267	.58085	.53264	.49334	8.80	.73985	.68676	.64389	.60768
6.44	.64469	.58302	.53488	.49561	8.84	.74112	.68816	.64540	.60925
6.48	.64670	.58518	.53711	.49787	8.88	.74236	.68956	.64689	.61081
6.52	.64871	.58732	.53933	.50011	8.92	.74363	.69095	.64837	.61236
6.56	.65069	.58944	.54152	.50235	8.96	.74486	.69232	.64985	.61389
6.60	.65266	.59155	.54371	.50457	9.00	.74610	.69369	.65131	.61542
6.64	.65460	.59365	.54588	.50677	9.04	.74732	.69505	.65277	.61694
6.68	.65653	.59572	.54803	.50896	9.08	.74852	.69640	.65421	.61845
6.72	.65845	.59779	.55018	.51114	9.12	.74973	.69774	.65565	.61995
6.76	.66035	.59983	.55230	.51331	9.16	.75092	.69907	.65707	.62144
6.80	.66224	.60187	.55442	.51546	9.20	.75212	.70039	.65849	.62292
6.84	.66411	.60389	.55651	.51760	9.24	.75329	.70170	.65990	.62440
6.88	.66596	.60589	.55860	.51972	9.28	.75445	.70300	.66130	.62586
6.92	.66781	.60788	.56067	.52184	9.32	.75564	.70430	.66268	.62732
6.96	.66963	.60985	.56273	.52394	9.36	.75678	.70558	.66406	.62876
7.00	.67145	.61181	.56477	.52602	9.40	.75794	.70686	.66544	.63020
7.04	.67325	.61376	.56680	.52810	9.44	.75907	.70812	.66680	.63163
7.08	.67502	.61569	.56882	.53016	9.48	.76018	.70938	.66815	.63304
7.12	.67680	.61760	.57082	.53221	9.52	.76133	.71063	.66950	.63445
7.16	.67855	.61951	.57281	.53424	9.56	.76243	.71187	.67083	.63586
7.20	.68029	.62140	.57478	.53627	9.60	.76354	.71311	.67216	.63725
7.24	.68201	.62327	.57675	.53828	9.64	.76464	.71433	.67348	.63863
7.28	.68372	.62513	.57870	.54028	9.68	.76570	.71555	.67479	.64001
7.32	.68543	.62698	.58063	.54226	9.72	.76681	.71675	.67609	.64138
7.36	.68711	.62882	.58256	.54424	9.76	.76788	.71795	.67738	.64274
7.40	.68879	.63064	.58447	.54620	9.80	.76895	.71914	.67867	.64409
7.44	.69045	.63245	.58636	.54815	9.84	.77001	.72033	.67995	.64543
7.48	.69209	.63424	.58825	.55008	9.88	.77105	.72150	.68122	.64676
7.52	.69374	.63602	.59012	.55201	9.92	.77211	.72267	.68248	.64809
7.56	.69535	.63779	.59198	.55392	9.96	.77314	.72383	.68373	.64941
7.60	.69696	.63955	.59383	.55582	10.00	.77418	.72498	.68497	.65072
7.64	.69856	.64129	.59567	.55771					
7.68	.70013	.64302	.59749	.55959					
7.72	.70171	.64474	.59930	.56146					
7.76	.70327	.64645	.60110	.56331					
7.80	.70482	.64814	.60289	.56516					
7.84	.70635	.64982	.60466	.56699					
7.88	.70786	.65149	.60642	.56881					
7.92	.70938	.65315	.60818	.57062					
7.96	.71088	.65479	.60991	.57241					
8.00	.71237	.65643	.61164	.57420					
8.04	.71385	.65805	.61336	.57598					
8.08	.71530	.65966	.61506	.57774					
8.12	.71676	.66126	.61676	.57949					
8.16	.71820	.66284	.61844	.58124					

TABLE III - VARIATION OF SHAPE PARAMETER H WITH MACH NUMBER M AND VELOCITY-PROFILE PARAMETER N

$$\left[H \equiv \frac{\delta^*}{\theta}\right]$$

(a) Subsonic flow

Mach number M	Velocity-profile parameter, N			
	5	7	9	11
0.100	1.40466	1.29006	1.22618	1.11961
.200	1.41866	1.30353	1.23934	1.13203
.300	1.44198	1.32596	1.26127	1.15272
.400	1.47463	1.35737	1.29199	1.18169
.500	1.51658	1.39773	1.33142	1.21894
.600	1.56785	1.44704	1.37965	1.26449
.700	1.62840	1.50531	1.43663	1.31836
.800	1.69821	1.57249	1.50233	1.38054
.900	1.77728	1.64860	1.57677	1.45103
1.000	1.86559	1.73364	1.65994	1.52987

TABLE III - VARIATION OF SHAPE PARAMETER H WITH MACH NUMBER M AND VELOCITY-PROFILE PARAMETER N - Continued

$$\left[H = \frac{\delta^*}{\theta}\right]$$

(b) Supersonic flow

Mach number	Velocity-profile parameter, N				Mach number	Velocity-profile parameter, N			
M	5	7	9	11	M	5	7	9	11
1.00	1.8656	1.7336	1.6599	1.6126	3.40	6.7118	6.4125	6.2452	6.1377
1.04	1.9035	1.7701	1.6956	1.6478	3.44	6.8364	6.5330	6.3634	6.2544
1.08	1.9429	1.8080	1.7327	1.6844	3.48	6.9624	6.6548	6.4830	6.3725
1.12	1.9837	1.8474	1.7712	1.7223	3.52	7.0898	6.7780	6.6039	6.4919
1.16	2.0261	1.8882	1.8111	1.7616	3.56	7.2187	6.9027	6.7261	6.6127
1.20	2.0699	1.9303	1.8524	1.8023	3.60	7.3490	7.0287	6.8498	6.7348
1.24	2.1151	1.9739	1.8950	1.8444	3.64	7.4807	7.1560	6.9748	6.8583
1.28	2.1619	2.0190	1.9391	1.8878	3.68	7.6138	7.2848	7.1011	6.9831
1.32	2.2101	2.0654	1.9845	1.9326	3.72	7.7483	7.4150	7.2288	7.1092
1.36	2.2597	2.1132	2.0314	1.9788	3.76	7.8843	7.5465	7.3579	7.2367
1.40	2.3108	2.1625	2.0796	2.0263	3.80	8.0217	7.6794	7.4883	7.3656
1.44	2.3634	2.2132	2.1292	2.0752	3.84	8.1605	7.8137	7.6201	7.4957
1.48	2.4175	2.2653	2.1802	2.1255	3.88	8.3007	7.9493	7.7532	7.6273
1.52	2.4730	2.3188	2.2325	2.1771	3.92	8.4424	8.0864	7.8877	7.7602
1.56	2.5300	2.3737	2.2863	2.2301	3.96	8.5854	8.2248	8.0236	7.8944
1.60	2.5884	2.4300	2.3414	2.2845	4.00	8.7300	8.3646	8.1608	8.0300
1.64	2.6483	2.4877	2.3980	2.3402	4.04	8.8759	8.5058	8.2994	8.1669
1.68	2.7096	2.5469	2.4559	2.3974	4.08	9.0232	8.6484	8.4394	8.3051
1.72	2.7724	2.6074	2.5152	2.4558	4.12	9.1719	8.7923	8.5807	8.4447
1.76	2.8367	2.6694	2.5758	2.5157	4.16	9.3221	8.9377	8.7233	8.5857
1.80	2.9024	2.7328	2.6379	2.5769	4.20	9.4737	9.0844	8.8673	8.7280
1.84	2.9695	2.7975	2.7013	2.6394	4.24	9.6267	9.2325	9.0127	8.9716
1.88	3.0382	2.8637	2.7661	2.7034	4.28	9.7811	9.3819	9.1594	9.0166
1.92	3.1082	2.9313	2.8323	2.7686	4.32	9.9370	9.5328	9.3075	9.1629
1.96	3.1797	3.0003	2.8999	2.8353	4.36	10.0943	9.6850	9.4569	9.3106
2.00	3.2527	3.0706	2.9688	2.9033	4.40	10.2530	9.8386	9.6077	9.4596
2.04	3.3271	3.1424	3.0391	2.9727	4.44	10.4130	9.9936	9.7599	9.6099
2.08	3.4029	3.2156	3.1108	3.0434	4.48	10.5746	10.1499	9.9134	9.7616
2.12	3.4802	3.2902	3.1839	3.1155	4.52	10.7375	10.3077	10.0682	9.9147
2.16	3.5589	3.3662	3.2583	3.1889	4.56	10.9019	10.4668	10.2245	10.0690
2.20	3.6391	3.4436	3.3341	3.2638	4.60	11.0677	10.6273	10.3820	10.2247
2.24	3.7207	3.5223	3.4113	3.3399	4.64	11.2349	10.7891	10.5410	10.3818
2.28	3.8038	3.6025	3.4899	3.4174	4.68	11.4035	10.9524	10.7013	10.5402
2.32	3.8883	3.6841	3.5698	3.4963	4.72	11.5735	11.1170	10.8629	10.7000
2.36	3.9742	3.7671	3.6511	3.5766	4.76	11.7450	11.2830	11.0259	10.8611
2.40	4.0616	3.8514	3.7338	3.6582	4.80	11.9178	11.4504	11.1903	11.0235
2.44	4.1504	3.9372	3.8179	3.7411	4.84	12.0921	11.6192	11.3560	11.1873
2.48	4.2407	4.0243	3.9033	3.8254	4.88	12.2678	11.7893	11.5230	11.3524
2.52	4.3324	4.1129	3.9901	3.9111	4.92	12.4449	11.9608	11.6914	11.5188
2.56	4.4255	4.2028	4.0782	3.9981	4.96	12.6234	12.1337	11.8612	11.6866
2.60	4.5201	4.2942	4.1678	4.0865	5.00	12.8034	12.3079	12.0324	11.8558
2.64	4.6161	4.3869	4.2587	4.1762	5.04	12.9848	12.4836	12.2048	12.0263
2.68	4.7135	4.4810	4.3509	4.2673	5.08	13.1676	12.6606	12.3787	12.1981
2.72	4.8124	4.5765	4.4446	4.3597	5.12	13.3518	12.8390	12.5539	12.3712
2.76	4.9127	4.6734	4.5396	4.4535	5.16	13.5374	13.0187	12.7304	12.5457
2.80	5.0144	4.7717	4.6359	4.5486	5.20	13.7245	13.1999	12.9083	12.7216
2.84	5.1175	4.8714	4.7337	4.6451	5.24	13.9129	13.3824	13.0876	12.8988
2.88	5.2221	4.9724	4.8328	4.7429	5.28	14.1027	13.5663	13.2682	13.0773
2.92	5.3282	5.0749	4.9332	4.8421	5.32	14.2940	13.7516	13.4502	13.2572
2.96	5.4356	5.1787	5.0351	4.9427	5.36	14.4867	13.9382	13.6335	13.4384
3.00	5.5445	5.2840	5.1383	5.0446	5.40	14.6809	14.1262	13.8182	13.6209
3.04	5.6548	5.3906	5.2428	5.1478	5.44	14.8763	14.3156	14.0042	13.8048
3.08	5.7665	5.4986	5.3488	5.2524	5.48	15.0733	14.5064	14.1916	13.9901
3.12	5.8797	5.6080	5.4560	5.3583	5.52	15.2717	14.6986	14.3803	14.1766
3.16	5.9943	5.7188	5.5647	5.4656	5.56	15.4714	14.8921	14.5704	14.3646
3.20	6.1103	5.8309	5.6747	5.5743	5.60	15.6727	15.0870	14.7619	14.5538
3.24	6.2278	5.9445	5.7861	5.6843	5.64	15.8752	15.2833	14.9547	14.7444
3.28	6.3466	6.0594	5.8988	5.7956	5.68	16.0792	15.4809	15.1488	14.9364
3.32	6.4670	6.1757	6.0129	5.9083	5.72	16.2847	15.6800	15.3443	15.1296
3.36	6.5887	6.2934	6.1284	6.0223	5.76	16.4915	15.8804	15.5412	15.3242

TABLE III - VARIATION OF SHAPE PARAMETER H WITH MACH NUMBER M AND VELOCITY-PROFILE PARAMETER N - Concluded

$$\left[H = \frac{\delta^*}{\theta}\right]$$

(b) Supersonic flow - Concluded

Mach number	Velocity-profile parameter, N				Mach number	Velocity-profile parameter, N			
M	5	7	9	11	M	5	7	9	11
5.80	16.6998	16.0822	15.7394	15.5202	8.20	31.7843	30.7061	30.1091	29.7299
5.84	16.9094	16.2853	15.9390	15.7175	8.24	32.0788	30.9908	30.5898	30.0077
5.88	17.1204	16.4898	16.1399	15.9162	8.28	32.3742	31.2778	30.6719	30.2866
5.92	17.3331	16.6957	16.3422	16.1161	8.32	32.6721	31.5661	30.9554	30.5670
5.96	17.5469	16.9030	16.5458	16.3175	8.36	32.9707	31.8560	31.2402	30.8488
6.00	17.7624	17.1117	16.7508	16.5201	8.40	33.2712	32.1471	31.5265	31.1318
6.04	17.9791	17.3217	16.9571	16.7241	8.44	33.5727	32.4396	31.8139	31.4162
6.08	18.1971	17.5331	17.1648	16.9294	8.48	33.8751	32.7336	32.1029	31.7020
6.12	18.4168	17.7469	17.3739	17.1361	8.52	34.1800	33.0288	32.3931	31.9889
6.16	18.6378	17.9601	17.5843	17.3441	8.56	34.4857	33.3254	32.6847	32.2774
6.20	18.8603	18.1755	17.7960	17.5535	8.60	34.7932	33.6234	32.9776	32.5671
6.24	19.0840	18.3925	18.0091	17.7642	8.64	35.1020	33.9230	33.2719	32.8583
6.28	19.3091	18.6107	18.2236	17.9763	8.68	35.4113	34.2236	33.5676	33.1506
6.32	19.5359	18.8304	18.4394	18.1897	8.72	35.7235	34.5258	33.8646	33.4445
6.36	19.7639	19.0514	18.6565	18.4043	8.76	36.0363	34.8293	34.1630	33.7395
6.40	19.9936	19.2739	18.8751	18.6204	8.80	36.3506	35.1343	34.4627	34.0361
6.44	20.2243	19.4976	19.0949	18.8378	8.84	36.6664	35.4406	34.7638	34.3339
6.48	20.4565	19.7228	19.3162	19.0565	8.88	36.9828	35.7481	35.0662	34.6330
6.52	20.6904	19.9493	19.5387	19.2766	8.92	37.3021	36.0573	35.3700	34.9335
6.56	20.9255	20.1772	19.7627	19.4980	8.96	37.6218	36.3677	35.6751	35.2353
6.60	21.1622	20.4065	19.9880	19.7208	9.00	37.9438	36.6794	35.9817	35.5384
6.64	21.4000	20.6371	20.2146	19.9449	9.04	38.2662	36.9926	36.2894	35.8429
6.68	21.6393	20.8692	20.4426	20.1704	9.08	38.5897	37.3072	36.5986	36.1488
6.72	21.8802	21.1026	20.6720	20.3971	9.12	38.9157	37.6230	36.9091	36.4559
6.76	22.1224	21.3374	20.9027	20.6252	9.16	39.2421	37.9402	37.2211	36.7646
6.80	22.3662	21.5736	21.1347	20.8548	9.20	39.5716	38.2590	37.5344	37.0744
6.84	22.6111	21.8111	21.3681	21.0855	9.24	39.9010	38.5789	37.8490	37.3855
6.88	22.8575	22.0500	21.6028	21.3177	9.28	40.2313	38.9003	38.1649	37.6981
6.92	23.1056	22.2903	21.8390	21.5512	9.32	40.5656	39.2232	38.4823	38.0120
6.96	23.3548	22.5319	22.0765	21.7860	9.36	40.8995	39.5474	38.8008	38.3272
7.00	23.6056	22.7749	22.3153	22.0221	9.40	41.2352	39.8730	39.1209	38.6437
7.04	23.8576	23.0193	22.5554	22.2596	9.44	41.5722	40.1998	39.4422	38.9616
7.08	24.1109	23.2651	22.7970	22.4984	9.48	41.9098	40.5280	39.7650	39.2810
7.12	24.3660	23.5122	23.0398	22.7386	9.52	42.2506	40.8578	40.0891	39.6014
7.16	24.6223	23.7608	23.2840	22.9801	9.56	42.5912	41.1887	40.4145	39.9234
7.20	24.8803	24.0107	23.5296	23.2230	9.60	42.9342	41.5212	40.7414	40.2466
7.24	25.1393	24.2619	23.7766	23.4672	9.64	43.2781	41.8552	41.0695	40.5713
7.28	25.3996	24.5146	24.0248	23.7127	9.68	43.6224	42.1902	41.3991	40.8973
7.32	25.6619	24.7687	24.2745	23.9596	9.72	43.9703	42.5267	41.7299	41.2244
7.36	25.9251	25.0240	24.5255	24.2078	9.76	44.3183	42.8646	42.0621	41.5532
7.40	26.1903	25.2808	24.7778	24.4574	9.80	44.6682	43.2040	42.3956	41.8831
7.44	26.4564	25.5390	25.0316	24.7083	9.84	45.0198	43.5448	42.7306	42.2144
7.48	26.7238	25.7985	25.2868	24.9606	9.88	45.3714	43.8867	43.0669	42.5471
7.52	26.9935	26.0594	25.5430	25.2142	9.92	45.7264	44.2302	43.4045	42.8809
7.56	27.2639	26.3217	25.8008	25.4691	9.96	46.0818	44.5750	43.7435	43.2163
7.60	27.5359	26.5853	26.0600	25.7253	10.00	46.4388	44.9212	44.0837	43.5531
7.64	27.8094	26.8503	26.3203	25.9829					
7.68	28.0836	27.1167	26.5822	26.2418					
7.72	28.3602	27.3846	26.8453	26.5021					
7.76	28.6376	27.6536	27.1099	26.7637					
7.80	28.9167	27.9243	27.3758	27.0267					
7.84	29.1971	28.1962	27.6430	27.2910					
7.88	29.4785	28.4693	27.9116	27.5566					
7.92	29.7621	28.7440	28.1816	27.8235					
7.96	30.0467	29.0201	28.4528	28.0919					
8.00	30.3328	29.2975	28.7255	28.3616					
8.04	30.6203	29.5762	28.9995	28.6326					
8.08	30.9087	29.8564	29.2748	28.9049					
8.12	31.1995	30.1379	29.5515	29.1786					
8.16	31.4909	30.4208	29.8297	29.4535					

1207

TABLE IV - VARIATION OF A WITH MACH NUMBER M AND VELOCITY-PROFILE PARAMETER N

$$\left[\underline{A} \equiv \int_{0.100}^{M} \psi_w \, e^{\int_{0.100}^{M_1} \varphi \, dM_1} \, dM_1 \right]$$

(a) Subsonic flow

Mach number M	Velocity-profile parameter, N			
	5	7	9	11
0.100	0	0	0	0
.200	4.90763	5.67833	6.53852	6.80255
.300	28.17632	31.23720	35.12561	35.12758
.400	93.48682	100.40804	110.93310	107.71321
.500	232.48958	243.59694	265.44898	251.84194
.600	481.47685	494.42310	532.76912	495.97768
.700	877.45287	885.98133	945.76453	866.51738
.800	1454.29779	1447.39366	1532.68505	1385.11728
.900	2240.82484	2201.14120	2314.61073	2066.81014
1.000	3269.30901	3161.36979	3303.93265	2919.05415

TABLE IV - VARIATION OF $\underline{A}$ WITH MACH NUMBER M AND VELOCITY-PROFILE PARAMETER N - Continued

$$\left[\underline{A} \equiv \int_1^M \nu_w \, e^{\int_1^{M_1} \varphi dM_1} \, dM_1\right]$$

(b) Supersonic flow

Mach number	Velocity-profile parameter, N				Mach number	Velocity-profile parameter, N			
M	5	7	9	11	M	5	7	9	11
1.00	0	0	0	0	3.40	39.83027	44.51024	50.17217	56.22780
1.04	.35033	.42255	.49685	.57207	3.44	40.35827	45.07350	50.79053	56.90900
1.08	.72903	.87739	1.03042	1.18548	3.48	40.87633	45.62556	51.39624	57.57603
1.12	1.13603	1.36425	1.60027	1.83963	3.52	41.38454	46.16658	51.98949	58.22908
1.16	1.57111	1.88267	2.20573	2.53372	3.56	41.88301	46.69669	52.57045	58.86838
1.20	2.03385	2.43199	2.84594	3.26663	3.60	42.37186	47.21605	53.13930	59.49412
1.24	2.52368	3.01139	3.51985	4.03709	3.64	42.85121	47.72481	55.69624	60.10654
1.28	3.03991	3.61988	4.22620	4.84366	3.68	43.32118	48.22313	54.24145	60.70584
1.32	3.58170	4.25635	4.96366	5.68473	3.72	43.78190	48.71117	54.77513	61.29229
1.36	4.14809	4.91957	5.73071	6.55855	3.76	44.23351	49.18910	55.29748	61.86608
1.40	4.73803	5.60820	6.52575	7.46321	3.80	44.67615	49.65710	55.80869	62.42745
1.44	5.35039	6.32081	7.34709	8.39678	3.84	45.10994	50.11532	56.30898	62.97664
1.48	5.98394	7.05592	8.19295	9.35725	3.88	45.53504	50.56395	56.79854	63.51389
1.52	6.63739	7.81196	9.06152	10.34246	3.92	45.95159	51.00315	57.27758	64.03939
1.56	7.30943	8.58734	9.95092	11.35031	3.96	46.35973	51.43311	57.74629	64.55342
1.60	7.99870	9.38047	10.85930	12.37867	4.00	46.75982	51.85400	58.20489	65.05618
1.64	8.70380	10.18969	11.78476	13.42539	4.04	47.15138	52.26598	58.65357	65.54794
1.68	9.42333	11.01338	12.72543	14.48832	4.08	47.53517	52.66923	59.09254	66.02890
1.72	10.15591	11.84993	13.67946	15.56536	4.12	47.91114	53.06393	59.52198	66.49930
1.76	10.90015	12.69773	14.64502	16.65451	4.16	48.27943	53.45024	59.94211	66.95935
1.80	11.65466	13.55523	15.62035	17.75374	4.20	48.64019	53.82834	60.35312	67.40922
1.84	12.41809	14.42089	16.60369	18.86108	4.24	48.99356	54.19840	60.75519	67.84921
1.88	13.18913	15.29323	17.59339	19.97467	4.28	49.33969	54.56057	61.14853	68.27953
1.92	13.96648	16.17080	18.58781	21.09270	4.32	49.67871	54.91503	61.53332	68.70037
1.96	14.74890	17.05222	19.58541	22.21348	4.36	50.01078	55.26195	61.90975	69.11197
2.00	15.53519	17.93616	20.58471	23.33531	4.40	50.33603	55.60147	62.27800	69.51452
2.04	16.32421	18.82138	21.58432	24.45666	4.44	50.65460	55.93376	62.63825	69.90820
2.08	17.11483	19.70665	22.58288	25.57607	4.48	50.96662	56.25898	62.99068	70.29323
2.12	17.90602	20.59084	23.57915	26.69212	4.52	51.27224	56.57727	63.33547	70.66980
2.16	18.69676	21.47288	24.57193	27.80351	4.56	51.57158	56.8880	63.67278	71.03814
2.20	19.48615	22.35175	25.56014	28.90903	4.60	51.86478	57.19372	64.00280	71.39839
2.24	20.27324	23.22653	26.54275	30.00758	4.64	52.15197	57.49216	64.32568	71.75077
2.28	21.05724	24.09631	27.51878	31.09810	4.68	52.43327	57.78427	64.64158	72.09542
2.32	21.83737	24.96031	28.48738	32.17962	4.72	52.70882	58.07020	64.95068	72.43257
2.36	22.61290	25.81775	29.44772	33.25125	4.76	52.97873	58.35008	65.25312	72.76240
2.40	23.38315	26.66794	30.39905	34.31221	4.80	53.24312	58.62405	65.54905	73.08503
2.44	24.14750	27.51024	31.34071	35.36177	4.84	53.50212	58.89225	65.83864	73.40068
2.48	24.90538	28.34409	32.27207	36.39926	4.88	53.75585	59.15480	66.12202	73.70950
2.52	25.65626	29.16894	33.19258	37.42409	4.92	54.00440	59.41183	66.39934	74.01162
2.56	26.39967	29.98433	34.10176	38.43573	4.96	54.24792	59.66347	66.67074	74.30724
2.60	27.13518	30.78984	34.99915	39.43374	5.00	54.48649	59.90984	66.93636	74.59645
2.64	27.86239	31.58509	35.88439	40.41767	5.04	54.72023	60.15107	67.19634	74.87947
2.68	28.58095	32.36975	36.75712	41.38720	5.08	54.94925	60.38727	67.45081	75.15643
2.72	29.29055	33.14351	37.61705	42.34203	5.12	55.17365	60.61855	67.69988	75.42746
2.76	29.99092	33.90614	38.46395	43.28192	5.16	55.39353	60.84503	67.94370	75.69272
2.80	30.68182	34.65743	39.29762	44.20668	5.20	55.60899	61.06681	68.18238	75.95233
2.84	31.36304	35.39719	40.11787	45.11610	5.24	55.82013	61.28402	68.41605	76.20643
2.88	32.03440	36.12529	40.92458	46.01010	5.28	56.02706	61.49676	68.64484	76.45514
2.92	32.69577	36.84160	41.71767	46.88857	5.32	56.22986	61.70512	68.86884	76.69862
2.96	33.34701	37.54605	42.49705	47.75149	5.36	56.42862	61.90920	69.08817	76.93695
3.00	33.98804	38.23857	43.26270	48.59881	5.40	56.62343	62.10912	69.30295	77.17029
3.04	34.61877	38.91913	44.01461	49.43053	5.44	56.81438	62.30495	69.51327	77.39872
3.08	35.23917	39.58772	44.75279	50.24671	5.48	57.00156	62.49680	69.71924	77.62240
3.12	35.84921	40.24435	45.47727	51.04741	5.52	57.18505	62.68476	69.92097	77.84141
3.16	36.44886	40.88904	46.18812	51.83269	5.56	57.36495	62.86891	70.11855	78.05591
3.20	37.03814	41.52185	46.88540	52.60267	5.60	57.54129	63.04936	70.31209	78.26598
3.24	37.61708	42.14283	47.56922	53.35747	5.64	57.71420	63.22617	70.50168	78.47172
3.28	38.18570	42.75207	48.23968	54.09722	5.68	57.88374	63.39943	70.68740	78.67321
3.32	38.74406	43.34964	48.89690	54.82209	5.72	58.04998	63.56923	70.86935	78.87056
3.36	39.29223	43.93566	49.54101	55.53221	5.76	58.21300	63.73565	71.04761	79.06388

TABLE IV - VARIATION OF $\underline{A}$ WITH MACH NUMBER M AND VELOCITY-PROFILE PARAMETER N - Concluded

$$\left[\underline{A} \equiv \int_1^M Y_w \, e^{\int_1^{M_1} \varphi dM_1} \, dM_1\right]$$

(b) Supersonic flow - Concluded

Mach number M	Velocity-profile parameter, N				Mach number M	Velocity-profile parameter, N			
	5	7	9	11		5	7	9	11
5.80	58.37287	63.89878	71.22229	79.25325	8.20	64.12830	69.69965	77.39276	85.91490
5.84	58.52965	64.05863	71.39344	79.43878	8.24	64.18276	69.75372	77.44980	85.97616
5.88	58.68342	64.21534	71.56116	79.62058	8.28	64.23636	69.80693	77.50592	86.03641
5.92	58.83425	64.36897	71.72554	79.79872	8.32	64.28913	69.85928	77.56112	86.09569
5.96	58.98219	64.51958	71.88663	79.97326	8.36	64.34107	69.91080	77.61544	86.15401
6.00	59.12732	64.66725	72.04453	80.14427	8.40	64.39221	69.96150	77.66888	86.21137
6.04	59.26969	64.81203	72.19930	80.31191	8.44	64.44255	70.01140	77.72146	86.26782
6.08	59.40937	64.95401	72.35102	80.47619	8.48	64.49212	70.06051	77.77321	86.32333
6.12	59.54640	65.09322	72.49975	80.63718	8.52	64.54092	70.10884	77.82413	86.37798
6.16	59.68086	65.22975	72.64557	80.79499	8.56	64.58898	70.15642	77.87424	86.43174
6.20	59.81280	65.36364	72.78853	80.94972	8.60	64.63630	70.20326	77.92356	86.48466
6.24	59.94227	65.49497	72.92872	81.10140	8.64	64.68290	70.24937	77.97211	86.53674
6.28	60.06932	65.62378	73.06618	81.25009	8.68	64.72880	70.29476	78.01989	86.58798
6.32	60.19403	65.75015	73.20099	81.39589	8.72	64.77399	70.33945	78.06692	86.63843
6.36	60.31642	65.87411	73.33321	81.53887	8.76	64.81851	70.38345	78.11322	86.68806
6.40	60.43655	65.99573	73.46288	81.67909	8.80	64.86236	70.42678	78.15880	86.73691
6.44	60.55447	66.11504	73.59006	81.81660	8.84	64.90555	70.46944	78.20368	86.78502
6.48	60.67024	66.23212	73.71483	81.95147	8.88	64.94810	70.51145	78.24786	86.83236
6.52	60.78388	66.34700	73.83722	82.08372	8.92	64.99002	70.55282	78.29136	86.87898
6.56	60.89546	66.45973	73.95730	82.21345	8.96	65.03131	70.59357	78.33420	86.92488
6.60	61.00502	66.57037	74.07511	82.34072	9.00	65.07200	70.63370	78.37638	86.97006
6.64	61.11259	66.67895	74.19070	82.46558	9.04	65.11208	70.67323	78.41792	87.01457
6.68	61.21822	66.78553	74.30415	82.58809	9.08	65.15158	70.71217	78.45883	87.05838
6.72	61.32196	66.89014	74.41544	82.70827	9.12	65.19050	70.75052	78.49912	87.10153
6.76	61.42383	66.99283	74.52467	82.82618	9.16	65.22885	70.78830	78.53881	87.14402
6.80	61.52389	67.09364	74.63188	82.94192	9.20	65.26664	70.82552	78.57790	87.18589
6.84	61.62216	67.19261	74.73711	83.05550	9.24	65.30389	70.86219	78.61640	87.22711
6.88	61.71870	67.28979	74.84040	83.16697	9.28	65.34060	70.89833	78.65433	87.26773
6.92	61.81353	67.38520	74.94179	83.27635	9.32	65.37678	70.93392	78.69169	87.30775
6.96	61.90669	67.47890	75.04134	83.38374	9.36	65.41245	70.96900	78.72851	87.34717
7.00	61.99822	67.57091	75.13907	83.48916	9.40	65.44760	71.00357	78.76477	87.38599
7.04	62.08815	67.66127	75.23502	83.59266	9.44	65.48225	71.03763	78.80051	87.42422
7.08	62.17651	67.75002	75.32924	83.69425	9.48	65.51642	71.07120	78.83572	87.46190
7.12	62.26334	67.83719	75.42176	83.79398	9.52	65.55009	71.10429	78.87041	87.49903
7.16	62.34866	67.92282	75.51262	83.89190	9.56	65.58330	71.13689	78.90460	87.53562
7.20	62.43251	68.00693	75.60186	83.98807	9.60	65.61603	71.16903	78.93830	87.57167
7.24	62.51492	68.08956	75.68950	84.08251	9.64	65.64831	71.20071	78.97150	87.60719
7.28	62.59592	68.17074	75.77558	84.17527	9.68	65.68014	71.23194	79.00423	87.64218
7.32	62.67554	68.25050	75.86014	84.26636	9.72	65.71152	71.26272	79.03649	87.67668
7.36	62.75380	68.32888	75.94321	84.35583	9.76	65.74247	71.29307	79.06828	87.71069
7.40	62.83074	68.40589	76.02482	84.44373	9.80	65.77299	71.32299	79.09962	87.74417
7.44	62.90638	68.48157	76.10499	84.53007	9.84	65.80309	71.35249	79.13051	87.77717
7.48	62.98074	68.55595	76.18377	84.61490	9.88	65.83277	71.38157	79.16097	87.80974
7.52	63.05386	68.62906	76.26118	84.69824	9.92	65.86205	71.41025	79.19099	87.84184
7.56	63.12575	68.70090	76.33725	84.78010	9.96	65.89093	71.43853	79.22059	87.87346
7.60	63.19645	68.77152	76.41200	84.86056	10.00	65.91942	71.46641	79.24978	87.90465
7.64	63.26597	68.84095	76.48546	84.93959					
7.68	63.33434	68.90919	76.55767	85.01729					
7.72	63.40159	68.97629	76.62864	85.09362					
7.76	63.46773	69.04226	76.69840	85.16867					
7.80	63.53278	69.10712	76.76698	85.24242					
7.84	63.59678	69.17090	76.83440	85.31491					
7.88	63.65974	69.23362	76.90069	85.38619					
7.92	63.72167	69.29530	76.96586	85.45627					
7.96	63.78261	69.35596	77.02994	85.52515					
8.00	63.84257	69.41563	77.09296	85.59288					
8.04	63.90156	69.47431	77.15493	85.65947					
8.08	63.95962	69.53204	77.21588	85.72493					
8.12	64.01674	69.58882	77.27582	85.78931					
8.16	64.07297	69.64469	77.33477	85.85262					

TABLE V - VARIATION OF $\underline{B}$ WITH MACH NUMBER M AND VELOCITY-PROFILE PARAMETER N

$$\left[\underline{B} = \int_{0.100}^{M} \Psi_s \, e^{\int_{0.100}^{M_1} \varphi dM_1} \, dM_1\right]$$

(a) Subsonic flow

Mach number M	Velocity-profile parameter, N			
	5	7	9	11
0.100	0	0	0	0
.200	4.92760	5.70129	6.56487	6.82980
.300	28.42363	31.50922	35.43010	35.42974
.400	94.92805	101.94268	112.62025	109.33747
.500	238.04224	249.36305	271.70006	257.71972
.600	497.89291	511.12627	550.67254	512.49115
.700	917.78388	926.32241	988.59400	905.38529
.800	1540.67351	1532.53301	1622.34001	1465.34709
.900	2407.32764	2363.03540	2483.87891	2216.43096
1.000	3565.86900	3444.65036	3598.25118	3176.37777

NACA

TABLE V - VARIATION OF $\underline{B}$ WITH MACH NUMBER M AND VELOCITY-PROFILE PARAMETER N - Continued

$$\left[\underline{B} \equiv \int_1^M \nu_s \, e^{\int_1^{M_1} \varphi dM_1} \, dM_1\right]$$

(b) Supersonic flow

Mach number M	Velocity-profile parameter, N				Mach number M	Velocity-profile parameter, N			
	5	7	9	11		5	7	9	11
1.00	0	0	0	0	3.40	66.54997	73.92654	83.04947	92.87096
1.04	.40101	.48366	.56872	.65480	3.44	67.79927	75.25925	84.51255	94.48275
1.08	.83875	1.00941	1.18547	1.36383	3.48	69.03943	76.58083	85.96255	96.07954
1.12	1.31394	1.57784	1.85076	2.12757	3.52	70.27024	77.89110	87.39931	97.66116
1.16	1.82712	2.18932	2.56490	2.94623	3.56	71.49152	79.18990	88.82267	99.22746
1.20	2.37865	2.84405	3.32795	3.81977	3.60	72.70309	80.47708	90.23252	100.77831
1.24	2.96873	3.54200	4.13975	4.74792	3.64	73.90479	81.75250	91.62872	102.31361
1.28	3.59738	4.28300	4.99993	5.73016	3.68	75.09649	83.01607	93.01119	103.83329
1.32	4.26446	5.06667	5.90794	6.76575	3.72	76.27807	84.26771	94.37986	105.33727
1.36	4.96968	5.89245	6.86301	7.85375	3.76	77.44941	85.50733	95.73468	106.82551
1.40	5.71260	6.75965	7.86422	8.99303	3.80	78.61044	86.73488	97.07560	108.29800
1.44	6.49266	7.66741	8.91048	10.18229	3.84	79.76107	87.95031	98.40259	109.75470
1.48	7.30915	8.61479	10.00058	11.42007	3.88	80.90124	89.15357	99.71563	111.19562
1.52	8.16126	9.60068	11.13318	12.70479	3.92	82.03089	90.34467	101.01475	112.62079
1.56	9.04807	10.62387	12.30683	14.03472	3.96	83.14998	91.52357	102.29993	114.03023
1.60	9.96859	11.68308	13.51996	15.40808	4.00	84.25847	92.69028	103.57119	115.42396
1.64	10.92170	12.77694	14.77094	16.82294	4.04	85.35635	93.84482	104.82858	116.80205
1.68	11.90626	13.90402	16.05808	18.27737	4.08	86.44360	94.98720	106.07212	118.16456
1.72	12.92105	15.06282	17.37962	19.76934	4.12	87.52022	96.11746	107.30188	119.51156
1.76	13.96479	16.25181	18.73376	21.29678	4.16	88.58621	97.23562	108.51792	120.84315
1.80	15.03615	17.46941	20.11867	22.85762	4.20	89.64159	98.34173	109.72030	122.15934
1.84	16.13380	18.71405	21.53251	24.44976	4.24	90.68638	99.43584	110.90909	123.46029
1.88	17.25637	19.98409	22.97342	26.07107	4.28	91.72060	100.51800	112.08437	124.74609
1.92	18.40247	21.27794	24.43955	27.71947	4.32	92.74428	101.58828	113.24623	126.01685
1.96	19.57070	22.59398	25.92906	29.39288	4.36	93.75746	102.64676	114.39475	127.27267
2.00	20.75967	23.93062	27.44012	31.08926	4.40	94.76019	103.69350	115.53005	128.51367
2.04	21.96799	25.28627	28.97094	32.80656	4.44	95.75251	104.72856	116.65220	129.73998
2.08	23.19428	26.65935	30.51974	34.54279	4.48	96.73448	105.75204	117.76132	130.95172
2.12	24.43720	28.04836	32.08483	36.29605	4.52	97.70615	106.76403	118.85753	132.14902
2.16	25.69538	29.45179	33.66447	38.06443	4.56	98.66759	107.76462	119.94094	133.33202
2.20	26.96750	30.86814	35.25702	39.84607	4.60	99.61187	108.75390	121.01166	134.50085
2.24	28.25228	32.29601	36.86090	41.63921	4.64	100.56005	109.73195	122.06980	135.65566
2.28	29.54845	33.73399	38.47455	43.44212	4.68	101.49120	110.69889	123.11549	136.79658
2.32	30.85479	35.18075	40.09648	45.25316	4.72	102.41240	111.65481	124.14886	137.92376
2.36	32.17010	36.63498	41.72523	47.07071	4.76	103.32372	112.59981	125.17001	139.03734
2.40	33.49323	38.09543	43.35943	48.89326	4.80	104.22526	113.53400	126.17910	140.13749
2.44	34.82307	39.56090	44.99774	50.71932	4.84	105.11708	114.45749	127.17624	141.22434
2.48	36.15855	41.03023	46.63890	52.54751	4.88	105.99927	115.37037	128.16154	142.29804
2.52	37.49862	42.50232	48.28170	54.37649	4.92	106.87191	116.27275	129.13514	143.35872
2.56	38.84229	43.97610	49.92498	56.20500	4.96	107.73511	117.16477	130.09720	144.40658
2.60	40.18862	45.45057	51.56764	58.03181	5.00	108.58891	118.04649	131.04780	145.44171
2.64	41.53668	46.92476	53.20862	59.85579	5.04	109.43346	118.91808	131.98714	146.46433
2.68	42.88560	48.39775	54.84694	61.67587	5.08	110.26882	119.77962	132.91531	147.47456
2.72	44.23455	49.86868	56.48167	63.49103	5.12	111.09504	120.63119	133.83241	148.47251
2.76	45.58275	51.33673	58.11193	65.30031	5.16	111.91227	121.47295	134.73861	149.45837
2.80	46.92945	52.80113	59.73689	67.10281	5.20	112.72058	122.30499	135.63403	150.43229
2.84	48.27394	54.26116	61.35578	68.89771	5.24	113.52007	123.12743	136.51882	151.39441
2.88	49.61554	55.71611	62.96785	70.68419	5.28	114.31087	123.94043	137.39314	152.34495
2.92	50.95361	57.16535	64.57240	72.46151	5.32	115.09303	124.74405	138.25708	153.28400
2.96	52.28755	58.60826	66.16881	74.22899	5.36	115.86663	125.53838	139.11074	154.21168
3.00	53.61681	60.04430	67.75648	75.98600	5.40	116.63180	126.32358	139.95431	155.12819
3.04	54.94085	61.47293	69.33486	77.73195	5.44	117.38860	127.09972	140.78788	156.03364
3.08	56.25917	62.89364	70.90343	79.46629	5.48	118.13715	127.86695	141.61160	156.92821
3.12	57.57130	64.30598	72.46173	81.18851	5.52	118.87752	128.62534	142.42557	157.81200
3.16	58.87680	65.70954	74.00931	82.89817	5.56	119.60983	129.37504	143.22994	158.68518
3.20	60.17527	67.10392	75.54577	84.59483	5.60	120.33417	130.11615	144.02484	159.54790
3.24	61.46634	68.48876	77.07074	86.27811	5.64	121.05063	130.84878	144.81040	160.40030
3.28	62.74966	69.86373	78.58388	87.94766	5.68	121.75930	131.57302	145.58672	161.24250
3.32	64.02490	71.22853	80.08490	89.60317	5.72	122.46026	132.28898	146.35392	162.07464
3.36	65.29176	72.58289	81.57351	91.24435	5.72	123.15360	132.99676	147.11212	162.89687

TABLE V - VARIATION OF $\underline{B}$ WITH MACH NUMBER M AND VELOCITY-PROFILE PARAMETER N - Concluded

$$\left[\underline{B} = \int_1^M v_s \, e^{\int_1^{M_1} \varphi dM_1} \, dM_1\right]$$

(b) Supersonic flow - Concluded

Mach number M	Velocity-profile parameter, N				Mach number M	Velocity-profile parameter, N			
	5	7	9	11		5	7	9	11
5.80	123.83945	133.69650	147.86147	163.70934	8.20	154.21493	164.28196	180.37806	198.80189
5.84	124.51786	134.38828	148.60207	164.51217	8.24	154.58300	164.64741	180.76357	199.21589
5.88	125.18892	135.07219	149.33401	165.30546	8.28	154.94763	165.00931	181.14587	199.62573
5.92	125.85275	135.74837	150.05747	166.08940	8.32	155.30887	165.36773	181.52320	200.03148
5.96	126.50941	136.41687	150.77251	166.86406	8.36	155.66676	165.72271	181.89743	200.43321
6.00	127.15900	137.07783	151.47927	167.62962	8.40	156.02134	166.07427	182.26799	200.83094
6.04	127.80163	137.73136	152.17787	168.38620	8.44	156.37265	166.42247	182.63493	201.22474
6.08	128.43736	138.37754	152.86842	169.13392	8.48	156.72073	166.76735	182.99831	201.61467
6.12	129.06625	139.01643	153.55098	169.87284	8.52	157.06562	167.10894	183.35816	202.00076
6.16	129.68842	139.64816	154.22570	170.60314	8.56	157.40737	167.44729	183.71454	202.38308
6.20	130.30395	140.27283	154.89268	171.32495	8.60	157.74601	167.78245	184.06748	202.76168
6.24	130.91291	140.89052	155.55203	172.03838	8.64	158.08157	168.11446	184.41703	203.13658
6.28	131.51539	141.50132	156.20385	172.74353	8.68	158.41409	168.44335	184.76323	203.50786
6.32	132.11150	142.10537	156.84829	173.44056	8.72	158.74361	168.76915	185.10612	203.87554
6.36	132.70130	142.70273	157.48540	174.12956	8.76	159.07016	169.09192	185.44574	204.23967
6.40	133.28485	143.29347	158.11528	174.81061	8.80	159.39378	169.41167	185.78214	204.60031
6.44	133.86223	143.87769	158.73804	175.48384	8.84	159.71451	169.72847	186.11536	204.95749
6.48	134.43355	144.45549	159.35379	176.14938	8.88	160.03238	170.04233	186.44544	205.31126
6.52	134.99886	145.02692	159.96261	176.80730	8.92	160.34742	170.35330	186.77240	205.66166
6.56	135.55828	145.59210	160.56461	177.45775	8.96	160.65967	170.66141	187.09630	206.00875
6.60	136.11179	146.15113	161.15988	178.10083	9.00	160.96916	170.96669	187.41718	206.35255
6.64	136.65956	146.70405	161.74849	178.73661	9.04	161.27592	171.26919	187.73507	206.69309
6.68	137.20163	147.25096	162.33056	179.36522	9.08	161.57999	171.56893	188.05002	207.03045
6.72	137.73807	147.79194	162.90617	179.98675	9.12	162.88139	171.86595	188.36204	207.36465
6.76	138.26894	148.32705	163.47539	180.60128	9.16	162.18015	172.16027	188.67118	207.69571
6.80	138.79433	148.85640	164.03833	181.20893	9.20	162.47632	172.45195	188.97749	208.02370
6.84	139.31430	149.38004	164.59507	181.80981	9.24	162.76991	172.74099	189.28097	208.34864
6.88	139.82892	149.89807	165.14571	182.40399	9.28	163.06097	173.02745	189.58169	208.67058
6.92	140.33826	150.41055	165.69031	182.99157	9.32	163.34951	173.31135	189.87966	208.98954
6.96	140.84241	150.91759	166.22899	183.57266	9.36	163.63557	173.59271	190.17493	209.30558
7.00	141.34141	151.41921	166.76181	184.14733	9.40	163.91918	173.87158	190.46753	209.61873
7.04	141.83533	151.91551	167.28883	184.71567	9.44	164.20035	174.14796	190.75748	209.92900
7.08	142.32423	152.40656	167.81015	185.27777	9.48	164.47913	174.42192	191.04483	210.23644
7.12	142.80819	152.89244	168.32586	185.83375	9.52	164.75554	174.69346	191.32959	210.54108
7.16	143.28726	153.37319	168.83601	186.38362	9.56	165.02960	174.96260	191.61180	210.84298
7.20	143.76149	153.84890	169.34067	186.92752	9.60	165.30135	175.22939	191.89150	211.14214
7.24	144.23097	154.31964	169.83995	187.46553	9.64	165.57082	176.49387	192.16870	211.43863
7.28	144.69574	154.78544	170.33388	187.99771	9.68	165.83801	175.75603	192.44344	211.73245
7.32	145.15587	155.24641	170.82257	188.52415	9.68	166.10296	176.01591	192.71575	212.02365
7.36	145.61142	155.70260	171.30609	189.04495	9.76	166.36570	176.27355	192.98566	212.31225
7.40	146.06243	156.15406	171.78448	189.56014	9.80	166.62625	176.52897	193.25321	212.59828
7.44	146.50898	156.60087	172.25783	190.06985	9.84	166.88464	176.78220	193.51841	212.88177
7.48	146.95112	157.04309	172.72622	190.57414	9.88	167.14089	177.03326	193.78131	213.16276
7.52	147.38891	157.48077	173.18970	191.07307	9.92	167.39503	177.28217	194.04191	213.44128
7.56	147.82237	157.91397	173.64832	191.56669	9.96	167.64708	177.52896	194.30025	213.71735
7.60	148.25159	158.34275	174.10216	192.05511	10.00	167.89706	177.77366	194.55635	213.99100
7.64	148.67661	158.76717	174.55129	192.53840					
7.68	149.09749	159.18729	174.99577	193.01661					
7.72	149.51428	159.60316	175.43567	193.48982					
7.76	149.92703	160.01484	175.87103	193.95809					
7.80	150.33580	160.42239	176.30193	194.42149					
7.84	150.74063	160.82585	176.72842	194.88009					
7.88	151.14159	161.22530	177.15058	195.33398					
7.92	151.53870	161.62077	177.56844	195.78319					
7.96	151.93202	162.01231	177.98206	196.22777					
8.00	152.32160	162.39999	178.39152	196.66781					
8.04	152.70749	162.78384	178.79687	197.10338					
8.08	153.08972	163.16392	179.19814	197.53451					
8.12	153.46834	163.54026	179.59539	197.96126					
8.16	153.84340	163.91293	179.98868	198.38371					

TABLE VI - VARIATION OF $\underline{C}$ WITH MACH NUMBER M AND VELOCITY-PROFILE PARAMETER N

$$\left[\underline{C} = \int_{0.100}^{M} \psi_w \, e^{-\int_{0.100}^{M_1} \varphi \, dM_1} \, dM_1\right]$$

(a) Subsonic flow

Mach number M	Velocity-profile parameter, N			
	5	7	9	11
0.100	0	0	0	0
.200	.39810	.49987	.60250	.67674
.300	.45070	.57082	.69147	.78359
.400	.46640	.59286	.71971	.81885
.500	.47304	.60245	.73219	.83486
.600	.47649	.60753	.73888	.84362
.700	.47853	.61059	.74294	.84905
.800	.47988	.61263	.74566	.85273
.900	.48082	.61408	.74761	.85541
1.000	.48152	.61518	.74909	.85746

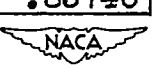

TABLE VI - VARIATION OF $\underline{C}$ WITH MACH NUMBER M AND VELOCITY-PROFILE PARAMETER N - Continued

$$\left[\underline{C} = \int_1^M v_w \, e^{-\int_1^{M_1} \varphi dM_1} \, dM_1\right]$$

(b) Supersonic flow

Mach number	Velocity-profile parameter, N				Mach number	Velocity-profile parameter, N			
M	5	7	9	11	M	5	7	9	11
1.00	0	0	0	0	3.40	9.33213	11.36144	13.27290	15.12415
1.04	.32103	.38855	.45765	.52746	3.44	9.51687	11.58170	13.52334	15.40213
1.08	.61490	.74502	.87793	1.01208	3.48	9.70563	11.80653	13.77872	15.68534
1.12	.88559	1.07405	1.26619	1.45994	3.52	9.89858	12.03610	14.03925	15.97400
1.16	1.13644	1.37952	1.62688	1.87609	3.56	10.09585	12.27059	14.30506	16.26825
1.20	1.37012	1.66458	1.96367	2.26474	3.60	10.29757	12.51017	14.57633	16.56826
1.24	1.58896	1.93192	2.27968	2.62948	3.64	10.50391	12.75497	14.85324	16.87425
1.28	1.79489	2.18382	2.57760	2.97333	3.68	10.71500	13.00517	15.13597	17.18637
1.32	1.98958	2.42226	2.85962	3.29886	3.72	10.93101	13.26095	15.42471	17.50485
1.36	2.17438	2.64883	3.12770	3.60824	3.76	11.15207	13.52244	15.71967	17.82987
1.40	2.35053	2.86500	3.38348	3.90340	3.80	11.37835	13.78986	16.02099	18.16161
1.44	2.51910	3.07199	3.62844	4.18601	3.84	11.61002	14.06340	16.32886	18.50026
1.48	2.68095	3.27088	3.86380	4.45750	3.88	11.84726	14.34320	16.64351	18.84605
1.52	2.83691	3.46262	4.09069	4.71914	3.92	12.09021	14.62947	16.96512	19.19917
1.56	2.98766	3.64805	4.31003	4.97202	3.96	12.33904	14.92240	17.29387	19.55984
1.60	3.13384	3.82790	4.52275	5.21715	4.00	12.59393	15.22218	17.63000	19.92825
1.64	3.27595	4.00283	4.72959	5.45539	4.04	12.85506	15.52903	17.97370	20.30464
1.68	3.41452	4.17343	4.93122	5.68755	4.08	13.12261	15.84313	18.32519	20.68920
1.72	3.55001	4.34019	5.12828	5.91431	4.12	13.39677	16.16467	18.68471	21.08220
1.76	3.68275	4.50363	5.32127	6.13628	4.16	13.67776	16.49389	19.05246	21.48384
1.80	3.81314	4.66414	5.51072	6.35409	4.20	13.96572	16.83098	19.42866	21.89436
1.84	3.94149	4.82213	5.69710	6.56824	4.24	14.26087	17.17617	19.81351	22.31400
1.88	4.06811	4.97796	5.88083	6.77921	4.28	14.56340	17.52970	20.20730	22.74300
1.92	4.19328	5.13194	6.06228	6.98742	4.32	14.87355	17.89176	20.61026	23.18161
1.96	4.31724	5.28436	6.24181	7.19328	4.36	15.19151	18.26263	21.02259	23.63007
2.00	4.44020	5.43552	6.41972	7.39712	4.40	15.51750	18.64251	21.44458	24.08866
2.04	4.56243	5.58571	6.59631	7.59934	4.44	15.85171	19.03167	21.87647	24.55763
2.08	4.68407	5.73512	6.77188	7.80024	4.48	16.19443	19.43032	22.31851	25.03722
2.12	4.80534	5.88399	6.94668	8.00012	4.52	16.54585	19.83875	22.77099	25.52773
2.16	4.92643	6.03256	7.12099	8.19928	4.56	16.90616	20.25720	23.23415	26.02941
2.20	5.04752	6.18101	7.29500	8.39796	4.60	17.27565	20.68592	23.70828	26.54255
2.24	5.16873	6.32952	7.46895	8.59644	4.64	17.65456	21.12520	24.19368	27.06745
2.28	5.29023	6.47832	7.64308	8.79492	4.68	18.04313	21.57533	24.69061	27.60440
2.32	5.41216	6.62755	7.81757	8.99364	4.72	18.44165	22.03656	25.19936	28.15371
2.36	5.53469	6.77738	7.99260	9.19284	4.76	18.85033	22.50914	25.72023	28.71564
2.40	5.65794	6.92798	8.16840	9.39271	4.80	19.26945	22.99341	26.25352	29.29056
2.44	5.78203	7.07949	8.34511	9.59343	4.84	19.69930	23.48967	26.79953	29.87874
2.48	5.90713	7.23208	8.52290	9.79522	4.88	20.14014	23.99819	27.35861	30.48050
2.52	6.03332	7.38592	8.70195	9.99826	4.92	20.59226	24.51931	27.93103	31.09618
2.56	6.16076	7.54114	8.88244	10.20274	4.96	21.05594	25.05332	28.51717	31.72612
2.60	6.28958	7.69786	9.06449	10.40884	5.00	21.53145	25.60054	29.11730	32.37060
2.64	6.41985	7.85625	9.24828	10.61669	5.04	22.01914	26.16133	29.73183	33.03007
2.68	6.55173	8.01644	9.43399	10.82651	5.08	22.51930	26.73602	30.36106	33.70484
2.72	6.68530	8.17856	9.62174	11.03844	5.12	23.03219	27.32488	31.00534	34.39521
2.76	6.82072	8.34273	9.81170	11.25270	5.16	23.55816	27.92832	31.66504	35.10159
2.80	6.95807	8.50911	10.00401	11.46942	5.20	24.09757	28.54670	32.34053	35.82436
2.84	7.09750	8.67783	10.19884	11.68873	5.24	24.65072	29.18037	33.03217	36.56388
2.88	7.23910	8.84902	10.39631	11.91081	5.28	25.21797	29.82970	33.74041	37.32060
2.92	7.38299	9.02284	10.59659	12.13587	5.32	25.79964	30.49506	34.46558	38.09485
2.96	7.52928	9.19937	10.79981	12.36400	5.36	26.39611	31.17685	35.20804	38.88704
3.00	7.67809	9.37878	11.00614	12.59538	5.40	27.00771	31.87544	35.96825	39.69759
3.04	7.82958	9.56119	11.21572	12.83018	5.44	27.63480	32.59120	36.74659	40.52687
3.08	7.98383	9.74677	11.42868	13.06857	5.48	28.27778	33.32459	37.54352	41.37539
3.12	8.14097	9.93565	11.64518	13.31073	5.52	28.93702	34.07600	38.35938	42.24350
3.16	8.30112	10.12795	11.86539	13.55679	5.56	29.61289	34.84589	39.19468	43.13171
3.20	8.46439	10.32379	12.08944	13.80688	5.60	30.30585	35.63463	40.04989	44.04045
3.24	8.63090	10.52334	12.31750	14.06122	5.64	31.01623	36.44269	40.92539	44.97018
3.28	8.80082	10.72674	12.54971	14.31995	5.68	31.74448	37.27054	41.82169	45.92133
3.32	8.97423	10.93411	12.78624	14.58324	5.72	32.49098	38.11856	42.73923	46.89438
3.36	9.15129	11.14562	13.02726	14.85126	5.76	33.25619	38.98727	43.67849	47.88981

TABLE VI - VARIATION OF $\underline{C}$ WITH MACH NUMBER M AND VELOCITY-PROFILE PARAMETER N - Concluded

$$\left[\underline{C} = \int_1^M \nu_w \, e^{-\int_1^{M_1} \varphi dM_1} \, dM_1\right]$$

(b) Supersonic flow - Concluded

Mach number M	Velocity-profile parameter, N				Mach number M	Velocity-profile parameter, N			
	5	7	9	11		5	7	9	11
5.80	34.04058	39.87719	44.63999	48.90818	8.20	138.57367	156.22375	167.73563	176.72228
5.84	34.84455	40.78872	45.62418	49.94991	8.24	141.76665	159.74325	171.41737	180.50350
5.88	35.66856	41.72235	46.63165	51.01549	8.28	145.02788	163.33682	175.17510	184.36130
5.92	36.51308	42.67865	47.66267	52.10553	8.32	148.35877	167.00594	179.01035	188.29712
5.96	37.37855	43.65802	48.71799	53.22048	8.36	151.76054	170.75199	182.92450	192.31239
6.00	38.26548	44.66107	49.79813	54.36092	8.40	155.23439	174.57621	186.91876	196.40834
6.04	39.17436	45.68835	50.90360	55.52740	8.44	158.78181	178.48022	190.99480	200.58656
6.08	40.10568	46.74034	52.03496	56.72044	8.48	162.40408	182.46537	195.15400	204.84844
6.12	41.05988	47.81754	53.19268	57.94056	8.52	166.10256	186.53319	199.39785	209.19544
6.16	42.03754	48.92055	54.37741	59.18840	8.56	169.87867	190.68514	203.72786	213.62907
6.20	43.03920	50.04996	55.58974	60.46455	8.60	173.73380	194.92271	208.14551	218.15080
6.24	44.06535	51.20636	56.83022	61.76957	8.64	177.66934	199.24745	212.65238	222.76218
6.28	45.11657	52.39030	58.09948	63.10406	8.68	181.68677	203.66088	217.25002	227.46481
6.32	46.19346	53.60248	59.39819	64.46876	8.72	185.78753	208.16460	221.94000	232.26019
6.36	47.29652	54.84342	60.72692	65.86415	8.76	189.97304	212.76014	226.72393	237.14984
6.40	48.42629	56.11371	62.08625	67.29091	8.80	194.24488	217.44915	231.60339	242.13544
6.44	49.58338	57.41401	63.47686	68.74968	8.84	198.60459	222.23331	236.58016	247.21872
6.48	50.76846	58.74501	64.89949	70.24119	8.88	203.05366	227.11426	241.65587	252.40126
6.52	51.98206	60.10730	66.35471	71.76602	8.92	207.59368	232.09363	246.83215	257.68471
6.56	53.22482	61.50162	67.84327	73.32492	8.96	212.22646	237.17347	252.11101	263.07105
6.60	54.49742	62.92867	69.36584	74.91859	9.00	216.95340	242.35520	257.49397	268.56171
6.64	55.80041	64.38901	70.92307	76.54764	9.04	221.77615	247.64056	262.98274	274.15853
6.68	57.13448	65.88341	72.51574	78.21285	9.08	226.69652	253.03162	268.57940	279.86345
6.72	58.50029	67.41263	74.14457	79.91495	9.12	231.71397	258.52988	274.28544	285.67802
6.76	59.89847	68.97729	75.81022	81.65464	9.16	236.83632	264.13726	280.10284	291.60414
6.80	61.32976	70.57820	77.51354	83.43273	9.20	242.05946	269.85587	286.03374	297.64390
6.84	62.79484	72.21609	79.25527	85.24996	9.24	247.38684	275.68726	292.07968	303.79886
6.88	64.29447	73.89176	81.03618	87.10709	9.28	252.82063	281.63370	298.24294	310.07122
6.92	65.82932	75.60595	82.85705	89.00494	9.32	258.36231	287.69679	304.52506	316.46286
6.96	67.40019	77.35953	84.71880	90.94443	9.36	264.01392	293.87883	310.92840	322.97536
7.00	69.00773	79.15324	86.62213	92.92625	9.40	269.77737	300.18173	317.45495	329.61134
7.04	70.65273	80.98789	88.56790	94.95120	9.44	275.65425	306.60730	324.10647	336.37229
7.08	72.33596	82.86432	90.55696	97.02018	9.48	281.64688	313.15791	330.88533	343.26059
7.12	74.05831	84.78343	92.59020	99.13410	9.52	287.75671	319.83524	337.79324	350.27793
7.16	75.82043	86.74601	94.66841	101.29372	9.56	293.98599	326.64168	344.83265	357.42663
7.20	77.62318	88.75295	96.79249	103.49994	9.60	300.33682	333.57950	352.00576	364.70905
7.24	79.46743	90.80518	98.96346	105.75377	9.64	306.81116	340.65083	359.31477	372.12725
7.28	81.35394	92.90351	101.18209	108.05598	9.68	313.41086	347.85752	366.76153	379.68307
7.32	83.28364	95.04897	103.44946	110.40765	9.72	320.13808	355.20202	374.34854	387.37896
7.36	85.25741	97.24251	105.76649	112.80970	9.76	326.99498	362.68658	382.07803	395.21710
7.40	87.27602	99.48492	108.13401	115.26296	9.80	333.98379	370.31362	389.95246	403.19990
7.44	89.34048	101.77732	110.55313	117.76854	9.84	341.10660	378.08541	397.97404	411.32964
7.48	91.45169	104.12067	113.02486	120.32745	9.88	348.36557	386.00431	406.14518	419.60865
7.52	93.61056	106.51594	115.55015	122.94063	9.92	355.76295	394.07276	414.46825	428.03928
7.56	95.81788	108.96399	118.12990	125.60894	9.96	363.30101	402.29309	422.94569	436.62392
7.60	98.07476	111.46603	120.76532	128.33364	10.00	370.98194	410.66765	431.57986	445.36484
7.64	100.38216	114.02309	123.45744	131.11571					
7.68	102.74105	116.63620	126.20734	133.95622					
7.72	105.15249	119.30643	129.01606	136.85630					
7.76	107.61745	122.03486	131.88477	139.81703					
7.80	110.13698	124.82266	134.81460	142.83954					
7.84	112.71211	127.67097	137.80668	145.92493					
7.88	115.34400	130.58097	140.86228	149.07450					
7.92	118.03361	133.55372	143.98240	152.28928					
7.96	120.78206	136.59041	147.16827	155.57042					
8.00	123.59064	139.69240	150.42129	158.91936					
8.04	126.46040	142.86089	153.74266	162.33723					
8.08	129.39237	146.09699	157.13345	165.82516					
8.12	132.38774	149.40192	160.59497	169.38441					
8.16	135.44781	152.77712	164.12863	173.01640					

TABLE VII - VARIATION OF $\underline{D}$ WITH MACH NUMBER M AND VELOCITY-PROFILE PARAMETER N

$$\left[\underline{D} = \int_{0.100}^{M} \psi_s \, e^{-\int_{0.100}^{M_1} \varphi \, dM_1} \, dM_1\right]$$

(a) Subsonic flow

Mach number M	Velocity-profile parameter, N			
	5	7	9	11
0.100	0	0	0	0
.200	.39908	.50111	.60400	.67845
.300	.45211	.57264	.69370	.78618
.400	.46806	.59505	.72242	.82203
.500	.47490	.60491	.73525	.83849
.600	.47849	.61020	.74222	.84762
.700	.48066	.61345	.74652	.85337
.800	.48210	.61564	.74946	.85734
.900	.48314	.61724	.75160	.86029
1.000	.48393	.61848	.75327	.86260

TABLE VII - VARIATION OF $\underline{D}$ WITH MACH NUMBER M AND VELOCITY-PROFILE PARAMETER N - Continued

$$\left[\underline{D} = \int_1^M \overline{v}_s \, e^{-\int_1^{M_1} \varphi dM_1} \, dM_1\right]$$

(b) Supersonic flow

Mach number	Velocity-profile parameter, N				Mach number	Velocity-profile parameter, N			
M	5	7	9	11	M	5	7	9	11
1.00	0	0	0	0	3.40	15.19799	18.47281	21.51765	24.44626
1.04	.36742	.44468	.52379	.60370	3.44	15.63507	18.99397	22.11021	25.10401
1.08	.70707	.85667	1.00954	1.16379	3.48	16.08696	19.53225	22.72159	25.78204
1.12	1.02306	1.24079	1.46280	1.68661	3.52	16.55426	20.08851	23.35255	26.48112
1.16	1.31887	1.60103	1.88819	2.17742	3.56	17.03758	20.66285	24.00383	27.20204
1.20	1.59737	1.94075	2.28958	2.64063	3.60	17.53757	21.25662	24.67622	27.94564
1.24	1.86097	2.26278	2.67026	3.07999	3.64	18.05486	21.87034	25.37050	28.71274
1.28	2.11172	2.56954	3.03300	3.49869	3.68	18.59015	22.50479	26.08751	29.50424
1.32	2.35137	2.86308	3.38022	3.89945	3.72	19.14415	23.16077	26.82809	30.32102
1.36	2.58147	3.14517	3.71397	4.28464	3.76	19.71755	23.83907	27.59313	31.16401
1.40	2.80329	3.41738	4.03607	4.65633	3.80	20.31116	24.54056	28.38354	32.03417
1.44	3.01801	3.68105	4.34808	5.01631	3.84	20.92571	25.26610	29.20023	32.93246
1.48	3.22661	3.93737	4.65138	5.36617	3.88	21.56199	26.01659	30.04419	33.85991
1.52	2.42998	4.18741	4.94720	5.70731	3.92	22.22088	26.79298	30.91641	34.81757
1.56	3.62890	4.43210	5.23666	6.04100	3.96	22.90318	27.59621	31.81791	35.80651
1.60	3.82410	4.67230	5.52073	6.36835	4.00	23.60979	28.42727	32.74975	36.82783
1.64	4.01619	4.90875	5.80029	6.69037	4.04	24.34165	29.28718	33.71302	37.88266
1.68	4.20580	5.14215	6.07615	7.00802	4.08	25.09967	30.17700	34.70883	38.97219
1.72	4.39344	5.37315	6.34908	7.32212	4.12	25.88482	31.09781	35.73836	40.09762
1.76	4.57963	5.60235	6.61973	7.63345	4.16	26.69811	32.05074	36.80279	41.26021
1.80	4.76480	5.83027	6.88875	7.94273	4.20	27.54056	33.03695	37.90336	42.46125
1.84	4.94937	6.05742	7.15673	8.25060	4.24	28.41325	34.05762	39.04133	43.70201
1.88	5.13371	6.28428	7.42421	8.55772	4.28	29.31731	35.11398	40.21801	44.98391
1.92	5.31823	6.51129	7.69171	8.86468	4.32	30.25384	36.20731	41.43475	46.30834
1.96	5.50329	6.73889	7.95972	9.17202	4.36	31.22403	37.33892	42.69293	47.67674
2.00	5.68924	6.96748	8.22873	9.48030	4.40	32.22908	38.51015	43.99398	49.09058
2.04	5.87639	7.19746	8.49918	9.79000	4.44	33.27025	39.72238	45.33937	50.55140
2.08	6.06509	7.42922	8.77150	10.10162	4.48	34.34881	40.97706	46.73062	52.06078
2.12	6.25561	7.66312	9.04613	10.41564	4.52	35.46608	42.27567	48.16930	53.62034
2.16	6.44829	7.89951	9.32347	10.73253	4.56	36.62348	43.61972	49.65701	55.23175
2.20	6.64342	8.13876	9.60393	11.05273	4.60	37.82240	45.01078	51.19543	56.89673
2.24	6.84126	8.38120	9.88791	11.37668	4.64	39.06428	46.45047	52.78623	58.61703
2.28	7.04215	8.62720	10.17580	11.70482	4.68	40.35062	47.94046	54.43119	60.39450
2.32	7.24635	8.87710	10.46799	12.03760	4.72	41.68298	49.48246	56.13212	62.23099
2.36	7.45420	9.13123	10.76487	12.37544	4.76	43.06293	51.07824	57.89086	64.12841
2.40	7.66595	9.38994	11.06683	12.71876	4.80	44.49217	52.72964	59.70937	66.08879
2.44	7.88190	9.65358	11.37426	13.06800	4.84	45.97231	54.43850	61.58959	68.11411
2.48	8.10235	9.92250	11.68755	13.42358	4.88	47.50515	56.20674	63.53353	70.20648
2.52	8.32760	10.19705	12.00710	27.78995	4.92	49.09248	58.03635	65.54329	72.36804
2.56	8.55795	10.47760	12.33330	14.15553	4.96	50.73617	59.92943	67.62106	74.60108
2.60	8.79370	10.76449	12.66656	14.53278	5.00	52.43803	61.88799	69.76894	76.90774
2.64	9.03521	11.05810	13.00730	14.91812	5.04	54.20014	63.91431	71.98936	79.29051
2.68	9.28278	11.35881	13.35592	15.31203	5.08	56.02450	66.01057	74.28457	81.75175
2.72	9.53672	11.66699	13.71286	15.71496	5.12	57.91308	68.17895	76.65688	84.29377
2.76	9.79739	11.98304	14.07854	16.12739	5.16	59.86810	70.42193	79.10887	86.91929
2.80	10.06513	12.30736	14.45342	16.54979	5.20	61.89176	72.74192	81.64308	89.63087
2.84	10.34030	12.64036	14.83794	16.98265	5.24	63.98633	75.14138	84.26207	92.43116
2.88	10.62327	12.98247	15.23257	17.42648	5.28	66.15425	77.62304	86.96872	95.32312
2.92	10.91440	13.33411	15.63778	17.88178	5.32	68.39780	80.18940	89.76560	98.30939
2.96	11.21410	13.69573	16.05406	18.34909	5.36	70.71937	82.84310	92.65549	101.39282
3.00	11.52275	14.06779	16.48191	18.82895	5.40	73.12166	85.58710	95.64149	104.57656
3.04	11.84076	14.45075	16.92185	19.32189	5.44	75.60714	88.42412	98.72641	107.86349
3.08	12.16855	14.84509	17.37441	19.82849	5.48	78.17859	91.35722	101.91347	111.25694
3.12	12.50655	15.25131	17.84013	20.34934	5.52	80.83867	94.38930	105.20568	114.75997
3.16	12.85522	15.66994	18.31956	20.88502	5.56	83.59036	97.52361	108.60643	118.37603
3.20	13.21500	16.10148	18.81329	21.43614	5.60	86.43651	100.76333	112.11904	122.10854
3.24	13.58637	16.54651	19.32190	22.00334	5.64	89.39015	104.11175	115.74692	125.96098
3.28	13.96985	17.00556	19.84599	22.58728	5.68	92.42435	107.57221	119.49354	129.93690
3.32	14.36593	17.47923	20.38621	23.18862	5.72	95.57223	111.14816	123.36251	134.03996
3.36	14.77514	17.96811	20.94321	23.80804	5.76	98.82699	114.84315	127.35751	138.27394

1207

TABLE VII - VARIATION OF D WITH MACH NUMBER M AND VELOCITY-PROFILE PARAMETER N - Concluded

$$\left[D = \int_1^M Y_s \cdot e^{-\int_1^{M_1} \varphi dM_1} dM_1\right]$$

NACA

(b) Supersonic flow - Concluded

Mach number	Velocity-profile parameter, N			
M	5	7	9	11
5.80	102.19219	118.66101	131.48250	142.64288
5.84	105.67108	122.60533	135.74123	147.15058
5.88	109.26719	126.67995	140.13766	151.80110
5.92	112.98429	130.88898	144.67610	156.59883
5.96	116.82588	135.23630	149.36054	161.54780
6.00	120.79595	139.72625	154.19549	166.65262
6.04	124.89849	144.36316	159.18544	171.91786
6.08	129.13742	149.15156	164.33484	177.34806
6.12	133.51664	154.09508	169.64807	182.94766
6.16	138.04069	159.19924	175.13026	188.72186
6.20	142.71385	164.46854	180.78626	194.67562
6.24	147.54056	169.90784	186.62111	200.81400
6.28	152.52538	175.52210	192.63992	207.14221
6.32	157.67333	181.31680	198.84836	213.66603
6.36	162.98893	187.29688	205.25150	220.39058
6.40	168.47705	193.46761	211.85480	227.32137
6.44	174.14283	199.83455	218.66402	234.46425
6.48	179.99167	206.40366	225.68526	241.82542
6.52	186.02863	213.18040	232.92419	249.41059
6.56	192.25944	220.17104	240.38725	257.22651
6.60	198.68944	227.38166	248.08071	265.27891
6.64	205.32462	234.81820	256.01066	273.57456
6.68	212.17086	242.48729	264.18399	282.12020
6.72	219.23411	250.39547	272.60740	290.92259
6.76	226.52032	258.54914	281.28745	299.98838
6.80	234.03616	266.95557	290.23163	309.32513
6.84	241.78805	275.62178	299.44716	318.94015
6.88	249.78265	284.55495	308.94143	328.84088
6.92	258.02670	293.76242	318.72196	339.03492
6.96	266.52765	303.25224	328.79706	349.53060
7.00	275.29213	313.03166	339.17414	360.33543
7.04	284.32750	323.10867	349.86139	371.45768
7.08	293.64131	333.49141	360.86717	382.90576
7.12	303.24151	344.18857	372.20039	394.68863
7.16	313.13580	355.20819	383.86932	406.81461
7.20	323.33157	366.55899	395.88285	419.29266
7.24	333.83815	378.25041	408.25071	432.13258
7.28	344.66318	390.29095	420.98156	445.34306
7.32	355.81576	402.69051	434.08556	458.93430
7.36	367.30473	415.45859	447.57245	472.91613
7.40	379.13850	428.60431	461.45155	487.29791
7.44	391.32696	442.13849	475.73391	502.09073
7.48	403.87966	456.07131	490.42997	517.30615
7.52	416.80597	470.41301	505.55022	532.95158
7.56	430.11516	485.17360	521.10479	549.04026
7.60	443.81803	500.36479	537.10577	565.58328
7.64	457.92492	515.99776	553.56453	582.59209
7.68	472.44650	532.08393	570.49281	600.07837
7.72	487.39337	548.63492	587.90239	618.05406
7.76	502.77662	565.66264	605.80545	636.53124
7.80	518.60769	583.17958	624.21465	655.52273
7.84	534.89806	601.19809	643.14267	675.04119
7.88	551.66023	619.73158	662.60325	695.10038
7.92	568.90534	638.79213	682.60873	715.71264
7.96	586.64600	658.39338	703.17286	736.89167
8.00	604.89544	678.54972	724.31039	758.65238
8.04	623.66648	699.27490	746.03540	781.00877
8.08	642.97142	720.58232	768.36144	803.97443
8.12	662.82375	742.48648	791.30332	827.56408
8.16	683.23811	765.00581	814.87712	851.79388

Mach number	Velocity-profile parameter, N			
M	5	7	9	11
8.20	704.22753	788.14653	839.09716	876.67806
8.24	725.80729	811.93295	863.98025	902.23354
8.28	747.99119	836.37739	889.54154	928.47535
8.32	770.79491	861.49685	915.79834	955.42084
8.36	794.23387	887.30784	942.76742	983.08678
8.40	818.32260	913.82609	970.46480	1011.48919
8.44	843.07810	941.07008	998.90924	1040.64673
8.48	868.51635	969.05692	1028.11822	1070.57675
8.52	894.65386	997.80451	1058.10984	1101.29738
8.56	921.50789	1027.33142	1088.90301	1132.82750
8.60	949.09585	1057.65626	1120.51666	1165.18604
8.64	977.43520	1088.79812	1152.97009	1198.39220
8.68	1006.54384	1120.77622	1186.28286	1232.46555
8.72	1036.44012	1153.61038	1220.47515	1267.42615
8.76	1067.14293	1187.32095	1255.56766	1303.29440
8.80	1098.67127	1221.92845	1291.58096	1340.09106
8.84	1131.04492	1257.45421	1328.53686	1377.83784
8.88	1164.28394	1293.91979	1366.45723	1416.55647
8.92	1198.40799	1331.34647	1405.36367	1456.26839
8.96	1233.43951	1369.75840	1445.28062	1496.99805
9.00	1269.39846	1409.17699	1486.22986	1538.76693
9.04	1306.30631	1449.62545	1528.23486	1581.59863
9.08	1344.18616	1491.12901	1571.32110	1625.51841
9.12	1383.05935	1533.71041	1615.51170	1670.54917
9.16	1422.94822	1577.39363	1660.83109	1716.71534
9.20	1463.87825	1622.20636	1707.30729	1764.04460
9.24	1505.87136	1668.17208	1754.96396	1812.56057
9.28	1548.95384	1715.31908	1803.82974	1862.29158
9.32	1593.14790	1763.67143	1853.92904	1913.26220
9.36	1638.48112	1813.25891	1905.29182	1965.50203
9.40	1684.97889	1864.10890	1957.94609	2019.03889
9.44	1732.66525	1916.24726	2011.91780	2073.89846
9.48	1781.57000	1969.70584	2067.23919	2130.11288
9.52	1831.71713	2024.51064	2123.93682	2187.70840
9.56	1883.13651	2080.69407	2182.04327	2246.71741
9.60	1935.85720	2138.28729	2241.59011	2307.17127
9.64	1989.90769	2197.32130	2302.60853	2369.10117
9.68	2045.31505	2257.82483	2365.12758	2432.53565
9.72	2102.11066	2319.83186	2429.18210	2497.50903
9.76	2160.32503	2383.37553	2494.80501	2564.05431
9.80	2219.98971	2448.48958	2562.03062	2632.20556
9.84	2281.13674	2515.20836	2630.89366	2701.99692
9.88	2343.79813	2583.56682	2701.42919	2773.46351
9.92	2408.00655	2653.59966	2773.67255	2846.63999
9.96	2473.79528	2725.34292	2847.66003	2921.56240
10.00	2541.19865	2798.83329	2923.42869	2998.26759

TABLE VIII - VARIATION OF $\underline{E}$ WITH MACH NUMBER M AND VELOCITY-PROFILE PARAMETER N

$$\left[\underline{E} = e^{-\int_{0.100}^{M} \varphi dM_1}\right]$$

(a) Subsonic flow

Mach number M	Velocity-profile parameter, N			
	5	7	9	11
0.100	1.0000000	1.0000000	1.0000000	1.0000000
.200	.0966699	.1045974	.1092891	.1176454
.300	.0251985	.0285359	.0305797	.0343666
.400	.0099328	.0116115	.0126636	.0146729
.500	.0049379	.0059131	.0065348	.0077527
.600	.0028542	.0034839	.0038905	.0047054
.700	.0018362	.0022766	.0025639	.0031517
.800	.0012804	.0016083	.0018239	.0022736
.900	.0009432	.0012079	.0013777	.0017387
1.000	.0007312	.0009530	.0010924	.0013937

TABLE VIII - VARIATION OF $\underline{E}$ WITH MACH NUMBER M AND VELOCITY-PROFILE PARAMETER N - Continued

$$\left[\underline{E} = e^{-\int_1^M \varphi dM_1}\right]$$

NACA

(b) Supersonic flow

Mach number	Velocity-profile parameter, N				Mach number	Velocity-profile parameter, N			
M	5	7	9	11	M	5	7	9	11
1.00	1.00000	1.00000	1.00000	1.00000	3.40	0.58555	0.61904	0.63006	0.63254
1.04	.91732	.92040	.92197	.92291	3.44	.59750	.63170	.64281	.64516
1.08	.84675	.85227	.85509	.85677	3.48	.60984	.64475	.65595	.65816
1.12	.78618	.79365	.79747	.79973	3.52	.62256	.65821	.66949	.67157
1.16	.73392	.74297	.74758	.75030	3.56	.63567	.67208	.68344	.68537
1.20	.68864	.69897	.70422	.70730	3.60	.64918	.68636	.69781	.69958
1.24	.64925	.66063	.66639	.66976	3.64	.66309	.70106	.71259	.71420
1.28	.61486	.62710	.63329	.63689	3.68	.67740	.71619	.72780	.72924
1.32	.58476	.59772	.60425	.60803	3.72	.69213	.73175	.74345	.74470
1.36	.55835	.57191	.57871	.58265	3.76	.70727	.74776	.75953	.76060
1.40	.53512	.54920	.55624	.56028	3.80	.72285	.76421	.77606	.77693
1.44	.51467	.52919	.53642	.54056	3.84	.73886	.78111	.79304	.79370
1.48	.49666	.51157	.51896	.52317	3.88	.75530	.79848	.81048	.81093
1.52	.48078	.49603	.50356	.50783	3.92	.77220	.81631	.82838	.82861
1.56	.46680	.48236	.49001	.49431	3.96	.78954	.83462	.84676	.84676
1.60	.45450	.47034	.47809	.48243	4.00	.80735	.85342	.86563	.86538
1.64	.44370	.45980	.46764	.47200	4.04	.82563	.87271	.88498	.88448
1.68	.43424	.45060	.45852	.46289	4.08	.84439	.89250	.90484	.90407
1.72	.42601	.44260	.45059	.45497	4.12	.86364	.91280	.92520	.92415
1.76	.41887	.43569	.44375	.44814	4.16	.88337	.93362	.94607	.94474
1.80	.41273	.42978	.43790	.44229	4.20	.90361	.95496	.96747	.96583
1.84	.40751	.42479	.43297	.43736	4.24	.92436	.97684	.98940	.98745
1.88	.40313	.42063	.42887	.43325	4.28	.94563	.99927	1.01188	1.00960
1.92	.39953	.41726	.42555	.42993	4.32	.96743	1.02224	1.03490	1.03229
1.96	.39664	.41460	.42295	.42731	4.36	.98976	1.04579	1.05849	1.05552
2.00	.39442	.41262	.42102	.42537	4.40	1.01264	1.06990	1.08264	1.07931
2.04	.39282	.41126	.41972	.42406	4.44	1.03607	1.09460	1.10737	1.10367
2.08	.39180	.41050	.41901	.42334	4.48	1.06007	1.11989	1.13270	1.12859
2.12	.39134	.41029	.41887	.42317	4.52	1.08465	1.14579	1.15862	1.15411
2.16	.39140	.41062	.41925	.42354	4.56	1.10980	1.17230	1.18515	1.18021
2.20	.39196	.41145	.42014	.42441	4.60	1.13556	1.19943	1.21229	1.20692
2.24	.39298	.41276	.42151	.42576	4.64	1.16191	1.22719	1.24007	1.23425
2.28	.39446	.41453	.42334	.42757	4.68	1.18888	1.25560	1.26849	1.26220
2.32	.39637	.41674	.42562	.42982	4.72	1.21648	1.28467	1.29756	1.29078
2.36	.39870	.41939	.42833	.43250	4.76	1.24471	1.31440	1.32729	1.32000
2.40	.40143	.42245	.43145	.43560	4.80	1.27358	1.34482	1.35769	1.34988
2.44	.40456	.42591	.43498	.43910	4.84	1.30311	1.37592	1.38878	1.38043
2.48	.40807	.42977	.43891	.44300	4.88	1.33331	1.40772	1.42056	1.41166
2.52	.41195	.43401	.44322	.44728	4.92	1.36419	1.44023	1.45305	1.44357
2.56	.41620	.43864	.44792	.45194	4.96	1.39576	1.47347	1.48626	1.47618
2.60	.42081	.44363	.45299	.45697	5.00	1.42803	1.50745	1.52019	1.50950
2.64	.42577	.44899	.45842	.46236	5.04	1.46101	1.54217	1.55487	1.54355
2.68	.43108	.45471	.46422	.46812	5.08	1.49472	1.57766	1.59031	1.57832
2.72	.43674	.46080	.47038	.47424	5.12	1.52916	1.61392	1.62651	1.61385
2.76	.44275	.46724	.47690	.48070	5.16	1.56435	1.65096	1.66349	1.65015
2.80	.44909	.47403	.48377	.48753	5.20	1.60031	1.68881	1.70126	1.68718
2.84	.45577	.48118	.49100	.49470	5.24	1.63703	1.72747	1.73983	1.72501
2.88	.46280	.48868	.49859	.50223	5.28	1.67454	1.76695	1.77923	1.76364
2.92	.47016	.49654	.50655	.51011	5.32	1.71285	1.80727	1.81945	1.80307
2.96	.47787	.50475	.51482	.51833	5.36	1.75197	1.84845	1.86052	1.84333
3.00	.48591	.51331	.52347	.52691	5.40	1.79192	1.89049	1.90245	1.88442
3.04	.49429	.52224	.53248	.53585	5.44	1.83270	1.93341	1.94524	1.92635
3.08	.50302	.53152	.54184	.54513	5.48	1.87433	1.97722	1.98892	1.96914
3.12	.51210	.54116	.55157	.55478	5.52	1.91682	2.02194	2.03350	2.01281
3.16	.52152	.55116	.56167	.56478	5.56	1.96020	2.06759	2.07900	2.05736
3.20	.53129	.56154	.57213	.57515	5.60	2.00446	2.11417	2.12542	2.10281
3.24	.54142	.57228	.58296	.58588	5.64	2.04963	2.16170	2.17278	2.14918
3.28	.55191	.58340	.59416	.59698	5.68	2.09572	2.21020	2.22110	2.19647
3.32	.56275	.59489	.60574	.60846	5.72	2.14274	2.25968	2.27038	2.24471
3.36	.57396	.60677	.61771	.62031	5.76	2.19070	2.31017	2.32067	2.29392

TABLE VIII - VARIATION OF $\frac{E}{E^*}$ WITH MACH NUMBER M AND VELOCITY-PROFILE PARAMETER N - Concluded

$$\left[\frac{E}{E^*} = e^{-\int_1^M \phi dM_1}\right]$$

(b) Supersonic flow - Concluded

Mach number	Velocity-profile parameter, N				Mach number	Velocity-profile parameter, N			
M	5	7	9	11	M	5	7	9	11
5.80	2.23963	2.36166	2.37195	2.34406	8.20	7.58628	7.99306	7.96007	7.78500
5.84	2.28954	2.41418	2.42424	2.39523	8.24	7.72817	8.14271	8.10829	7.92893
5.88	2.34044	2.46774	2.47757	2.44738	8.28	7.87226	8.29469	8.25883	8.07509
5.92	2.39235	2.52235	2.53194	2.50065	8.32	8.01858	8.44904	8.41170	8.22350
5.96	2.44527	2.57805	2.58737	2.55475	8.36	8.16716	8.60578	8.56692	8.37419
6.00	2.49924	2.63483	2.64389	2.60999	8.40	8.31802	8.76494	8.72454	8.52719
6.04	2.55426	2.69273	2.70150	2.66630	8.44	8.47120	8.92655	8.88458	8.68252
6.08	2.61034	2.75175	2.76022	2.72368	8.48	8.62670	9.09064	9.04706	8.84022
6.12	2.66751	2.81190	2.82007	2.78216	8.52	8.78457	9.25724	9.21202	9.00030
6.16	2.72578	2.87322	2.88106	2.84174	8.56	8.94484	9.42637	9.37948	9.16281
6.20	2.78517	2.93571	2.94322	2.90246	8.60	9.10752	9.59807	9.54948	9.32776
6.24	2.84569	2.99940	3.00655	2.96431	8.64	9.27264	9.77237	9.72204	9.49518
6.28	2.90736	3.06429	3.07108	3.02733	8.68	9.44024	9.94929	9.89719	9.66511
6.32	2.97019	3.13042	3.13683	3.09151	8.72	9.61034	10.12886	10.07496	9.83757
6.36	3.03421	3.19779	3.20380	3.15690	8.76	9.78297	10.31112	10.25539	10.01258
6.40	3.09943	3.26642	3.27203	3.22349	8.80	9.95816	10.49610	10.43850	10.19019
6.44	3.16586	3.33633	3.34152	3.29151	8.84	10.13594	10.68383	10.62432	10.37042
6.48	3.23353	3.40755	3.41230	3.36037	8.88	10.31633	10.87434	10.81289	10.55329
6.52	3.30245	3.48008	3.48438	3.43069	8.92	10.49937	11.06766	11.00423	10.73885
6.56	3.37264	3.55396	3.55778	3.50230	8.96	10.68508	11.26382	11.19838	10.92711
6.60	3.44412	3.62918	3.63252	3.57520	9.00	10.87350	11.46286	11.39538	11.11812
6.64	3.51690	3.70579	3.70862	3.64942	9.04	11.06465	11.66481	11.59524	11.31190
6.68	3.59101	3.78379	3.78610	3.72497	9.08	11.25857	11.86969	11.79800	11.50847
6.72	3.66646	3.86320	3.86498	3.80188	9.12	11.45528	12.07754	12.00369	11.70788
6.76	3.74327	3.94405	3.94527	3.88015	9.16	11.65482	12.28840	12.21236	11.91015
6.80	3.82146	4.02636	4.02701	3.95982	9.20	11.85722	12.50230	12.42402	12.11532
6.84	3.90104	4.11014	4.11019	4.04089	9.24	12.06250	12.71926	12.63872	12.32341
6.88	3.98205	4.19541	4.19486	4.12340	9.28	12.27070	12.93934	12.85648	12.53446
6.92	4.06449	4.28220	4.28102	4.20735	9.32	12.48184	13.16255	13.07734	12.74851
6.96	4.14839	4.37052	4.36870	4.29277	9.36	12.69597	13.38893	13.30134	12.96557
7.00	4.23376	4.46041	4.45792	4.37968	9.40	12.91311	13.61853	13.52850	13.18570
7.04	4.32063	4.55187	4.54869	4.46809	9.44	13.13329	13.85136	13.75887	13.40891
7.08	4.40901	4.64493	4.64105	4.55804	9.48	13.35655	14.08747	13.99247	13.63525
7.12	4.49894	4.73961	4.73501	4.64953	9.52	13.58292	14.32690	14.22935	13.86475
7.16	4.59041	4.83593	4.83059	4.74259	9.56	13.81243	14.56967	14.46953	14.09743
7.20	4.68347	4.93392	4.92781	4.83724	9.60	14.04512	14.81582	14.71305	14.33334
7.24	4.77812	5.03360	5.02670	4.93350	9.64	14.28101	15.06540	14.95995	14.57251
7.28	4.87439	5.13499	5.12727	5.03140	9.68	14.52015	15.31843	15.21027	14.81497
7.32	4.97230	5.23810	5.22956	5.13094	9.72	14.76256	15.57495	15.46403	15.06076
7.36	5.07187	5.34298	5.33358	5.23216	9.76	15.00828	15.83500	15.72128	15.30992
7.40	5.17313	5.44962	5.43935	5.33508	9.80	15.25735	16.09861	15.98205	15.56247
7.44	5.27608	5.55807	5.54691	5.43972	9.84	15.50979	16.36583	16.24638	15.81846
7.48	5.38077	5.66835	5.65626	5.54609	9.88	15.76564	16.63669	16.51431	16.07791
7.52	5.48720	5.78047	5.76744	5.65423	9.92	16.02494	16.91123	16.78588	16.34088
7.56	5.59540	5.89446	5.88046	5.76416	9.96	16.28772	17.18948	17.06111	16.60738
7.60	5.70539	6.01035	5.99535	5.87589	10.00	16.55401	17.47149	17.34005	16.87747
7.64	5.81720	6.12816	6.11214	5.98945					
7.68	5.93085	6.24791	6.23086	6.10487					
7.72	6.04636	6.36963	6.35151	6.22217					
7.76	6.16375	6.49334	6.47413	6.34137					
7.80	6.28305	6.61907	6.59874	6.46249					
7.84	6.40429	6.74684	6.72537	6.58557					
7.88	6.52747	6.87669	6.85405	6.71061					
7.92	6.65264	7.00863	6.98479	6.83766					
7.96	6.77981	7.14269	7.11763	6.96672					
8.00	6.90901	7.27889	7.25258	7.09784					
8.04	7.04026	7.41727	7.38968	7.23102					
8.08	7.17358	7.55785	7.52895	7.36631					
8.12	7.30901	7.70066	7.67042	7.50371					
8.16	7.44657	7.84572	7.81412	7.64327					

TABLE IX - VARIATION OF $\underline{F}$ WITH MACH NUMBER M AND VELOCITY-PROFILE PARAMETER N

$$\left[\underline{F} = e^{\int_{0.100}^{M} \varphi dM_1}\right]$$

(a) Subsonic flow

Mach number M	Velocity-profile parameter, N			
	5	7	9	11
0.100	1.00000	1.00000	1.00000	1.00000
.200	10.34448	9.56047	9.15004	8.50012
.300	39.68497	35.04360	32.70139	29.09806
.400	100.67640	86.12166	78.96629	68.15294
.500	202.51727	109.11741	153.02743	128.98686
.600	350.36128	287.03727	257.03315	212.52031
.700	544.60092	439.26097	390.03557	317.29234
.800	780.98726	621.77891	548.27530	439.82313
.900	1060.19229	827.91431	725.83398	575.15348
1.000	1367.58348	1049.26411	915.43551	717.52915

TABLE IX - VARIATION OF F WITH MACH NUMBER M AND VELOCITY-PROFILE PARAMETER N - Continued

$$\left[F = e^{\int_1^M \varphi dM_1}\right]$$

NACA

(b) Supersonic flow

Mach number	Velocity-profile parameter, N				Mach number	Velocity-profile parameter, N			
M	5	7	9	11	M	5	7	9	11
1.00	1.00000	1.00000	1.00000	1.00000	3.40	1.70781	1.61541	1.58715	1.58093
1.04	1.09013	1.08649	1.08463	1.08353	3.44	1.67363	1.58304	1.55568	1.55001
1.08	1.18099	1.17334	1.16946	1.16717	3.48	1.63977	1.55098	1.52451	1.51938
1.12	1.27198	1.26000	1.25397	1.25043	3.52	1.60626	1.51927	1.49367	1.48905
1.16	1.36254	1.34694	1.33764	1.33280	3.56	1.57314	1.48792	1.46318	1.45906
1.20	1.45213	1.43067	1.42001	1.41382	3.60	1.54041	1.45696	1.43306	1.42943
1.24	1.54024	1.51371	1.50062	1.49306	3.64	1.50810	1.42641	1.40332	1.40016
1.28	1.62638	1.59463	1.57906	1.57013	3.68	1.47623	1.39627	1.37400	1.37129
1.32	1.71010	1.67302	1.65496	1.64465	3.72	1.44482	1.36658	1.34509	1.34281
1.36	1.79101	1.74853	1.72797	1.71630	3.76	1.41388	1.33733	1.31661	1.31475
1.40	1.86874	1.82084	1.79780	1.78481	3.80	1.38342	1.30855	1.28857	1.28712
1.44	1.94298	1.88966	1.86419	1.84992	3.84	1.35345	1.28025	1.26098	1.25992
1.48	2.01346	1.95478	1.92694	1.91143	3.88	1.32397	1.25239	1.23384	1.23316
1.52	2.07995	2.01599	1.98585	1.96917	3.92	1.29501	1.22502	1.20717	1.20684
1.56	2.14226	2.07315	2.04079	2.02301	3.96	1.26655	1.19815	1.18097	1.18097
1.60	2.20024	2.12613	2.09166	2.07286	4.00	1.23861	1.17176	1.15523	1.15556
1.64	2.25380	2.17485	2.13839	2.11864	4.04	1.21119	1.14586	1.12996	1.13061
1.68	2.30286	2.21928	2.18095	2.16033	4.08	1.18428	1.12045	1.10517	1.10612
1.72	2.34739	2.25939	2.21932	2.19793	4.12	1.15790	1.09553	1.08085	1.08208
1.76	2.38739	2.29520	2.25352	2.23145	4.16	1.13203	1.07110	1.05700	1.05850
1.80	2.42288	2.32676	2.28361	2.26094	4.20	1.10667	1.04716	1.03362	1.03538
1.84	2.45392	2.35412	2.30964	2.28646	4.24	1.08183	1.02371	1.01071	1.01271
1.88	2.48058	2.37737	2.33170	2.30811	4.28	1.05750	1.00074	.98826	.99049
1.92	2.50297	2.39661	2.34990	2.32599	4.32	1.03367	.97824	.96627	.96872
1.96	2.52120	2.41197	2.36435	2.34020	4.36	1.01035	.95622	.94474	.94740
2.00	2.53540	2.42356	2.37518	2.35087	4.40	.98752	.93466	.92367	.92652
2.04	2.54571	2.43155	2.38254	2.35815	4.44	.96518	.91357	.90304	.90607
2.08	2.55229	2.43606	2.38656	2.36218	4.48	.94333	.89294	.88285	.88606
2.12	2.55531	2.43728	2.38740	2.36309	4.52	.92196	.87276	.86310	.86647
2.16	2.55492	2.43535	2.38522	2.36106	4.56	.90106	.85303	.84378	.84730
2.20	2.55131	2.43044	2.38018	2.35623	4.60	.88063	.83373	.82488	.82855
2.24	2.54465	2.42275	2.37244	2.34877	4.64	.86065	.81487	.80640	.81021
2.28	2.53512	2.41238	2.36217	2.33882	4.68	.84113	.79643	.78834	.79227
2.32	2.52290	2.39955	2.34953	2.32656	4.72	.82205	.77841	.77068	.77473
2.36	2.50816	2.38442	2.33467	2.31212	4.76	.80340	.76080	.75342	.75757
2.40	2.49108	2.36715	2.31775	2.29568	4.80	.78519	.74360	.73654	.74080
2.44	2.47183	2.34790	2.29894	2.27737	4.84	.76739	.72679	.72006	.72441
2.48	2.45057	2.32682	2.27837	2.25734	4.88	.75001	.71037	.70395	.70839
2.52	2.42748	2.30407	2.25619	2.23574	4.92	.73304	.69433	.68821	.69273
2.56	2.40269	2.27980	2.23255	2.21270	4.96	.71646	.67867	.67283	.67743
2.60	2.37638	2.25413	2.20757	2.18833	5.00	.70027	.66337	.65781	.66247
2.64	2.34868	2.22722	2.18140	2.16280	5.04	.68446	.64844	.64314	.64786
2.68	2.31973	2.19919	2.15415	2.13620	5.08	.66902	.63385	.62881	.63358
2.72	2.28968	2.17016	2.12593	2.10866	5.12	.65395	.61961	.61481	.61964
2.76	2.25863	2.14025	2.09688	2.08028	5.16	.63924	.60571	.60115	.60601
2.80	2.22672	2.10957	2.06708	2.05117	5.20	.62488	.59213	.58780	.59271
2.84	2.19407	2.07823	2.03664	2.02142	5.24	.61086	.57888	.57477	.57971
2.88	2.16077	2.04632	2.00566	1.99113	5.28	.59718	.56595	.56204	.56701
2.92	2.12693	2.01394	1.97423	1.96038	5.32	.58382	.55332	.54962	.55461
2.96	2.09264	1.98119	1.94242	1.92926	5.36	.57079	.54099	.53748	.54250
3.00	2.05800	1.94813	1.91032	1.89785	5.40	.55806	.52896	.52564	.53067
3.04	2.02309	1.91485	1.87801	1.86621	5.44	.54564	.51722	.51407	.51912
3.08	1.98798	1.88141	1.84555	1.83441	5.48	.53352	.50576	.50278	.50784
3.12	1.95276	1.84789	1.81300	1.80252	5.52	.52170	.49457	.49176	.49682
3.16	1.91748	1.81434	1.78042	1.77069	5.56	.51015	.48366	.48100	.48606
3.20	1.88220	1.78083	1.74787	1.73868	5.60	.49889	.47300	.47050	.47555
3.24	1.84699	1.74739	1.71540	1.70683	5.64	.48789	.46260	.46024	.46529
3.28	1.81190	1.71410	1.68305	1.67509	5.68	.47716	.45245	.45023	.45528
3.32	1.77698	1.68097	1.65087	1.64350	5.72	.46669	.44254	.44045	.44549
3.36	1.74227	1.64806	1.61889	1.61210	5.76	.45647	.43287	.43091	.43594

1207

TABLE IX - VARIATION OF F WITH MACH NUMBER M AND VELOCITY-PROFILE PARAMETER N - Concluded

$$\left[F = e^{\int_1^M \varphi dM_1}\right]$$

(b) Supersonic flow - Concluded

Mach number	Velocity-profile parameter, N				Mach number	Velocity-profile parameter, N			
M	5	7	9	11	M	5	7	9	11
5.80	0.44650	0.42343	0.42159	0.42661	8.20	0.13182	0.12511	0.12563	0.12845
5.84	.43677	.41422	.41250	.41750	8.24	.12940	.12281	.12333	.12612
5.88	.42727	.40523	.40362	.40860	8.28	.12703	.12056	.12108	.12384
5.92	.41800	.39646	.39495	.39991	8.32	.12471	.11836	.11888	.12160
5.96	.40895	.38789	.38649	.39143	8.36	.12244	.11620	.11673	.11942
6.00	.40012	.37953	.37823	.38314	8.40	.12022	.11409	.11462	.11727
6.04	.39150	.37137	.37017	.37505	8.44	.11805	.11203	.11255	.11517
6.08	.38309	.36341	.36229	.36715	8.48	.11592	.11000	.11053	.11312
6.12	.37488	.35563	.35460	.35943	8.52	.11384	.10802	.10855	.11111
6.16	.36687	.34804	.34709	.35190	8.56	.11180	.10609	.10662	.10914
6.20	.35904	.34063	.33976	.34454	8.60	.10980	.10419	.10472	.10721
6.24	.35141	.33340	.33261	.33735	8.64	.10784	.10233	.10286	.10532
6.28	.34396	.32634	.32562	.33033	8.68	.10593	.10051	.10104	.10347
6.32	.33668	.31945	.31879	.32347	8.72	.10405	.09873	.09926	.10165
6.36	.32958	.31272	.31213	.31677	8.76	.10222	.09698	.09751	.09987
6.40	.32264	.30615	.30562	.31022	8.80	.10042	.09527	.09580	.09813
6.44	.31587	.29973	.29926	.30383	8.84	.09866	.09360	.09412	.09643
6.48	.30926	.29347	.29306	.29759	8.88	.09693	.09196	.09248	.09476
6.52	.30281	.28735	.28700	.29149	8.92	.09524	.09035	.09087	.09312
6.56	.29650	.28138	.28107	.28553	8.96	.09359	.08878	.08930	.09158
6.60	.29035	.27554	.27529	.27971	9.00	.09197	.08724	.08775	.08994
6.64	.28434	.26985	.26964	.27402	9.04	.09038	.08573	.08624	.08840
6.68	.27847	.26429	.26412	.26846	9.08	.08882	.08425	.08476	.08689
6.72	.27274	.25885	.25873	.26305	9.12	.08730	.08280	.08331	.08541
6.76	.26715	.25355	.25347	.25772	9.16	.08580	.08138	.08188	.08396
6.80	.26168	.24836	.24832	.25254	9.20	.08434	.07999	.08049	.08254
6.84	.25634	.24330	.24330	.24747	9.24	.08290	.07862	.07912	.08115
6.88	.25113	.23836	.23839	.24252	9.28	.08150	.07728	.07778	.07978
6.92	.24603	.23352	.23359	.23768	9.32	.08012	.07597	.07647	.07844
6.96	.24106	.22881	.22890	.23295	9.36	.07877	.07469	.07518	.07713
7.00	.23620	.22419	.22432	.22833	9.40	.07744	.07343	.07392	.07584
7.04	.23145	.21969	.21984	.22381	9.44	.07614	.07220	.07268	.07458
7.08	.22681	.21529	.21547	.21939	9.48	.07487	.07099	.07147	.07334
7.12	.22227	.21099	.21119	.21508	9.52	.07362	.06980	.07028	.07213
7.16	.21785	.20679	.20701	.21086	9.56	.07240	.06864	.06911	.07094
7.20	.21352	.20268	.20293	.20673	9.60	.07120	.06750	.06797	.06977
7.24	.20929	.19866	.19894	.20270	9.64	.07002	.06638	.06685	.06862
7.28	.20515	.19474	.19504	.19875	9.68	.06887	.06528	.06575	.06750
7.32	.20111	.19091	.19122	.19490	9.72	.06774	.06421	.06467	.06640
7.36	.19717	.18716	.18749	.19113	9.76	.06663	.06315	.06361	.06532
7.40	.19331	.18350	.18385	.18744	9.80	.06554	.06212	.06257	.06426
7.44	.18953	.17992	.18028	.18383	9.84	.06448	.06110	.06155	.06322
7.48	.18585	.17642	.17680	.18031	9.88	.06343	.06011	.06055	.06220
7.52	.18224	.17300	.17339	.17686	9.92	.06240	.05915	.05957	.06120
7.56	.17872	.16965	.17005	.17349	9.96	.06140	.05818	.05861	.06021
7.60	.17527	.16638	.16680	.17019	10.00	.06041	.05724	.05767	.05925
7.64	.17190	.16318	.16361	.16696					
7.68	.16861	.16005	.16049	.16380					
7.72	.16539	.15700	.15744	.16072					
7.76	.16224	.15400	.15446	.15770					
7.80	.15916	.15108	.15154	.15474					
7.84	.15615	.14822	.14869	.15185					
7.88	.15320	.14542	.14590	.14902					
7.92	.15032	.14268	.14317	.14625					
7.96	.14750	.14000	.14050	.14354					
8.00	.14474	.13738	.13788	.14089					
8.04	.14204	.13482	.13532	.13829					
8.08	.13940	.13231	.13282	.13575					
8.12	.13682	.12986	.13037	.13327					
8.16	.13429	.12746	.12797	.13083					

TABLE X - VARIATION OF REFLECTION-THICKNESS RATIO λ/δ WITH MACH NUMBER M AND VELOCITY-PROFILE PARAMETER N

Mach number	Velocity-profile parameter, N				Mach number	Velocity-profile parameter, N			
M	5	7	9	11	M	5	7	9	11
1.00	1.0000	1.0000	1.0000	1.0000	3.40	0.3692	0.2969	0.2501	0.2169
1.04	.9034	.8678	.8340	.8026	3.44	.3708	.2986	.2517	.2185
1.08	.8191	.7581	.7026	.6550	3.48	.3724	.3003	.2534	.2201
1.12	.7499	.6721	.6043	.5450	3.52	.3740	.3020	.2551	.2218
1.16	.6922	.6034	.5290	.4664	3.56	.3757	.3037	.2568	.2234
1.20	.6438	.5479	.4704	.4074	3.60	.3773	.3055	.2585	.2251
1.24	.6028	.5026	.4242	.3623	3.64	.3790	.3072	.2603	.2268
1.28	.5679	.4654	.3874	.3274	3.68	.3807	.3090	.2620	.2285
1.32	.5381	.4345	.3577	.3000	3.72	.3824	.3108	.2638	.2302
1.36	.5125	.4088	.3336	.2781	3.76	.3841	.3126	.2655	.2319
1.40	.4903	.3871	.3138	.2607	3.80	.3858	.3144	.2673	.2336
1.44	.4711	.3688	.2974	.2464	3.84	.3875	.3162	.2691	.2353
1.48	.4544	.3533	.2839	.2348	3.88	.3893	.3180	.2709	.2370
1.52	.4399	.3400	.2725	.2253	3.92	.3910	.3198	.2727	.2387
1.56	.4271	.3287	.2630	.2174	3.96	.3928	.3216	.2745	.2405
1.60	.4160	.3190	.2549	.2108	4.00	.3945	.3234	.2763	.2422
1.64	.4062	.3107	.2482	.2054	4.04	.3963	.3252	.2781	.2439
1.68	.3976	.3035	.2424	.2008	4.08	.3981	.3271	.2799	.2457
1.72	.3901	.2973	.2376	.1970	4.12	.3998	.3289	.2817	.2474
1.76	.3834	.2920	.2335	.1939	4.16	.4016	.3308	.2835	.2492
1.80	.3776	.2874	.2300	.1913	4.20	.4034	.3326	.2853	.2509
1.84	.3725	.2835	.2271	.1891	4.24	.4052	.3344	.2871	.2527
1.88	.3680	.2802	.2247	.1873	4.28	.4070	.3363	.2889	.2545
1.92	.3641	.2773	.2227	.1859	4.32	.4087	.3381	.2907	.2562
1.96	.3607	.2749	.2211	.1848	4.36	.4105	.3400	.2926	.2580
2.00	.3577	.2729	.2197	.1840	4.40	.4123	.3418	.2944	.2597
2.04	.3552	.2712	.2187	.1834	4.44	.4141	.3437	.2962	.2615
2.08	.3530	.2699	.2179	.1830	4.48	.4159	.3455	.2980	.2633
2.12	.3512	.2688	.2174	.1827	4.52	.4177	.3473	.2998	.2650
2.16	.3496	.2680	.2170	.1827	4.56	.4195	.3492	.3017	.2668
2.20	.3483	.2674	.2169	.1828	4.60	.4212	.3510	.3035	.2686
2.24	.3473	.2670	.2169	.1830	4.64	.4230	.3529	.3053	.2704
2.28	.3465	.2667	.2170	.1833	4.68	.4248	.3547	.3071	.2721
2.32	.3459	.2667	.2173	.1838	4.72	.4266	.3565	.3089	.2739
2.36	.3454	.2668	.2177	.1843	4.76	.4283	.3584	.3108	.2756
2.40	.3452	.2670	.2182	.1850	4.80	.4301	.3602	.3126	.2774
2.44	.3451	.2674	.2188	.1857	4.84	.4319	.3620	.3144	.2792
2.48	.3452	.2679	.2195	.1865	4.88	.4336	.3638	.3162	.2809
2.52	.3454	.2685	.2203	.1873	4.92	.4354	.3657	.3180	.2827
2.56	.3457	.2692	.2211	.1883	4.96	.4372	.3675	.3198	.2844
2.60	.3461	.2699	.2221	.1893	5.00	.4389	.3693	.3216	.2862
2.64	.3467	.2708	.2231	.1903	5.04	.4407	.3711	.3234	.2879
2.68	.3473	.2717	.2241	.1914	5.08	.4424	.3729	.3252	.2897
2.72	.3480	.2728	.2253	.1926	5.12	.4441	.3747	.3269	.2914
2.76	.3488	.2738	.2264	.1937	5.16	.4459	.3765	.3287	.2932
2.80	.3497	.2750	.2277	.1950	5.20	.4476	.3783	.3305	.2949
2.84	.3507	.2762	.2289	.1962	5.24	.4493	.3801	.3323	.2967
2.88	.3517	.2774	.2303	.1976	5.28	.4510	.3819	.3341	.2984
2.92	.3528	.2787	.2316	.1989	5.32	.4528	.3836	.3358	.3001
2.96	.3539	.2800	.2330	.2003	5.36	.4545	.3854	.3376	.3018
3.00	.3551	.2814	.2344	.2017	5.40	.4562	.3872	.3393	.3036
3.04	.3564	.2828	.2359	.2031	5.44	.4579	.3889	.3411	.3053
3.08	.3576	.2843	.2373	.2045	5.48	.4596	.3907	.3428	.3070
3.12	.3590	.2858	.2389	.2060	5.52	.4612	.3924	.3446	.3087
3.16	.3603	.2873	.2404	.2075	5.56	.4629	.3942	.3463	.3104
3.20	.3617	.2888	.2420	.2090	5.60	.4646	.3959	.3481	.3121
3.24	.3632	.2904	.2435	.2106	5.64	.4663	.3976	.3498	.3138
3.28	.3647	.2920	.2451	.2121	5.68	.4679	.3994	.3515	.3155
3.32	.3662	.2936	.2468	.2137	5.72	.4696	.4011	.3532	.3172
3.36	.3677	.2953	.2484	.2153	5.76	.4712	.4028	.3550	.3189

TABLE X - VARIATION OF REFLECTION-THICKNESS RATIO λ/δ WITH MACH NUMBER M AND VELOCITY-PROFILE PARAMETER N - Concluded

NACA

Mach number	Velocity-profile parameter, N				Mach number	Velocity-profile parameter, N			
M	5	7	9	11	M	5	7	9	11
5.80	0.4729	0.4045	0.3567	0.3206	8.20	0.5590	0.4954	0.4489	0.4126
5.84	.4745	.4062	.3584	.3223	8.24	.5602	.4968	.4503	.4139
5.88	.4761	.4079	.3601	.3239	8.28	.5614	.4981	.4516	.4153
5.92	.4777	.4096	.3618	.3256	8.32	.5627	.4994	.4530	.4167
5.96	.4793	.4113	.3635	.3273	8.36	.5639	.5007	.4543	.4180
6.00	.4810	.4130	.3651	.3289	8.40	.3651	.5020	.4557	.4194
6.04	.4826	.4146	.3668	.3306	8.44	.5663	.5033	.4570	.4207
6.08	.4842	.4163	.3685	.3323	8.48	.5675	.5046	.4583	.4221
6.12	.4857	.4180	.3702	.3339	8.52	.5687	.5059	.4597	.4234
6.16	.4873	.4196	.3718	.3355	8.56	.5699	.5071	.4610	.4247
6.20	.4889	.4213	.3735	.3372	8.60	.5711	.5084	.4623	.4261
6.24	.4905	.4229	.3751	.3388	8.64	.5723	.5097	.4636	.4274
6.28	.4920	.4245	.3768	.3405	8.68	.5734	.5109	.4649	.4287
6.32	.4936	.4262	.3784	.3421	8.72	.5746	.5122	.4662	.4300
6.36	.4951	.4278	.3801	.3437	8.76	.5758	.5135	.4675	.4313
6.40	.4967	.4294	.3817	.3453	8.80	.5769	.5147	.4688	.4326
6.44	.4982	.4310	.3833	.3469	8.84	.5781	.5159	.4701	.4339
6.48	.4997	.4326	.3849	.3485	8.88	.5792	.5172	.4713	.4352
6.52	.5012	.4342	.3865	.3501	8.92	.5804	.5184	.4726	.4365
6.56	.5027	.4358	.3881	.3517	8.96	.5815	.5196	.4739	.4378
6.60	.5043	.4374	.3897	.3533	9.00	.5826	.5208	.4751	.4391
6.64	.5058	.4390	.3913	.3549	9.04	.5837	.5220	.4764	.4404
6.68	.5072	.4405	.3929	.3565	9.08	.5849	.5233	.4776	.4416
6.72	.5087	.4421	.3945	.3580	9.12	.5860	.5245	.4789	.4429
6.76	.5102	.4436	.3961	.3596	9.16	.5871	.5257	.4801	.4441
6.80	.5117	.4452	.3976	.3612	9.20	.5882	.5268	.4813	.4454
6.84	.5131	.4467	.3992	.3627	9.24	.5893	.5280	.4826	.4466
6.88	.5146	.4483	.4008	.3643	9.28	.5904	.5292	.4838	.4479
6.92	.5160	.4498	.4023	.3658	9.32	.5914	.5304	.4850	.4491
6.96	.5175	.4513	.4039	.3674	9.36	.5925	.5315	.4862	.4504
7.00	.5189	.4528	.4054	.3689	9.40	.5936	.5327	.4874	.4516
7.04	.5204	.4544	.4069	.3704	9.44	.5947	.5339	.4886	.4528
7.08	.5218	.4559	.4085	.3720	9.48	.5957	.5350	.4898	.4540
7.12	.5232	.4574	.4100	.3735	9.52	.5968	.5362	.4910	.4553
7.16	.5246	.4589	.4115	.3750	9.56	.5979	.5373	.4922	.4565
7.20	.5260	.4603	.4130	.3765	9.60	.5989	.5385	.4934	.4577
7.24	.5274	.4618	.4145	.3780	9.64	.5999	.5396	.4946	.4589
7.28	.5288	.4633	.4160	.3795	9.68	.6010	.5407	.4958	.4601
7.32	.5302	.4648	.4175	.3810	9.72	.6020	.5418	.4969	.4613
7.36	.5316	.4662	.4190	.3825	9.76	.6031	.5430	.4981	.4625
7.40	.5329	.4677	.4205	.3840	9.80	.6041	.5441	.4993	.4636
7.44	.5343	.4691	.4220	.3855	9.84	.6051	.5452	.5004	.4648
7.48	.5356	.4706	.4234	.3869	9.88	.6061	.5463	.5016	.4660
7.52	.5370	.4720	.4249	.3884	9.92	.6071	.5474	.5027	.4672
7.56	.5383	.4734	.4264	.3899	9.96	.6081	.5485	.5039	.4683
7.60	.5397	.4748	.4278	.3913	10.00	.6091	.5496	.5050	.4695
7.64	.5410	.4760	.4288	.3920					
7.68	.5423	.4777	.4307	.3942					
7.72	.5437	.4791	.4321	.3957					
7.76	.5450	.4805	.4336	.3971					
7.80	.5463	.4819	.4350	.3985					
7.84	.5476	.4832	.4364	.4000					
7.88	.5489	.4846	.4378	.4014					
7.92	.5501	.4860	.4392	.4028					
7.96	.5514	.4874	.4406	.4042					
8.00	.5527	.4887	.4420	.4056					
8.04	.5540	.4901	.4434	.4070					
8.08	.5552	.4914	.4448	.4084					
8.12	.5565	.4928	.4462	.4098					
8.16	.5577	.4941	.4476	.4112					

TABLE XI

SUMMARY OF TYPICAL NOZZLE BOUNDARY-LAYER CALCULATIONS

[Values of δ, θ, δ^*, and λ listed are relative to values obtained for $k = 0.30$.]

k	N (throat)	N (test section)	δ	θ	δ^*	λ
Test-section Mach number, 2.08						
0.25	5.90	6.38	0.915	1.006	1.036	1.070
.30	7.08	7.66	1.000	1.000	1.000	1.000
.39	9.21	9.95	1.155	.991	.958	.920
Test-section Mach number, 7.00						
0.25	5.72	5.07	0.960	0.986	1.006	1.027
.30	6.87	6.08	1.000	1.000	1.000	1.000
.39	8.93	7.91	1.074	1.018	.992	.959

TABLE XII

SECONDARY WAVE STRENGTHS OBTAINED BY CHARACTERISTICS ANALYSIS OF MACH WAVE BOUNDARY-LAYER INTERACTION $M_1 = 2.44$, $N = 5$

[Primary or incident wave strength: +1.000]

Location number	Wave strength	Location number	Wave strength
0	-0.00291800	25	0.02931285
1	- .00359997	26	-.03835323
2	- .00409983	27	.04548135
3	- .00448471	28	-.02984755
4	- .00481443	29	.04408122
5	- .00509892	30	-.02862546
6	- .00531820	31	.04221899
7	- .00554232	32	-.02765037
8	- .00575678	33	.04042821
9	- .00597492	34	-.02659263
10	- .00618321	35	.03881986
11	- .00640518	36	-.02553515
12	- .00663364	37	.03731339
13	- .00688571	38	-.02447908
14	- .00714522	39	.03587558
15	- .00743806	40	-.02345762
16	- .00775829	41	.03447333
17	- .00811766	42	-.02250068
18	- .00848494	43	.03312750
19	- .00880291	44	-.02167685
20	- .00901364	45	.03158638
21	- .00878372	46	-.02117528
22	- .00224388	47	.02977436
23	.00852988	48	-.02129959
24	.97931981	49	.02524097
		50	-.02325054

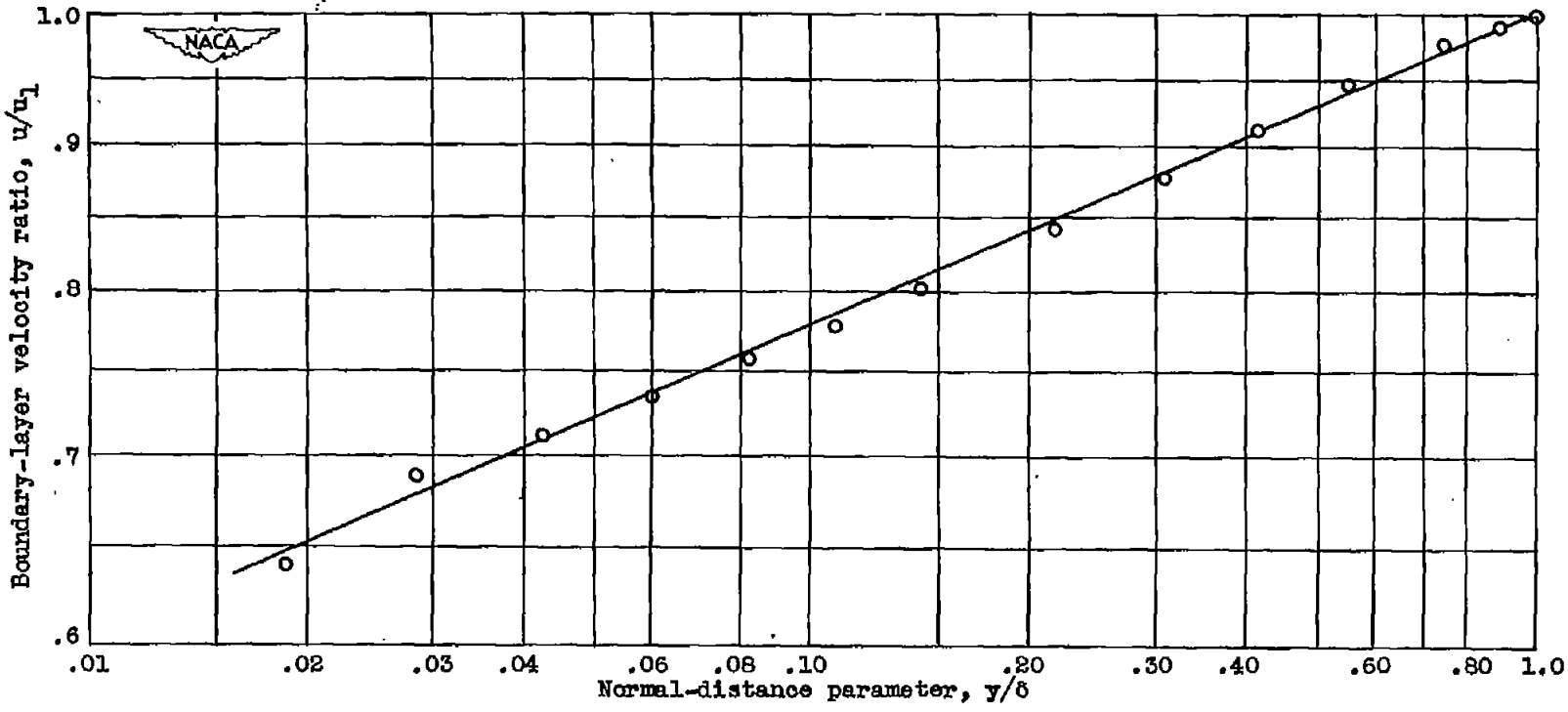

Figure 1. - Comparison of power-law profile and experimental profile obtained in a supersonic nozzle at a stream Mach number of 2.

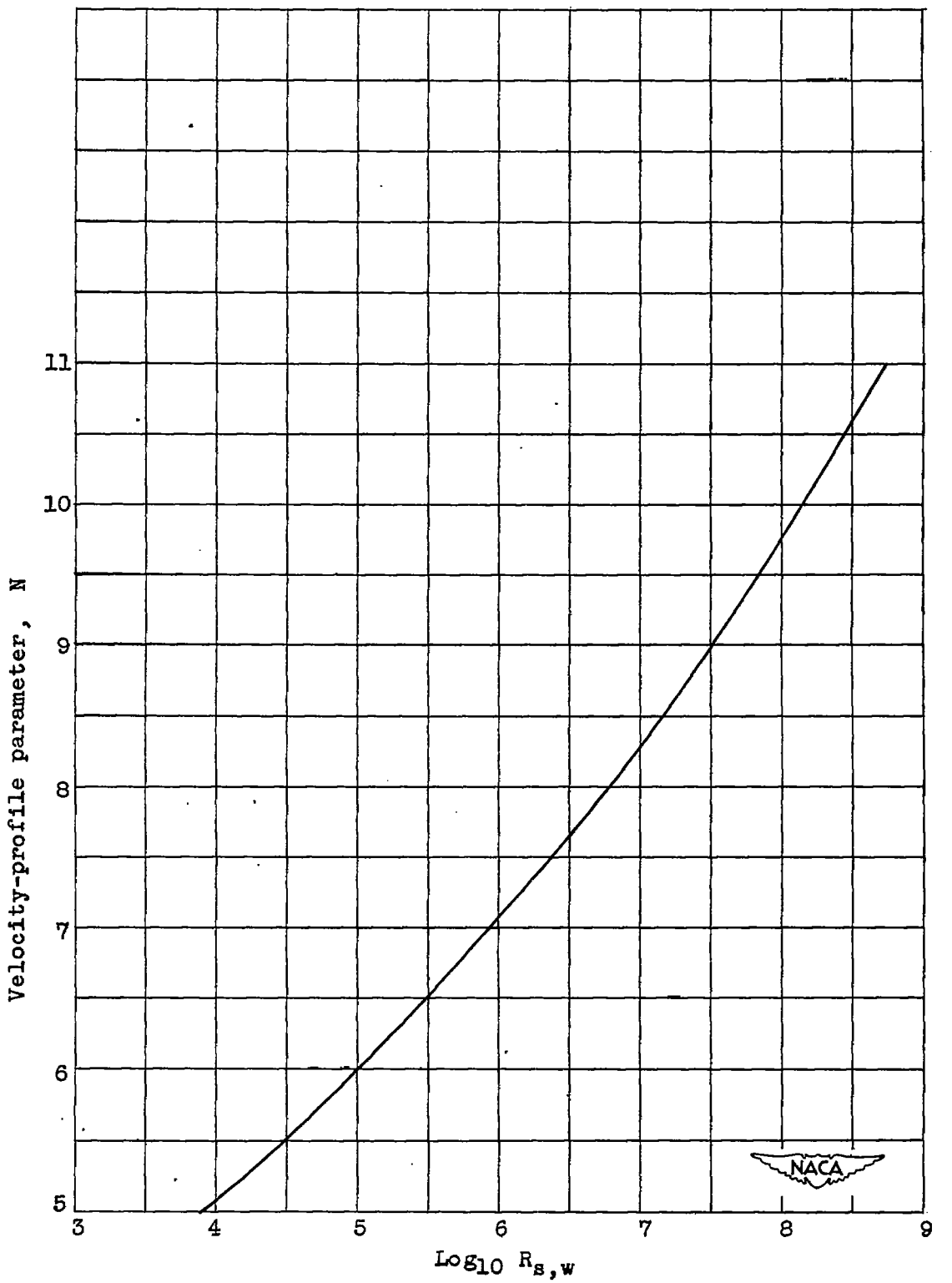

Figure 2. - Variation of velocity-profile parameter with Reynolds number for $k = 0.3$ and $\frac{u}{u_1} = 1$.

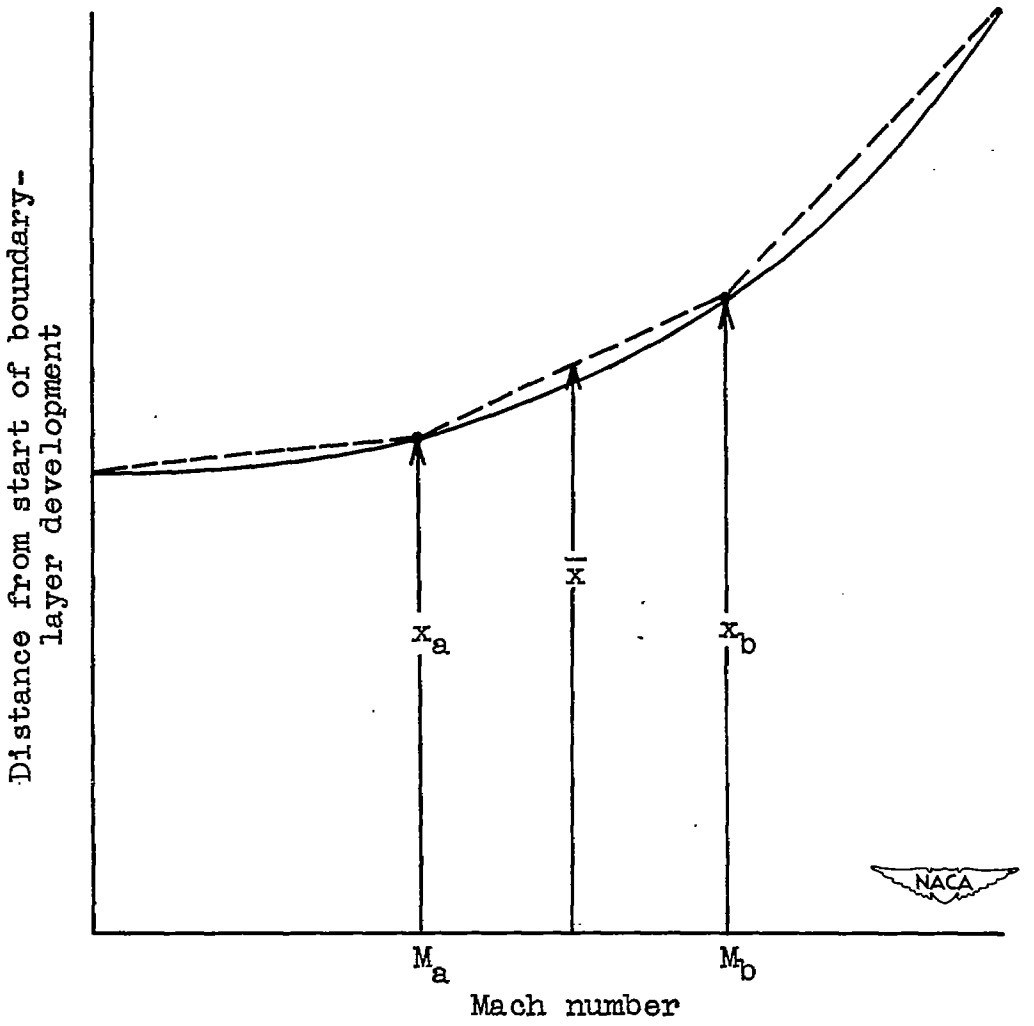

Figure 3. - Method of approximating potential-flow Mach number distribution.

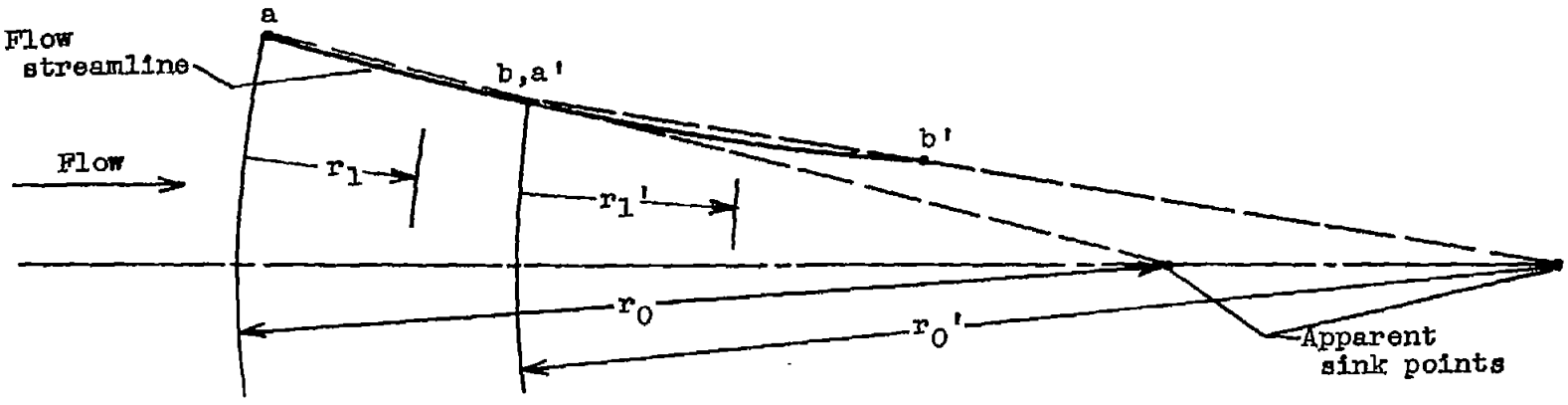

(a) Converging flow.

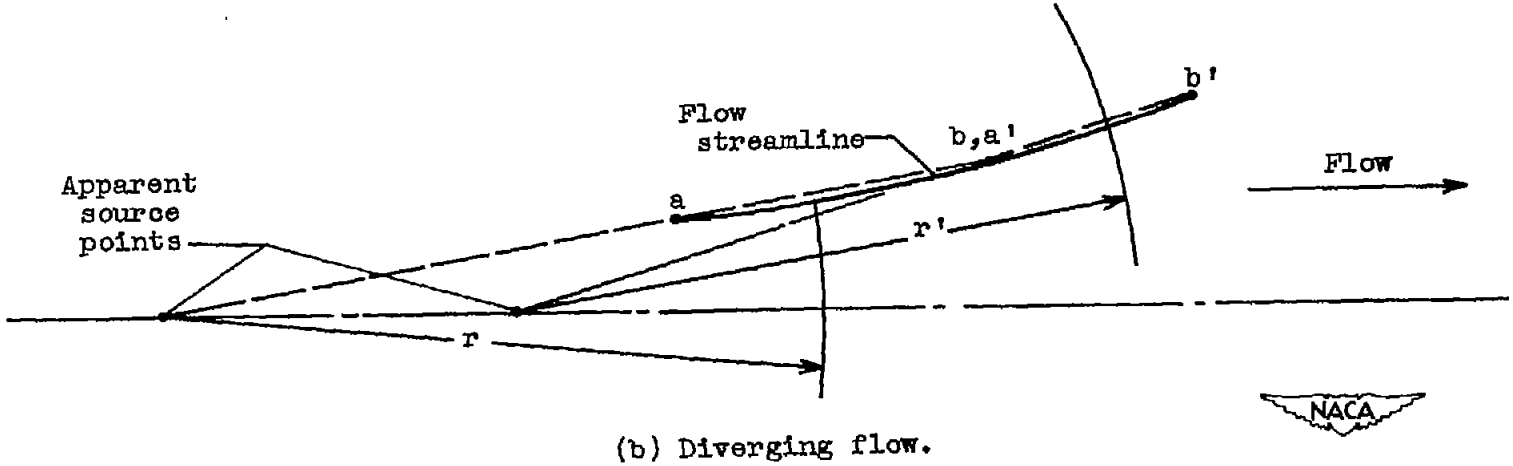

(b) Diverging flow.

Figure 4. - Method of approximating convergent and divergent flows as radial flows.

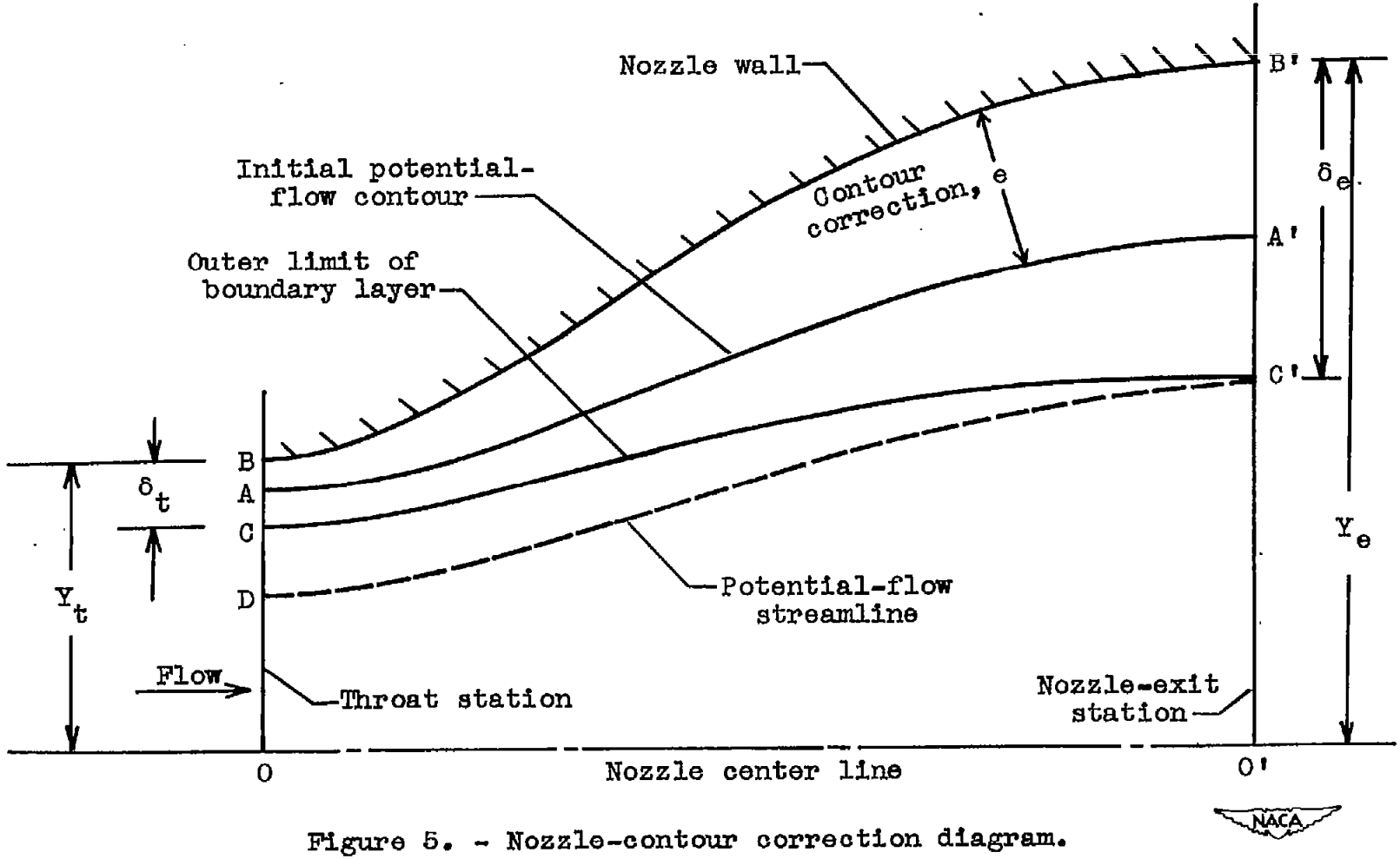

Figure 5. - Nozzle-contour correction diagram.

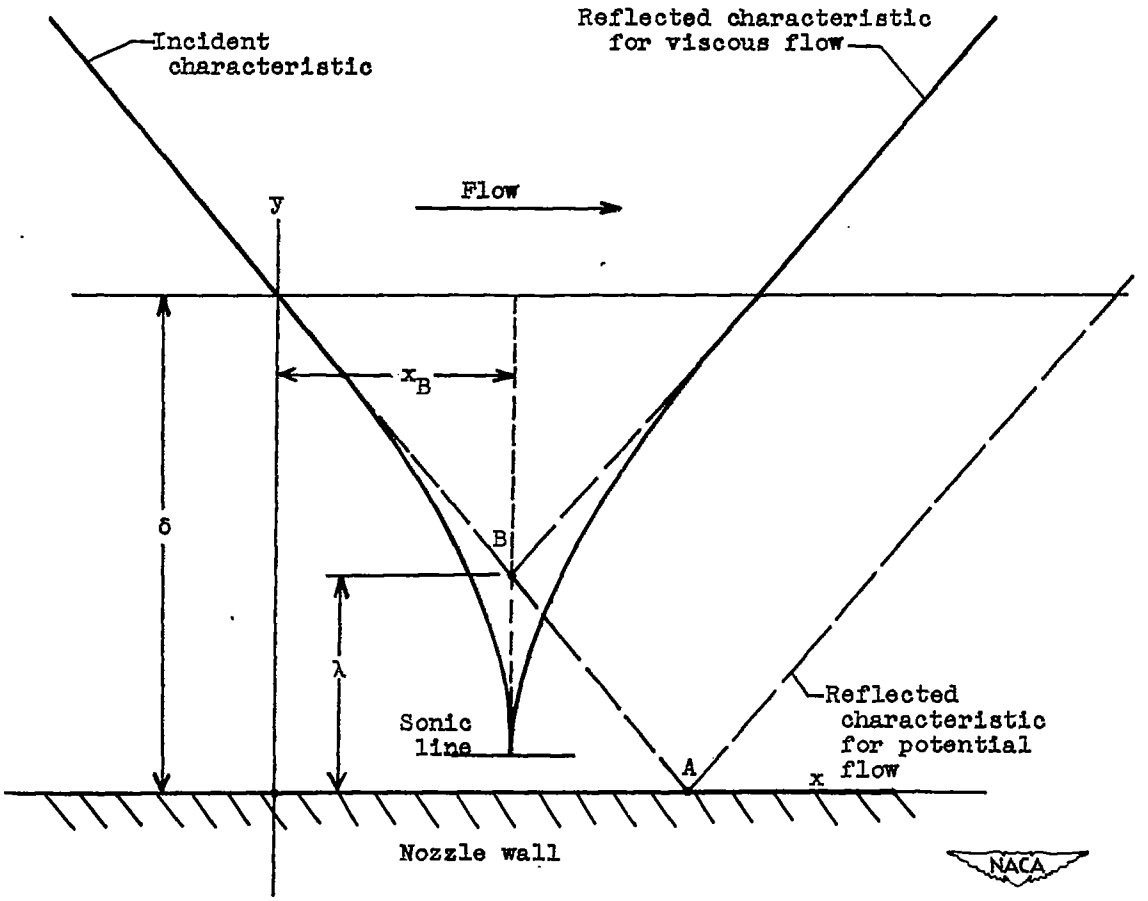

Figure 6. - Comparison of wave reflection for viscous and potential flows.

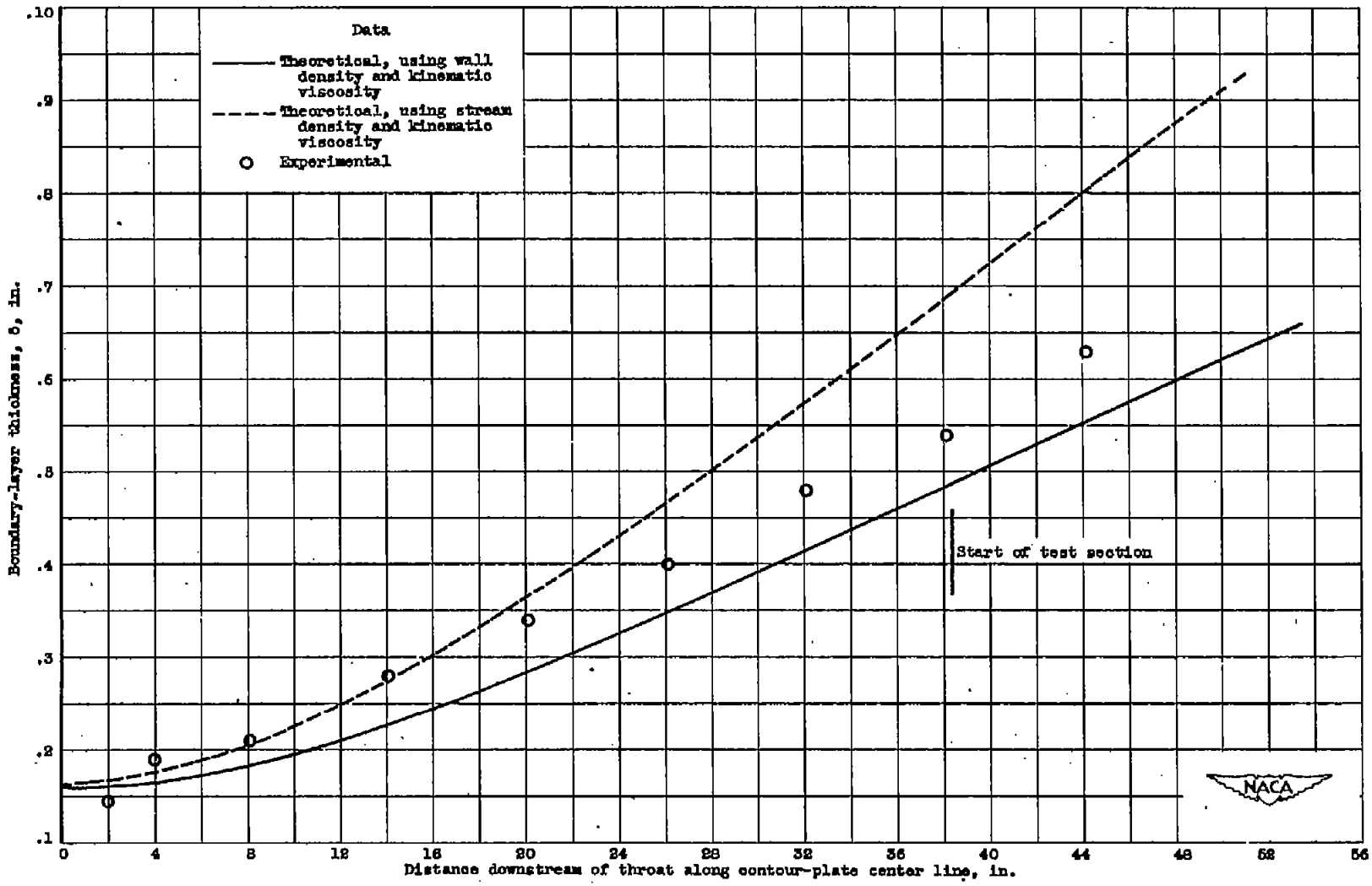

(a) Boundary-layer thickness.

Figure 7. - Comparison of theoretical and experimental boundary-layer development along contour-plate center line of 3.84- by 10-inch Mach number 2.08 supersonic tunnel.

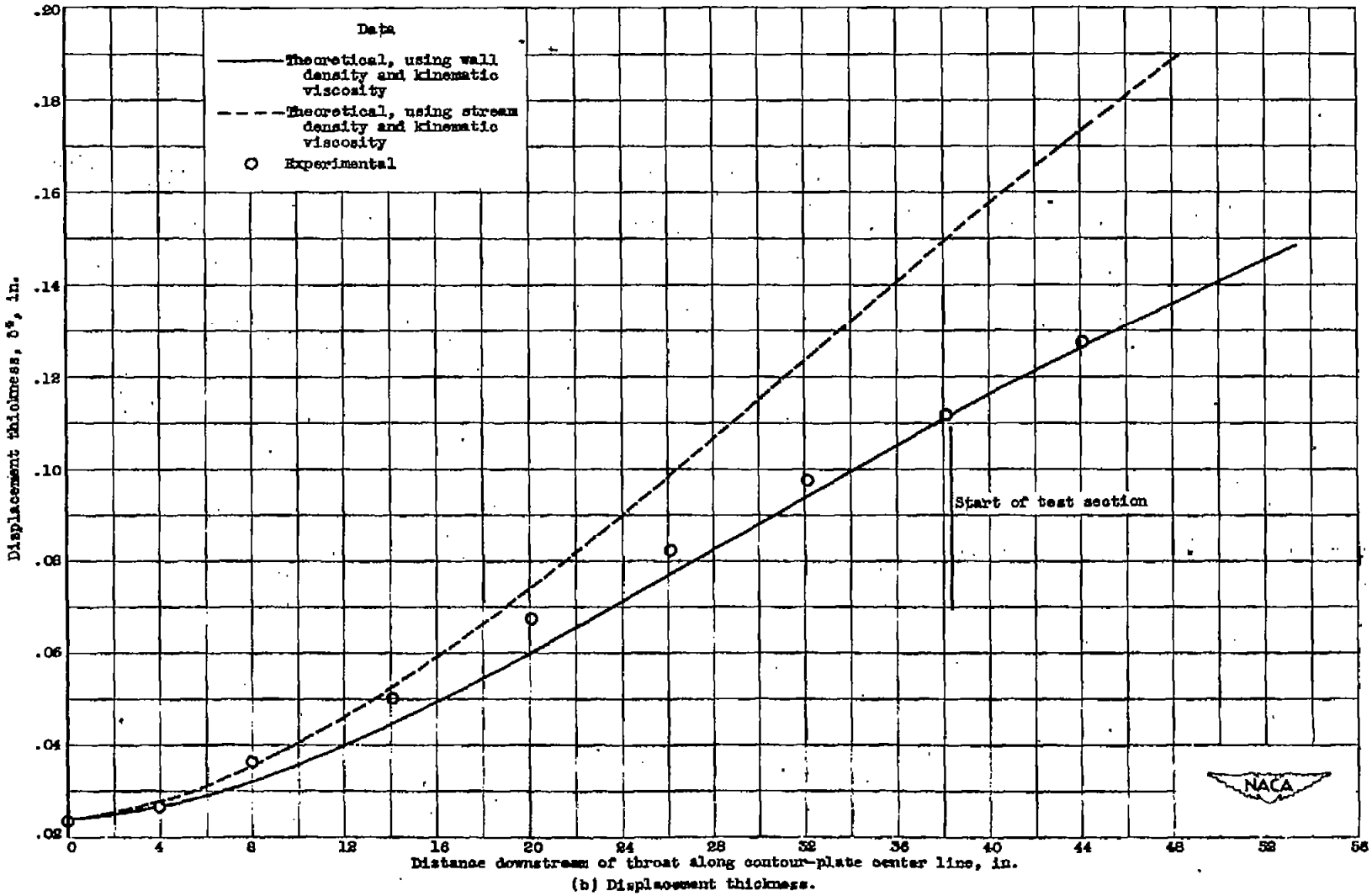

(b) Displacement thickness.

Figure 7. - Continued. Comparison of theoretical and experimental boundary-layer development along contour-plate center line of 3.94- by 10-inch Mach number 2.08 supersonic tunnel.

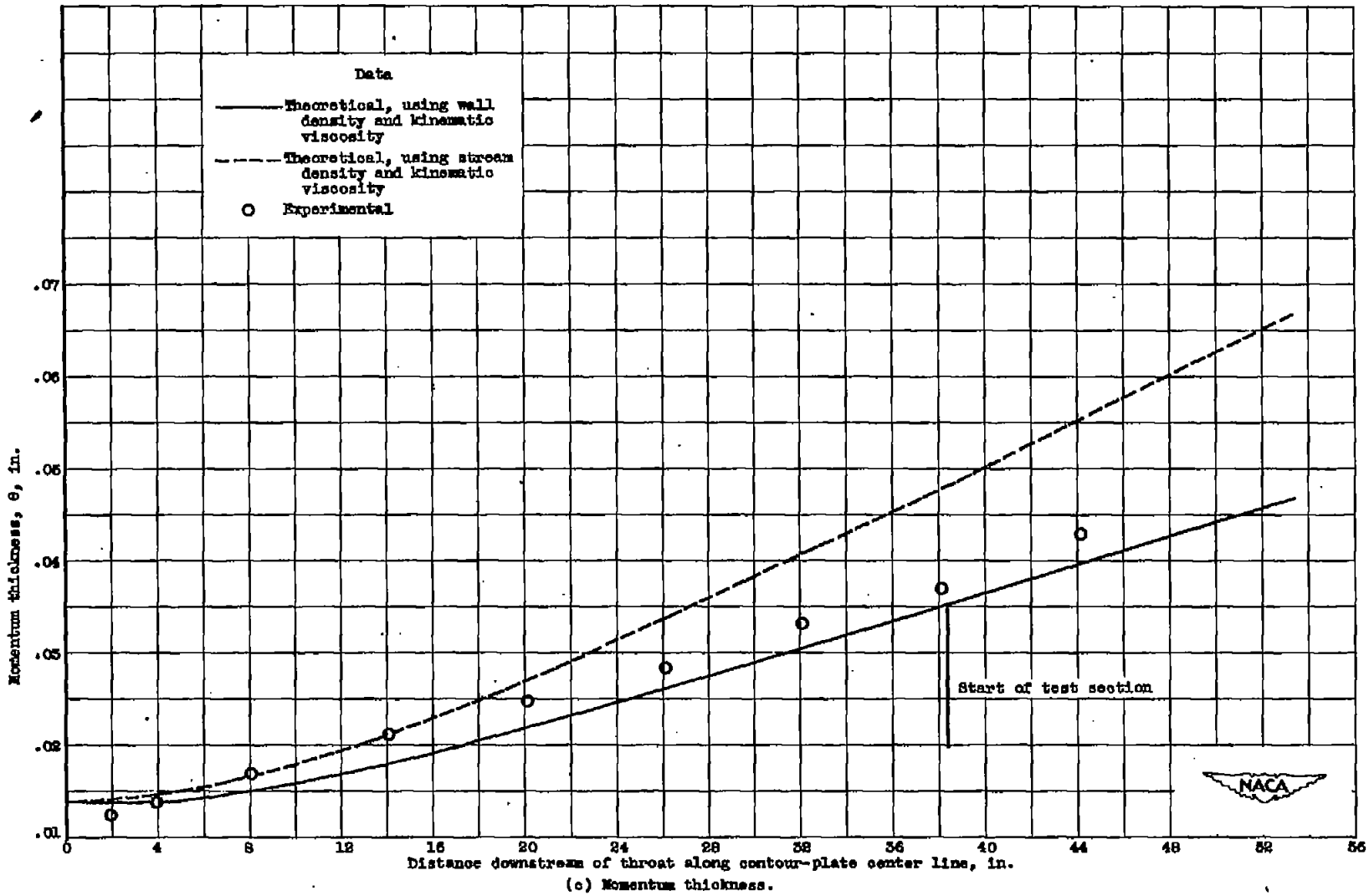

(c) Momentum thickness.

Figure 7. – Concluded. Comparison of theoretical and experimental boundary-layer development along contour-plate center line of 3.84- by 10-inch Mach number 2.08 supersonic tunnel.

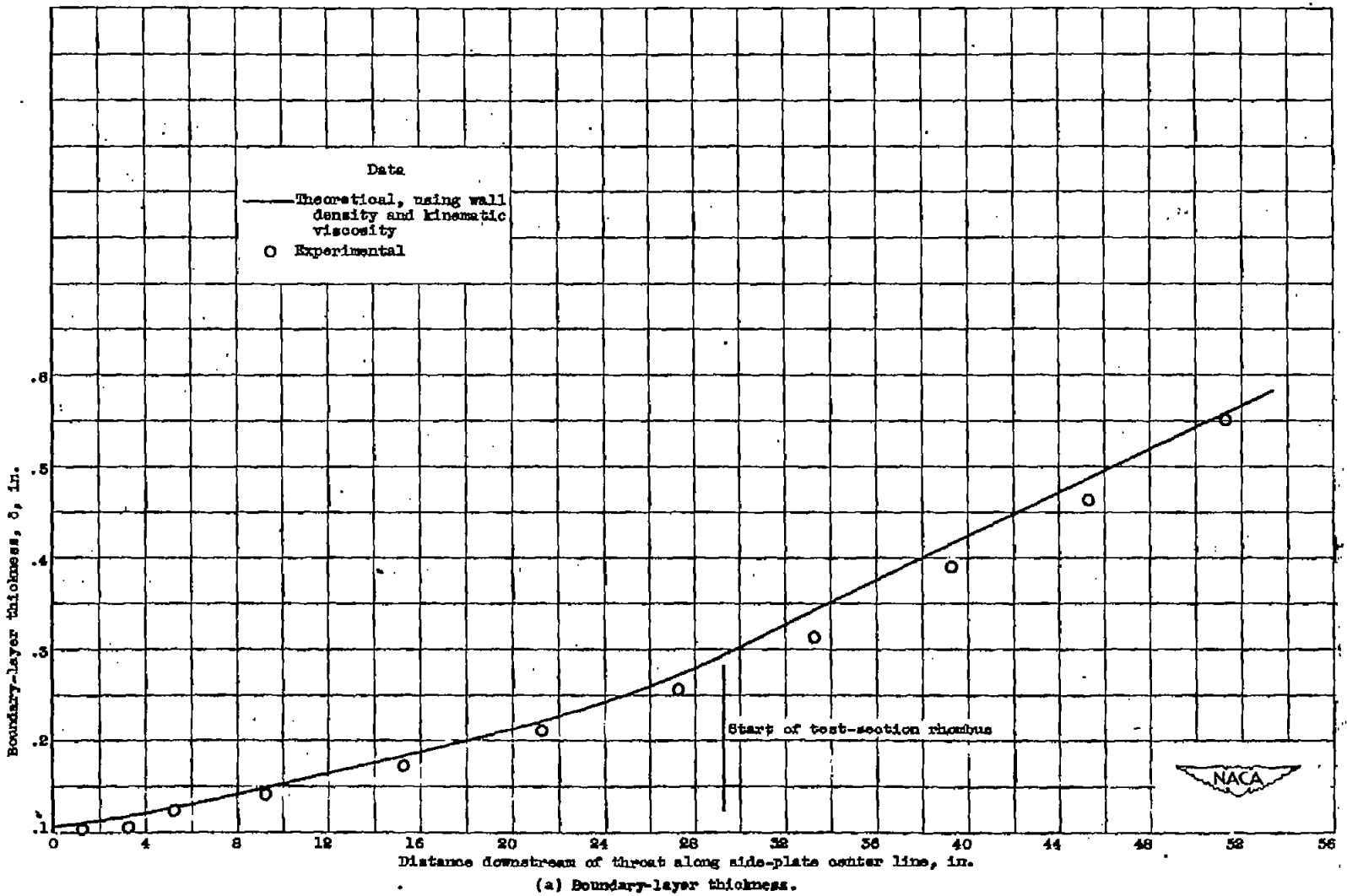

(a) Boundary-layer thickness.

Figure 8. - Comparison of theoretical and experimental boundary-layer development along side-plate center line of 3.84- by 10-inch Mach number 2.08 supersonic tunnel.

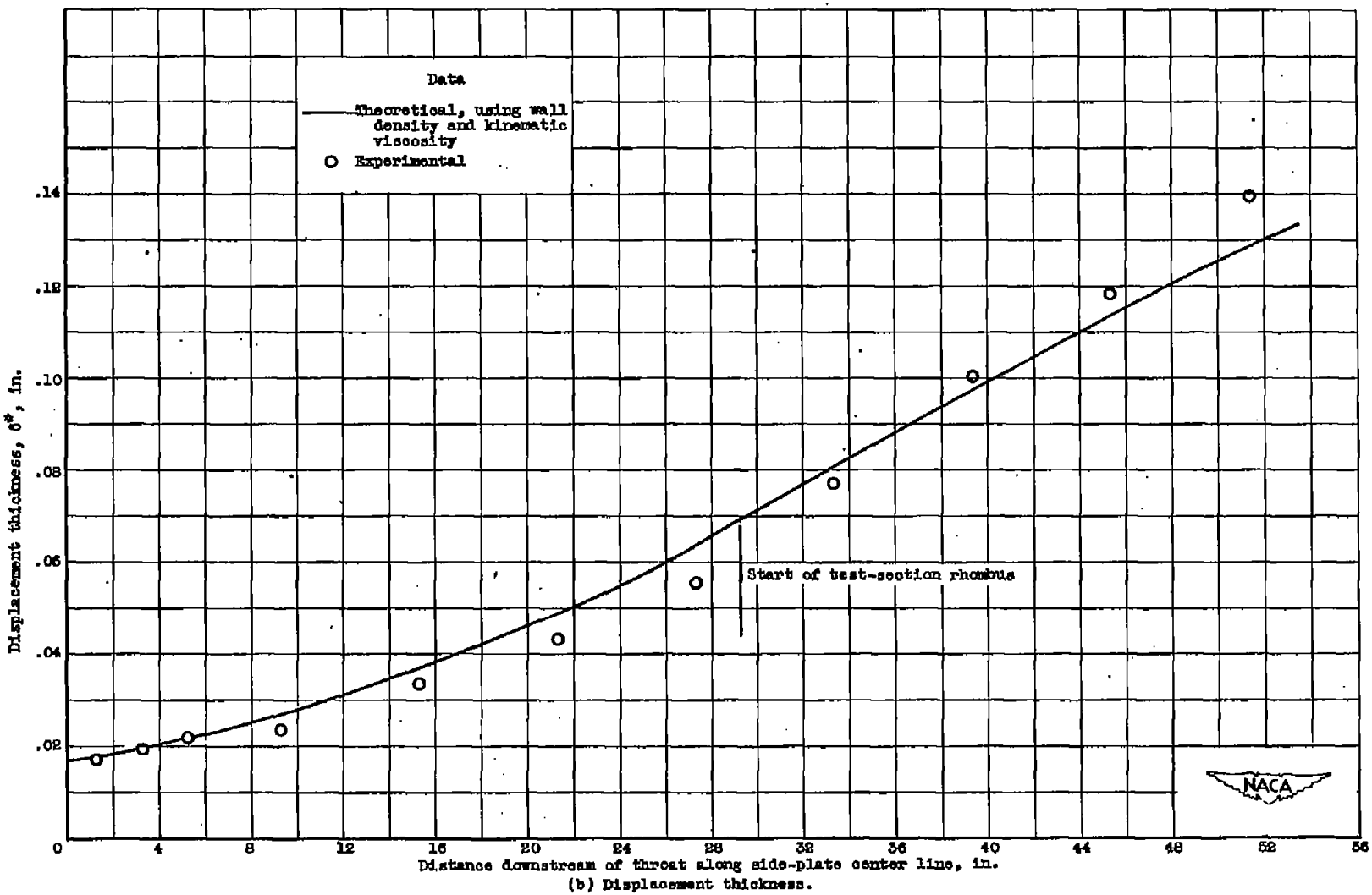

(b) Displacement thickness.

Figure 8. - Continued. Comparison of theoretical and experimental boundary-layer development along side-plate center line of 3.84- by 10-inch Mach number 2.08 supersonic tunnel.

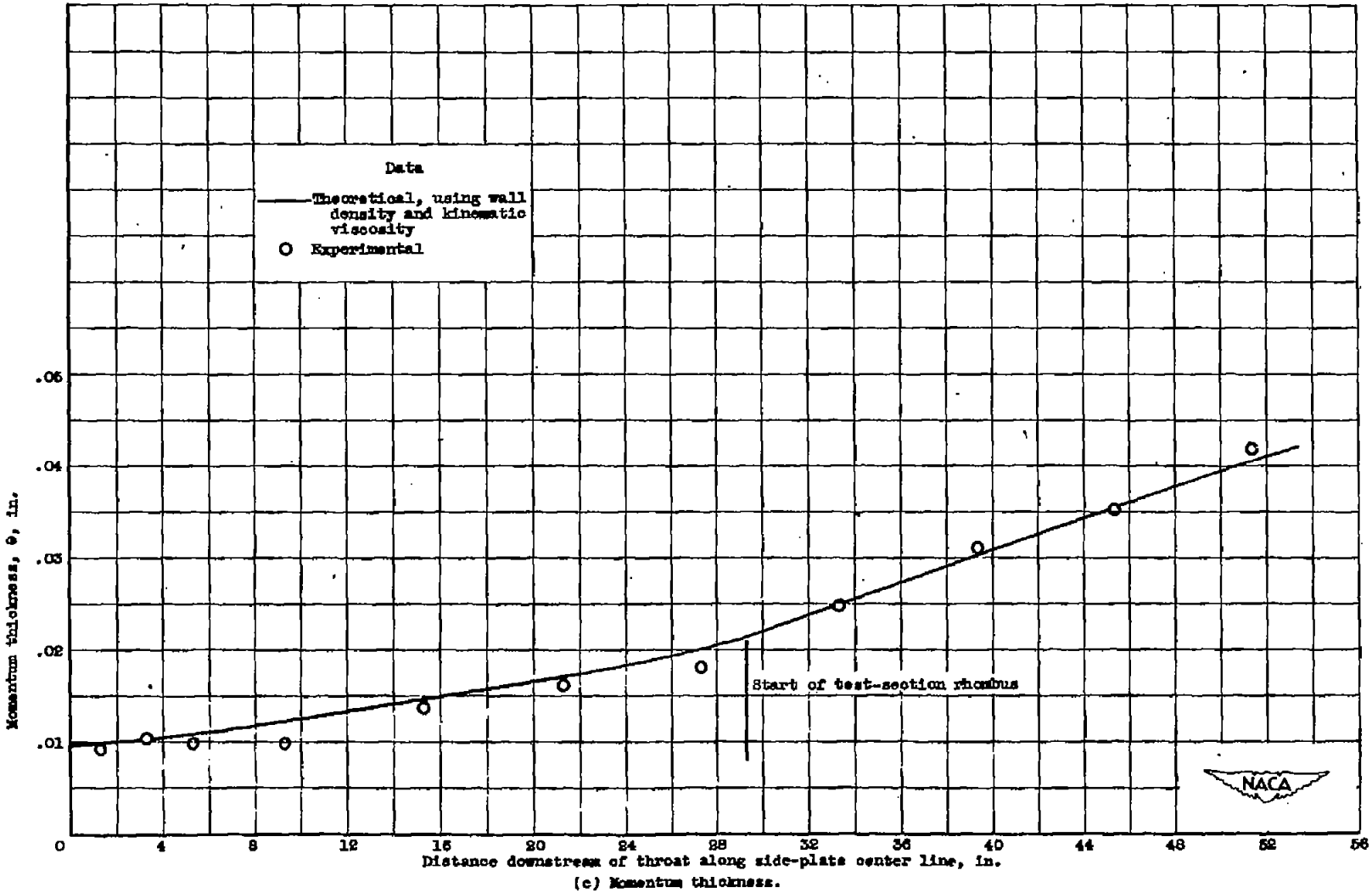

(c) Momentum thickness.

Figure 8. - Concluded. Comparison of theoretical and experimental boundary-layer development along side-plate center line of 3.84- by 10-inch Mach number 2.08 supersonic tunnel.

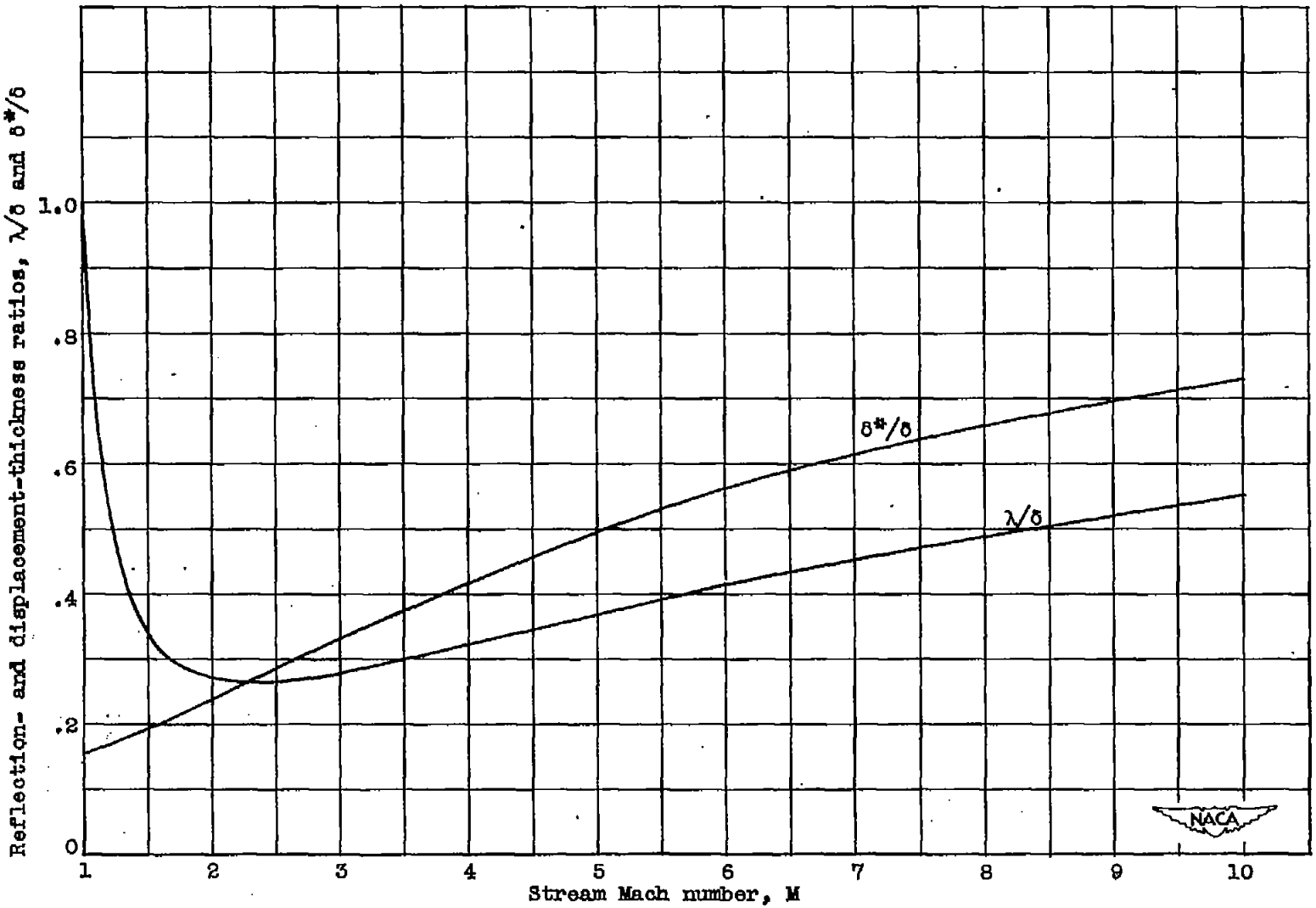

Figure 9. - Comparison of reflection- and displacement-thickness ratios for velocity-profile parameter of 7.

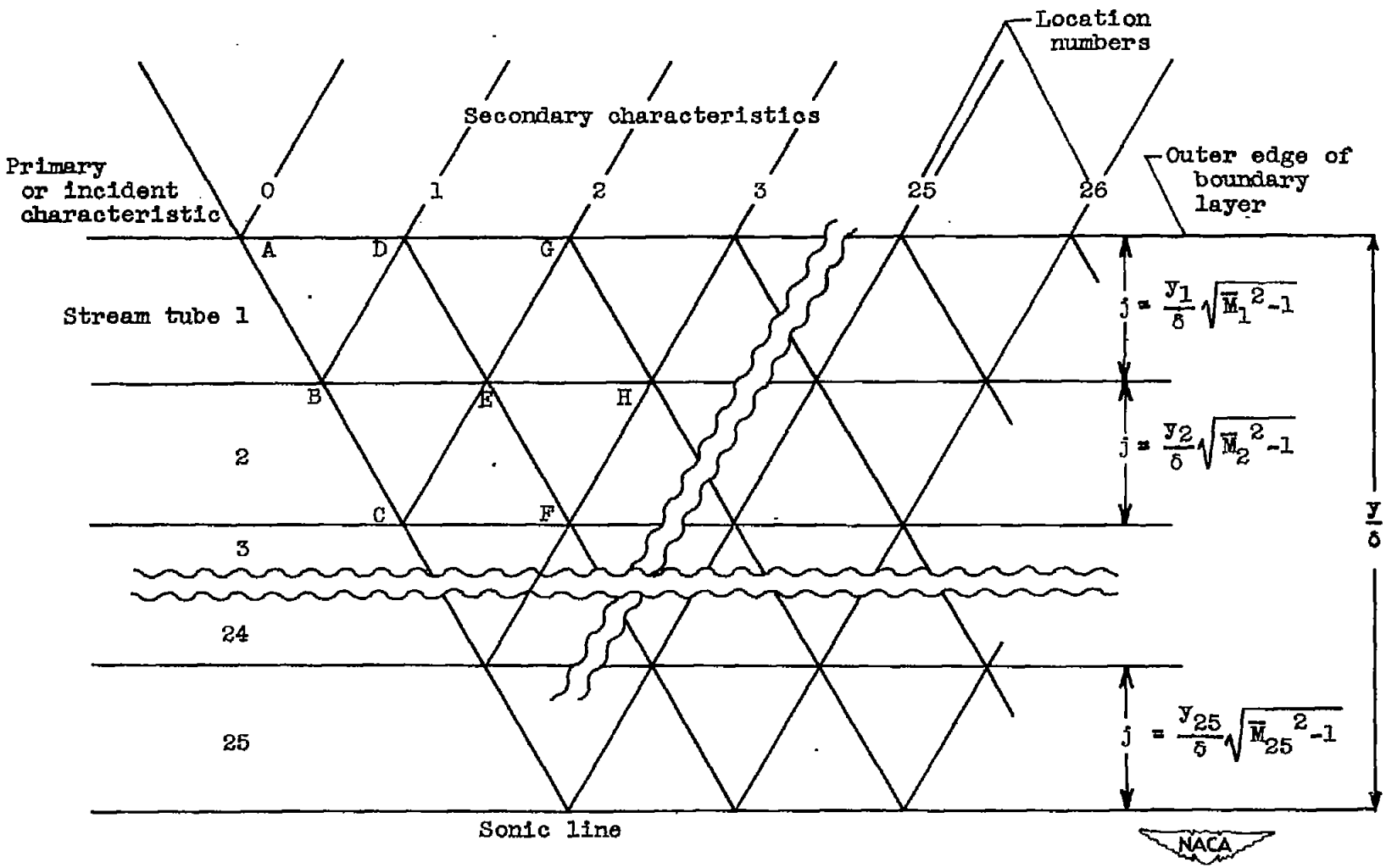

Figure 10. - Characteristic network used in obtaining interaction of Mach wave and boundary layer.